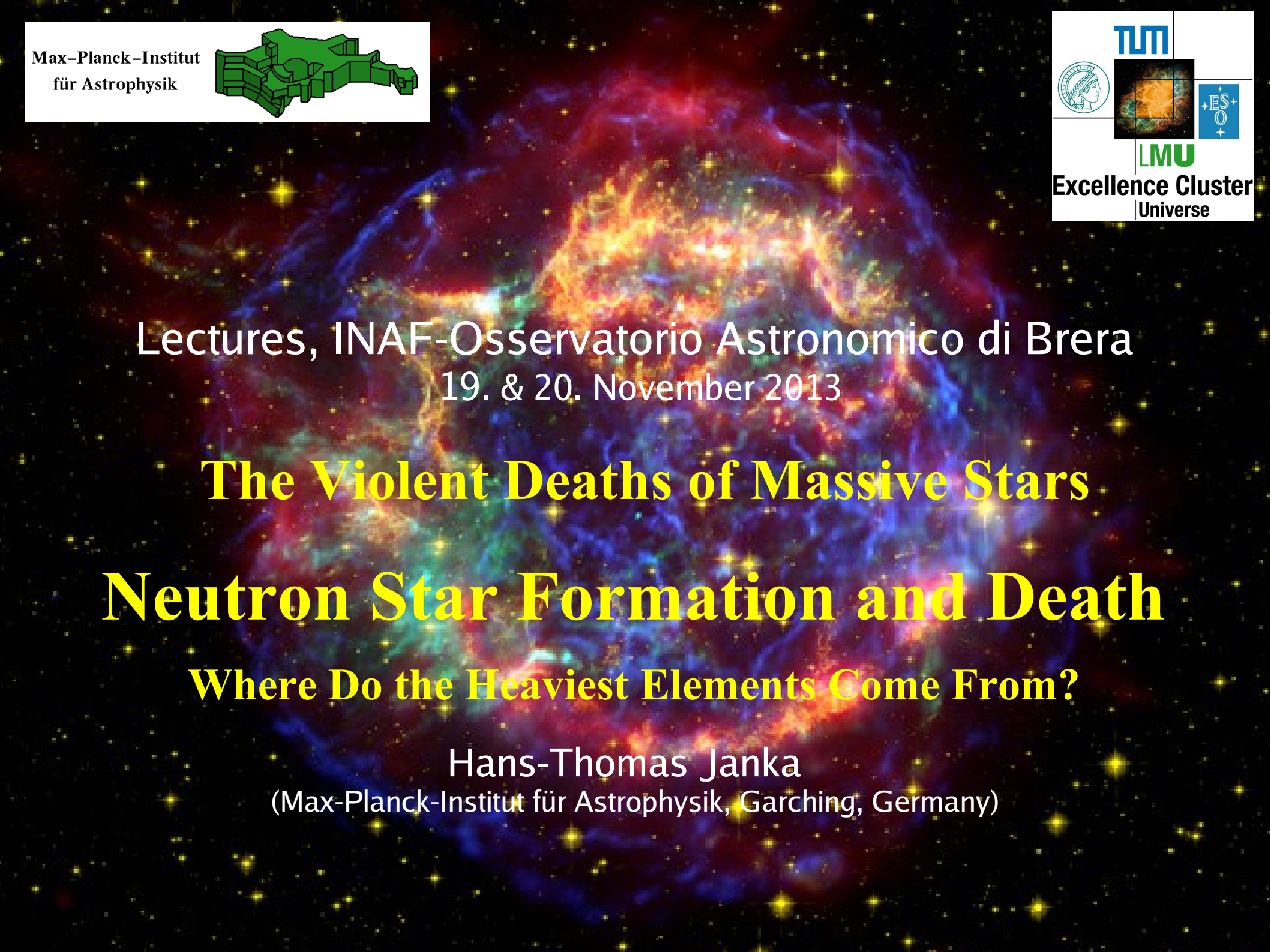

Lectures, INAF-Osservatorio Astronomico di Brera

19. & 20. November 2013

The Violent Deaths of Massive Stars

Neutron Star Formation and Death

Where Do the Heaviest Elements Come From?

Hans-Thomas Janka

(Max-Planck-Institut für Astrophysik, Garching, Germany)

Contents

Lecture I:

- Supernovae: classification and phenomenology
- Basics of stellar evolution & death scenarios in overview
- White dwarfs and thermonuclear supernovae

Lecture II:

- Gravitational (core-collapse) supernovae: evolution stages
- SN modeling: some technical aspects
- Status of 2D and 3D SN modeling

Lecture III:

- Supernova models: Predictions of observable signals
- Neutron stars: birth and death
- Black holes and gamma-ray bursts: Sources of heavy elements

Some Observable Consequences of Neutrino-driven Explosions (continued)

Observational consequences and indirect evidence for neutrino heating and hydrodynamic instabilities at the onset of stellar explosions:

- Neutrino signals (characteristic modulations)
  (Marek et al. 2009; Müller E. et al. 2012; Lund et al. 2010, 2012; Tamborra et al. 2013)
- Gravitational-wave signals
  (Marek et al. 2009; Müller E. et al. 2012; Müller B. et al. 2012)
- Neutron star and BH kicks
  (Scheck et al. 2004, 2006; Wongwathanat et al. 2010, 2012; Janka 2013)
- Asymmetric mass ejection & large-scale radial mixing
  (Kifonidis et al. 2005, Hammer er al. 2010, Wongwathanat et al., in prep.)
- Progenitor – explosion – remnant connection (Ugliano et al. 2012)
- Lightcurve shape, spectral features (electromagnetic emission)
- Nucleosynthesis (e.g., Pruet et al. 2006, Wanajo et al. 2011,2013)

Detecting Core-Collapse SN Signals

Superkamiokande

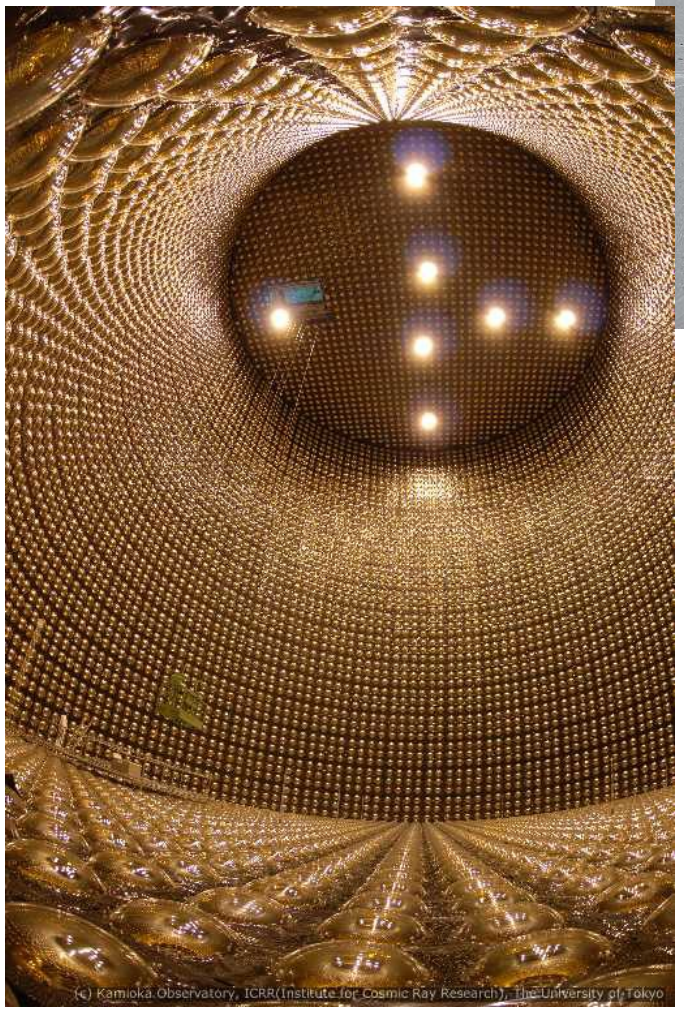

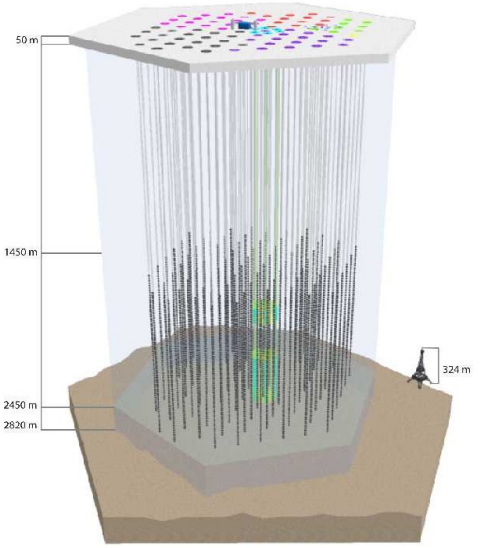

IceCube

VIRGO

Schematic Neutrino Light Curves

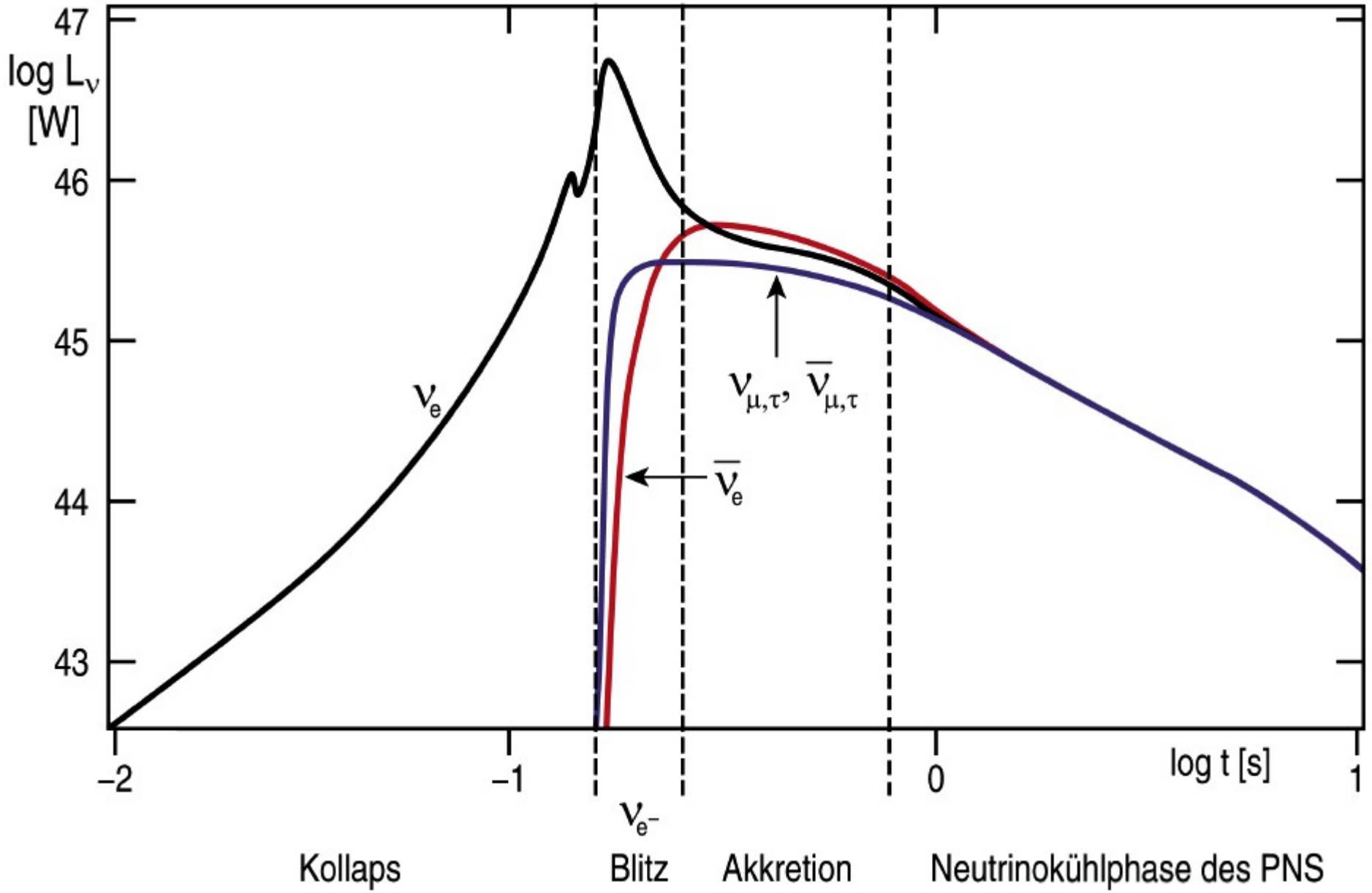

3D Core-Collapse Models: Neutrino Signals

11.2, 20, 27 M_{sun} progenitors (WHW 2002)

SASI produces modulations of neutrino emission and gravitational-wave signal.

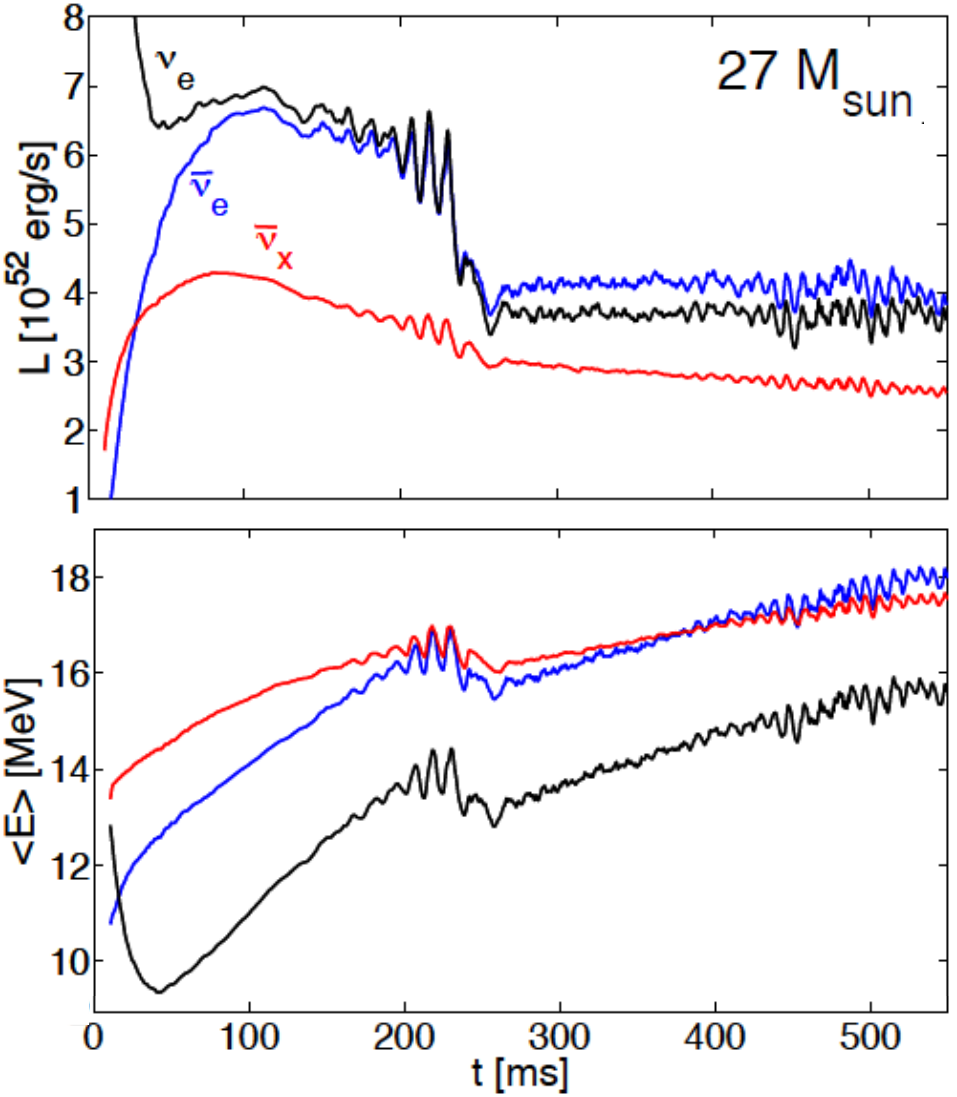

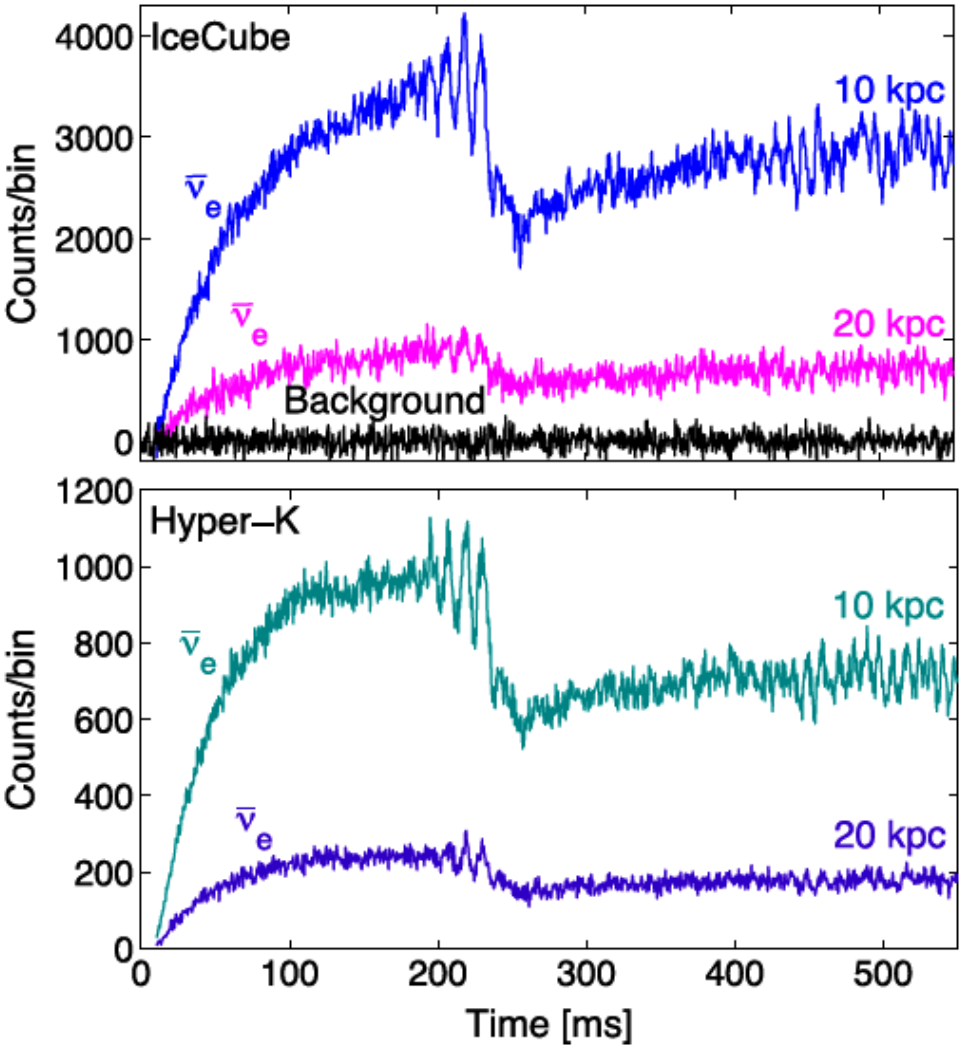

(Tamborra et al., PRL 111, 121104 (2013); arXiv:1307.7936)

3D Core-Collapse Models: Neutrino Signals

11.2, 20, 27 M_{sun} progenitors (WHW 2002)

SASI produces modulations of neutrino emission and gravitational-wave signal.

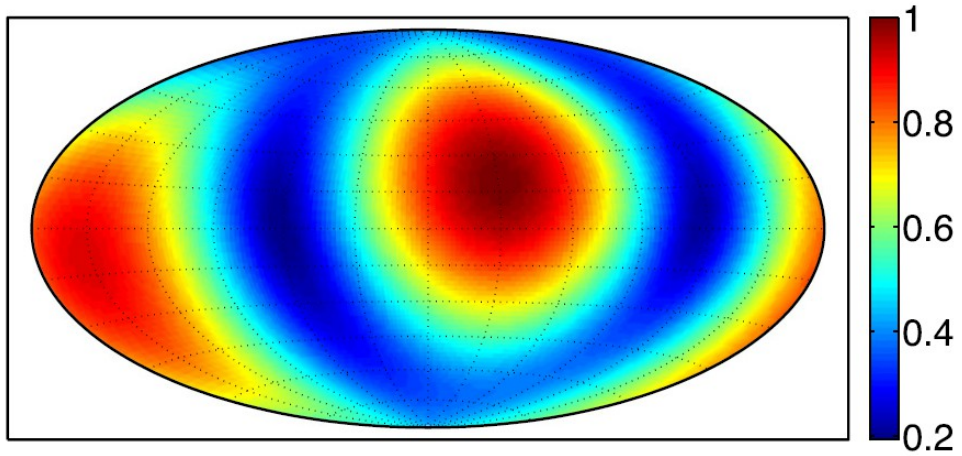

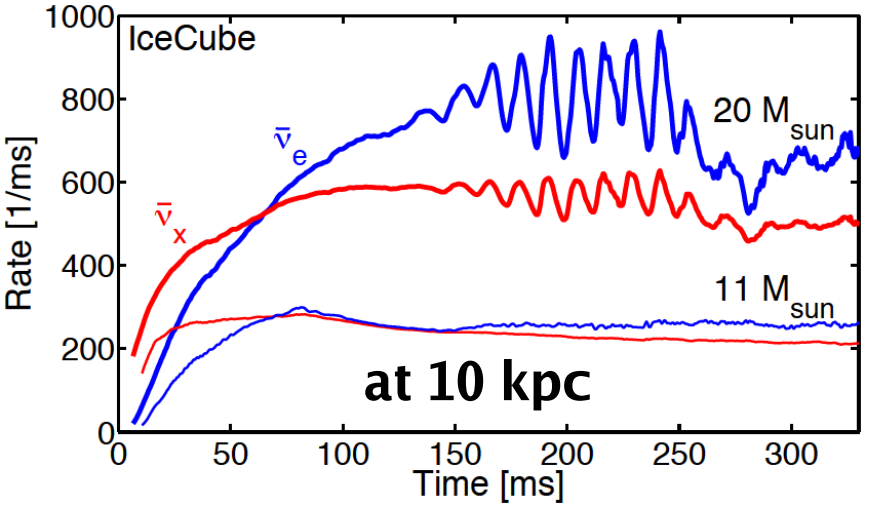

$$f_{\mathrm{SASI}}^{-1} \sim \int_{R_{\mathrm{NS}}}^{R_{\mathrm{S}}} \frac{dr}{|v|} + \int_{R_{\mathrm{NS}}}^{R_{\mathrm{S}}} \frac{dr}{c_{\mathrm{s}} - |v|}$$

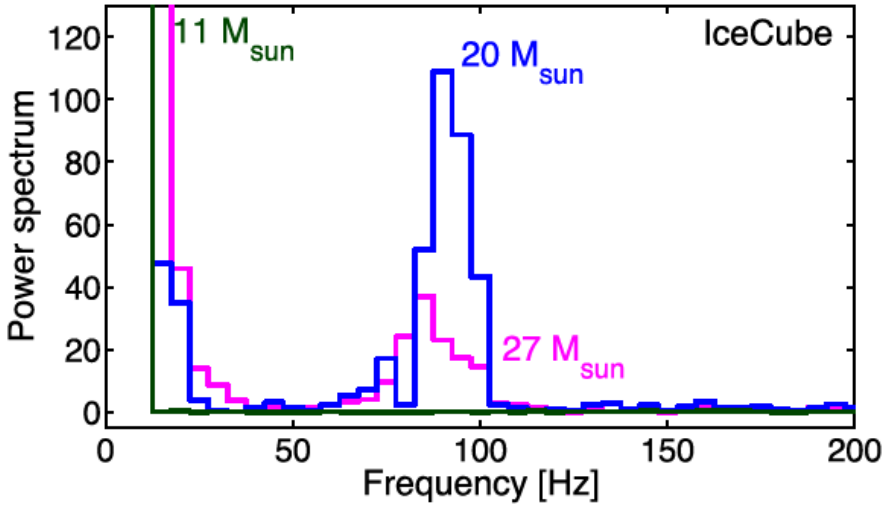

(Tamborra et al., PRL 111, 121104 (2013); arXiv:1307.7936)

Gravitational Waves for 2D SN Explosions

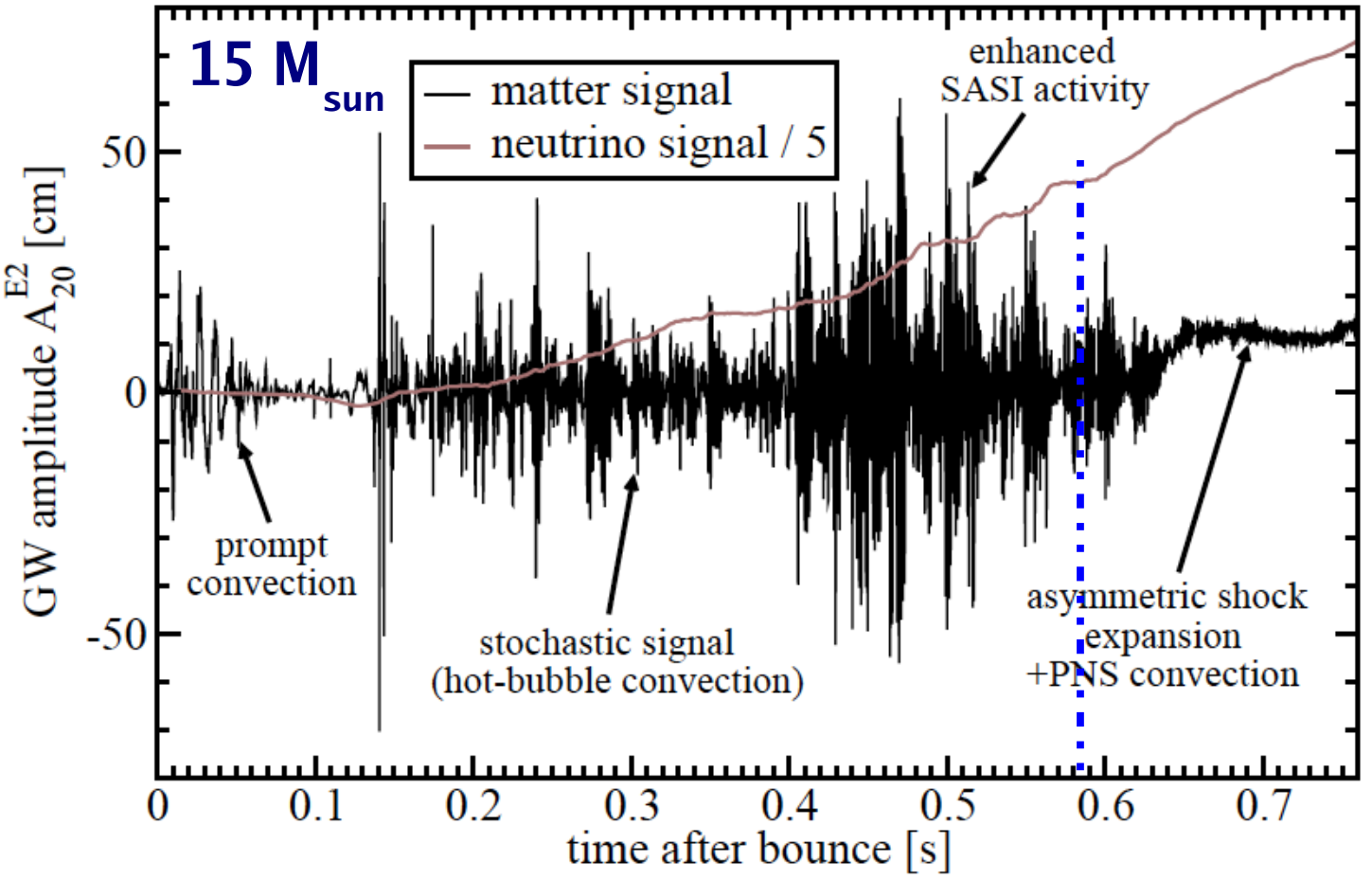

(Müller, THJ, & Marek, ApJ 766 (2013) 43)

$$h = \frac{1}{8}\sqrt{\frac{15}{\pi}}\sin^2\Theta\frac{A_{20}^{E2}}{R}$$

$$h_\nu = \frac{2G}{c^4 R}\int_0^t L_\nu(t')\alpha_\nu(t')\,dt'$$

$$\alpha_\nu = \frac{1}{L_\nu}\int \pi \sin\theta\,(2|\cos\theta| - 1)\frac{dL_\nu}{d\Omega}d\Omega$$

Gravitational Waves for 2D SN Explosions

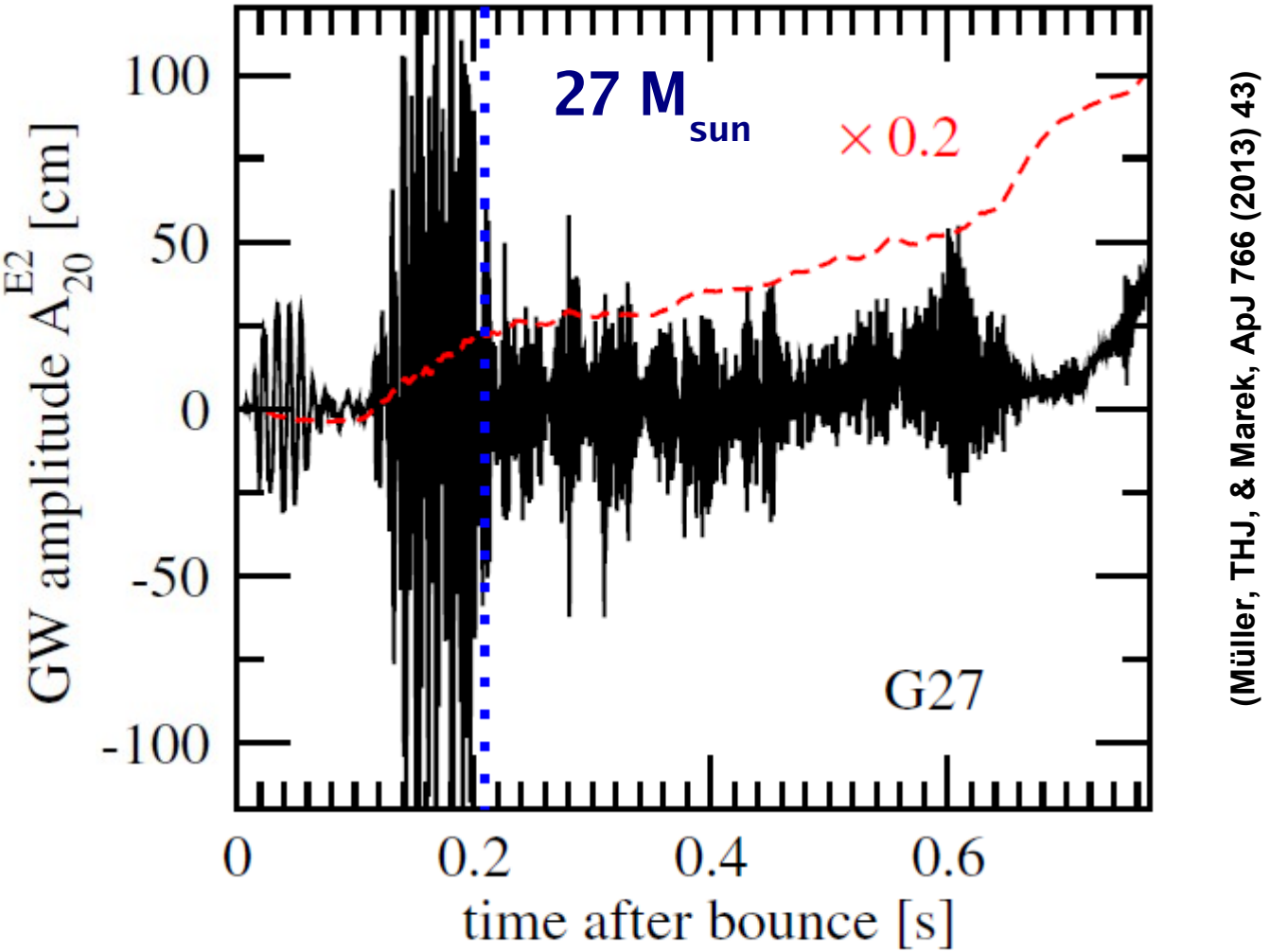

(Müller, THJ, & Marek, ApJ 766 (2013) 43)

GW amplitudes in 2D are considerably larger than in 3D.
No template character, in 3D strongly direction dependent.

3D Core-Collapse Models: Gravitational Waves

27 M_{sun} progenitor (WHW 2002)

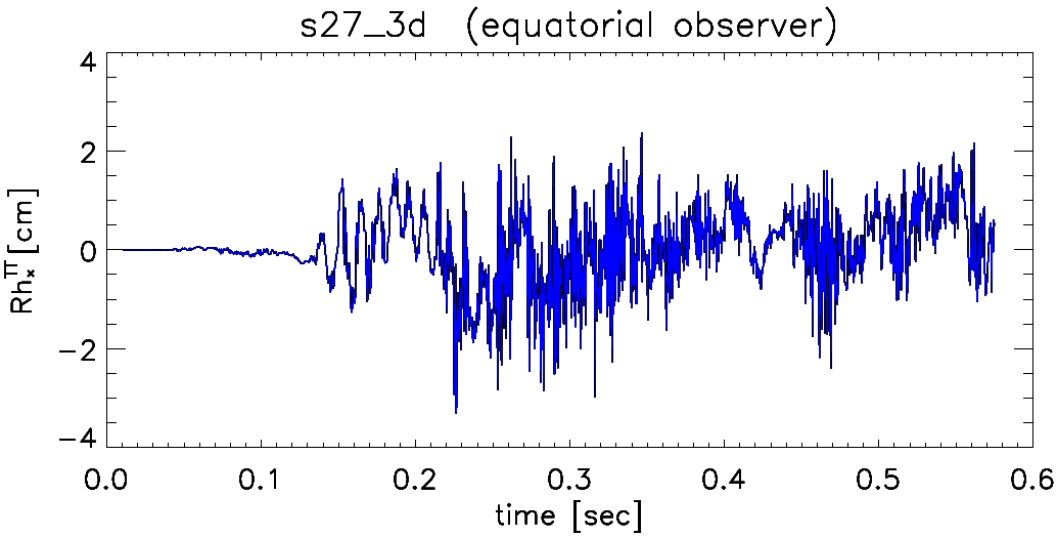

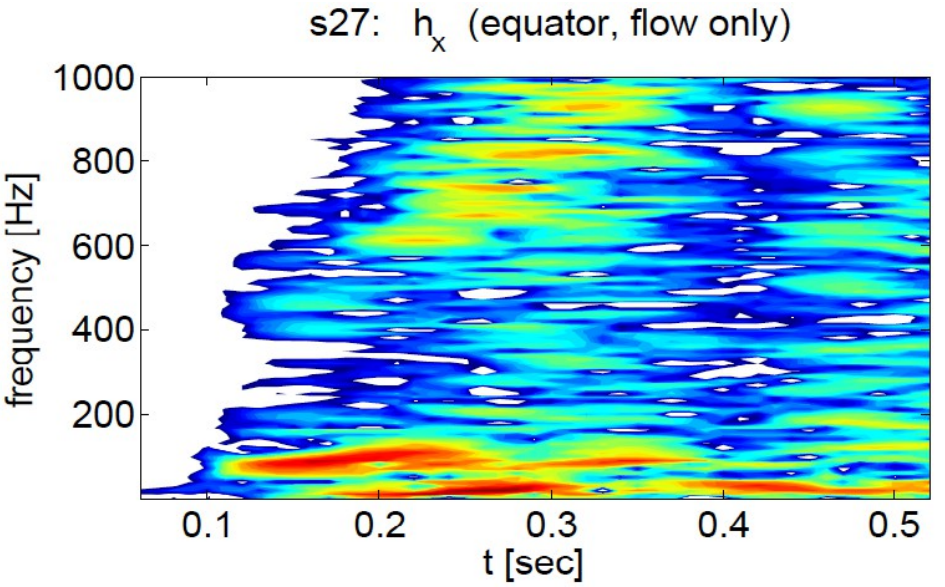

Preliminary analysis
by E. Müller of
model from
F. Hanke et al.,
ApJ 770 (2013) 66

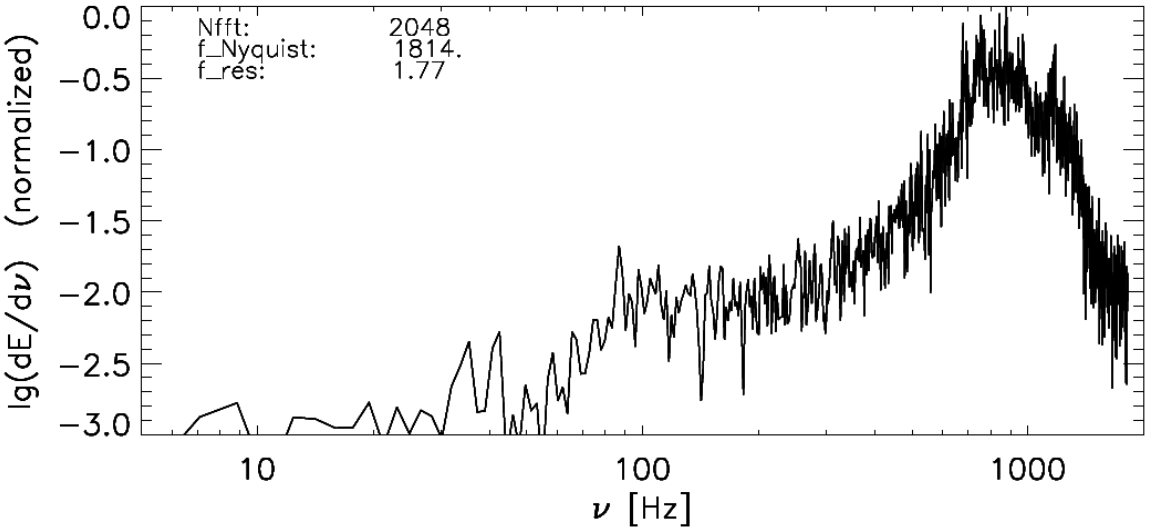

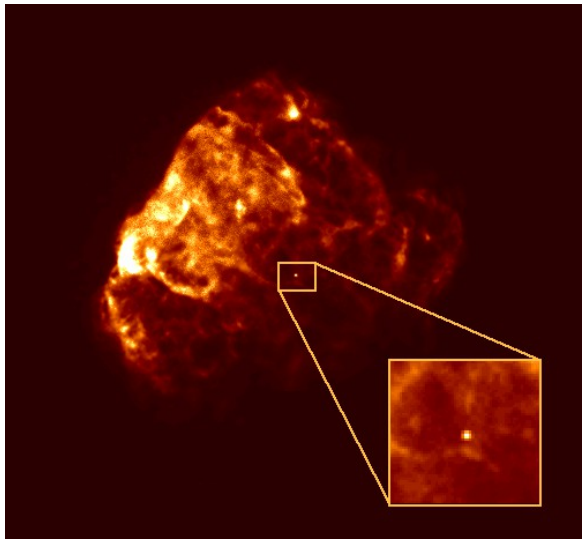

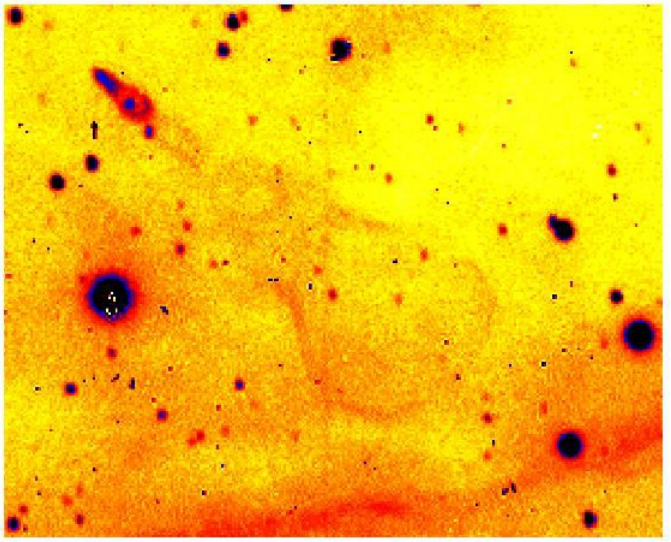

Neutron Star Kicks in 3D SN Explosions

Parametric neutrino-driven explosion simulations:

Neutrino core luminosity of proto-NS chosen;
Accretion luminosity calculated with simple (grey) transport scheme

Neutron Star Recoil in 3D Explosion Models

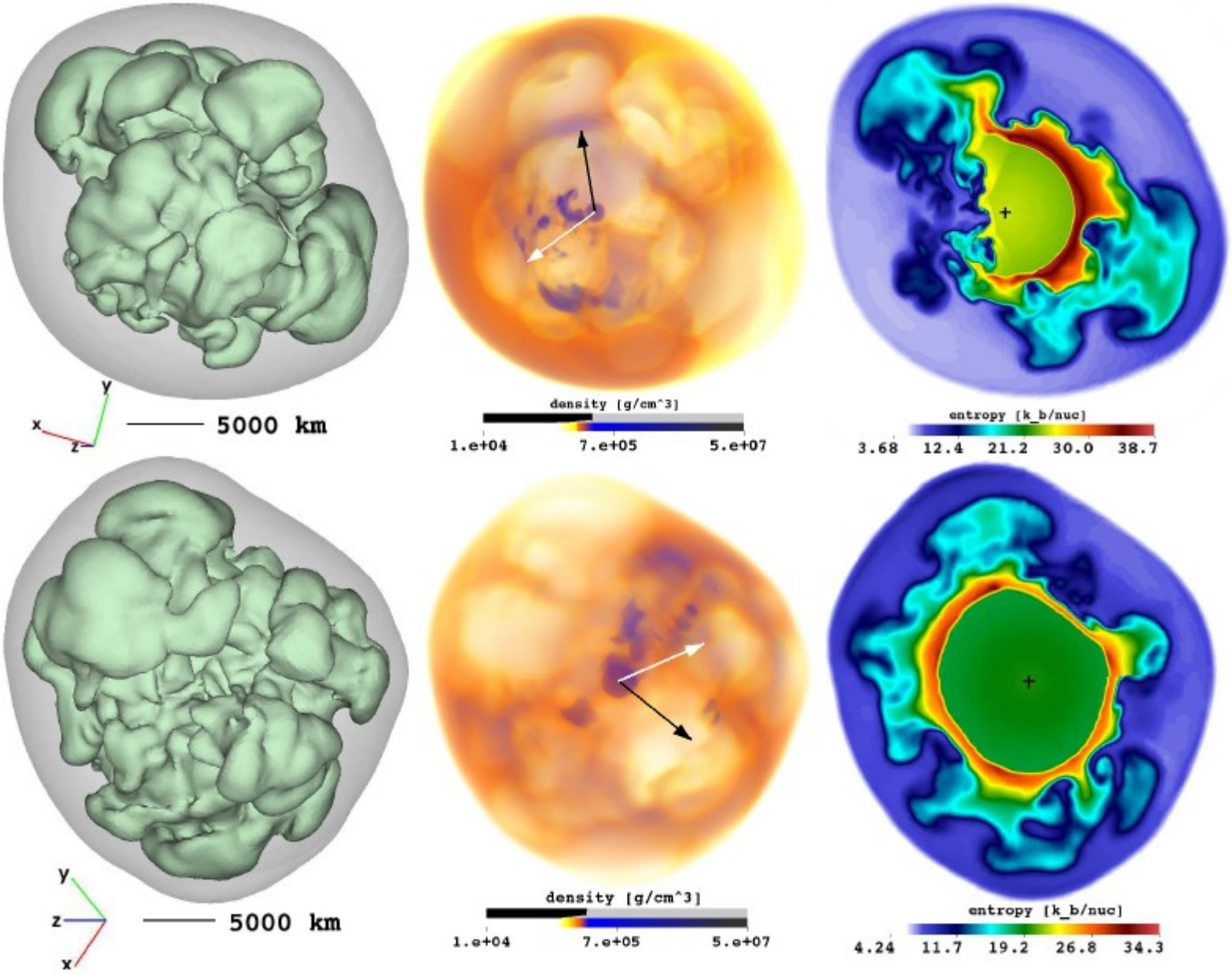

Wongwathanarat, Janka, Müller, ApJL 725 (2010) 106; A&A 552 (2013) A126

Neutron Star Recoil by "Gravitational Tug-Boat" Mechanism

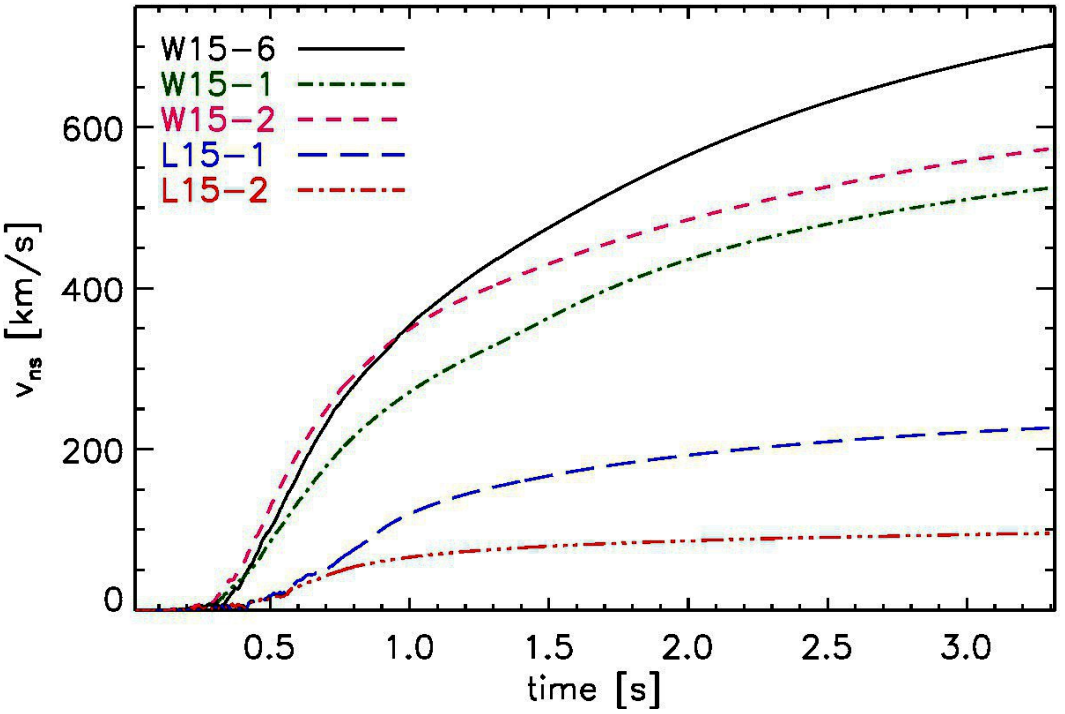

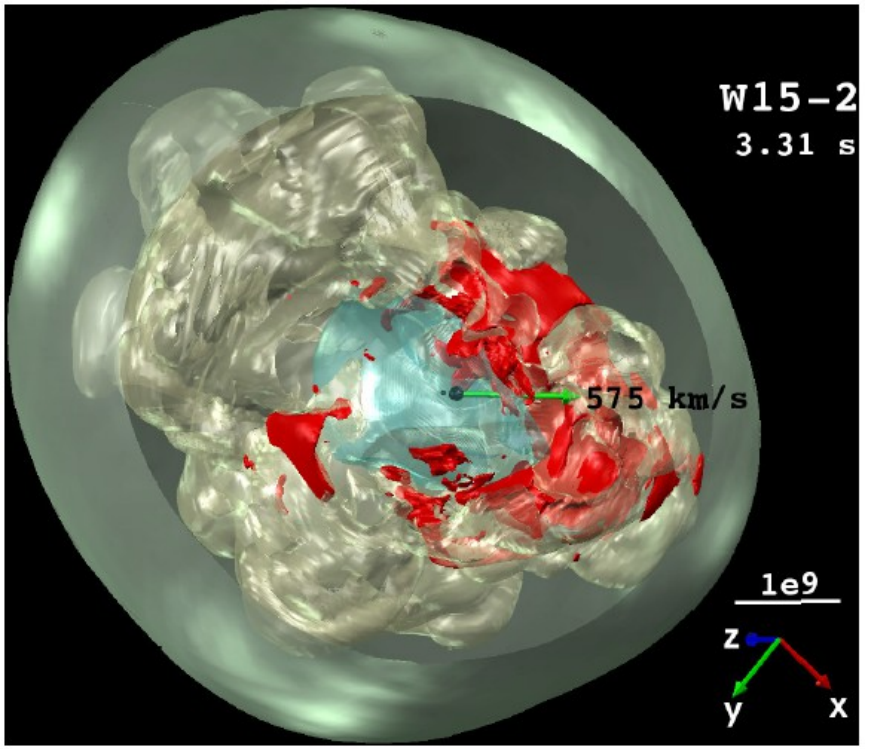

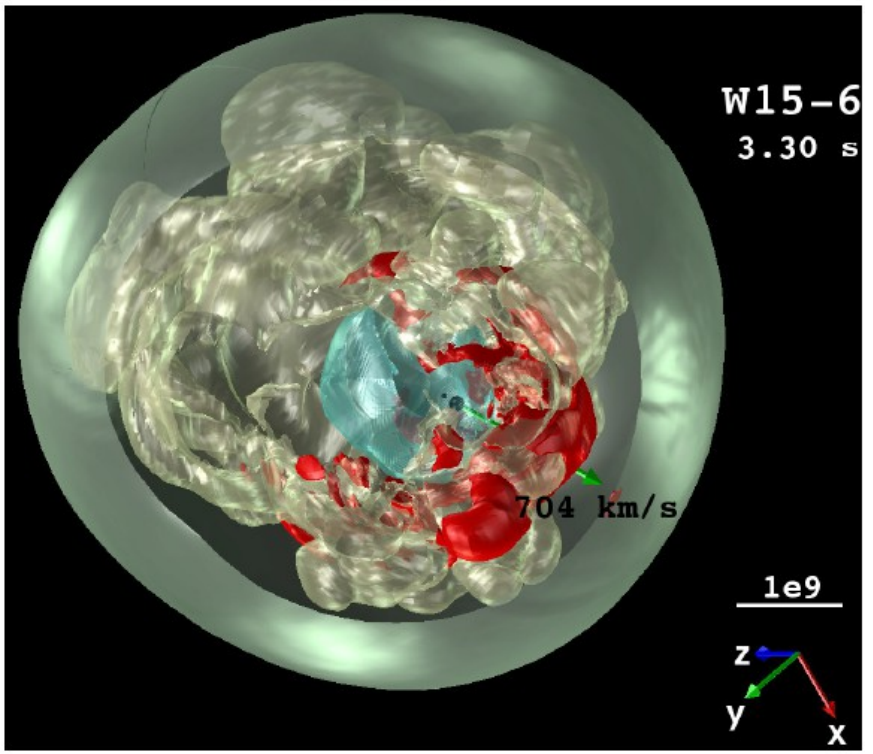

Wongwathanarat, Janka, Müller, ApJL 725 (2010) 106;
A&A 552 (2013) A126

Neutron Star Recoil by "Gravitational Tug-Boat" Mechanism

@ t = 1.4 s @ t = 3.3 s

Model	M_{ns} [$M_\odot$]	t_{exp} [ms]	E_{exp} [B]	v_{ns} [km/s]	a_{ns} [km/s^2]	$v_{ns,\nu}$ [km/s]	$\alpha_{k\nu}$ [°]	v_{ns}^{long} [km/s]	a_{ns}^{long} [km/s^2]	$J_{ns,46}$ [10^{46} g cm^2/s]	α_{sk} [°]	T_{spin} [ms]
W15-1	1.37	246	1.12	331	167	2	151	524	44	1.51	117	652
W15-2	1.37	248	1.13	405	133	1	12	575	49	1.56	58	632
W15-3	1.36	250	1.11	267	102	1	16	-	-	1.13	105	864
W15-4	1.38	272	0.94	262	111	4	16	-	-	1.27	43	785
W15-5-lr	1.41	289	0.83	373	165	2	12	-	-	1.63	28	625
W15-6	1.39	272	0.90	437	222	2	136	704	71	0.97	127	1028
W15-7	1.37	258	1.07	215	85	1	81	-	-	0.45	48	2189
W15-8	1.41	289	0.72	336	168	3	160	-	-	4.33	104	235
L15-1	1.58	422	1.13	161	69	5	135	227	16	1.89	148	604
L15-2	1.51	382	1.74	78	14	1	150	[illegible]	[illegible]	1.04	62	1041
L15-3	1.62	478	0.84	31	27	1	51	-	-	1.55	123	750
L15-4-lr	1.64	502	0.75	199	123	4	120	-	-	1.39	93	846
L15-5	1.66	516	0.62	267	209	3	147	542	106	1.72	65	695
N20-1-lr	1.40	311	1.93	157	42	7	118	-	-	5.30	122	190
N20-2	1.28	276	3.12	101	12	4	159	-	-	7.26	43	127
N20-3	1.38	299	1.98	125	15	5	138	[illegible]	[illegible]	4.42	54	225
N20-4	1.45	334	1.35	98	18	1	98	125	9	2.04	45	512
B15-1	1.24	164	1.25	92	16	1	97	102	1	1.03	155	866
B15-2	1.24	162	1.25	143	37	1	140	-	-	0.12	162	7753
B15-3	1.26	175	1.04	85	19	1	24	99	3	0.44	148	2050

Wongwathanarat, Janka, Müller, A&A 552 (2013) A126

Neutron Star Recoil by "Gravitational Tug-Boat" Mechanism

NS kick statistics of a set of more than 70 neutrino-driven explosion simulations in 2D:

(Scheck et al., PRL 92 (2004) 011103; A&A 457 (2006) 963)

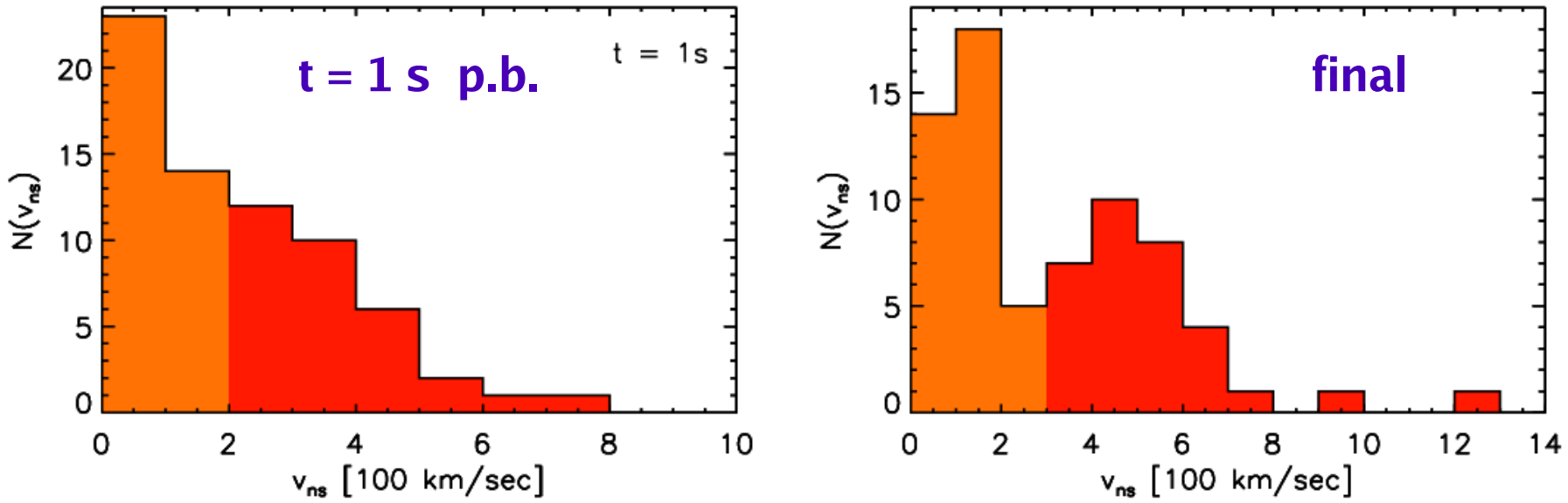

Fig. 20. Histograms of the neutron star velocity distribution for the 70 models of Tables A.1−A.5. The left panel shows the velocity distribution at $t = 1$ s (solid black line). The darker shaded area corresponds to the fraction of models whose neutron stars are moving with more than 200 km s^{-1} one second after bounce. The same models are displayed with dark shading also in the right panel, which shows the final velocity distribution as obtained by extrapolation with Eq. (8).

Neutron Star Kicks of Galactic NS-LMXBs

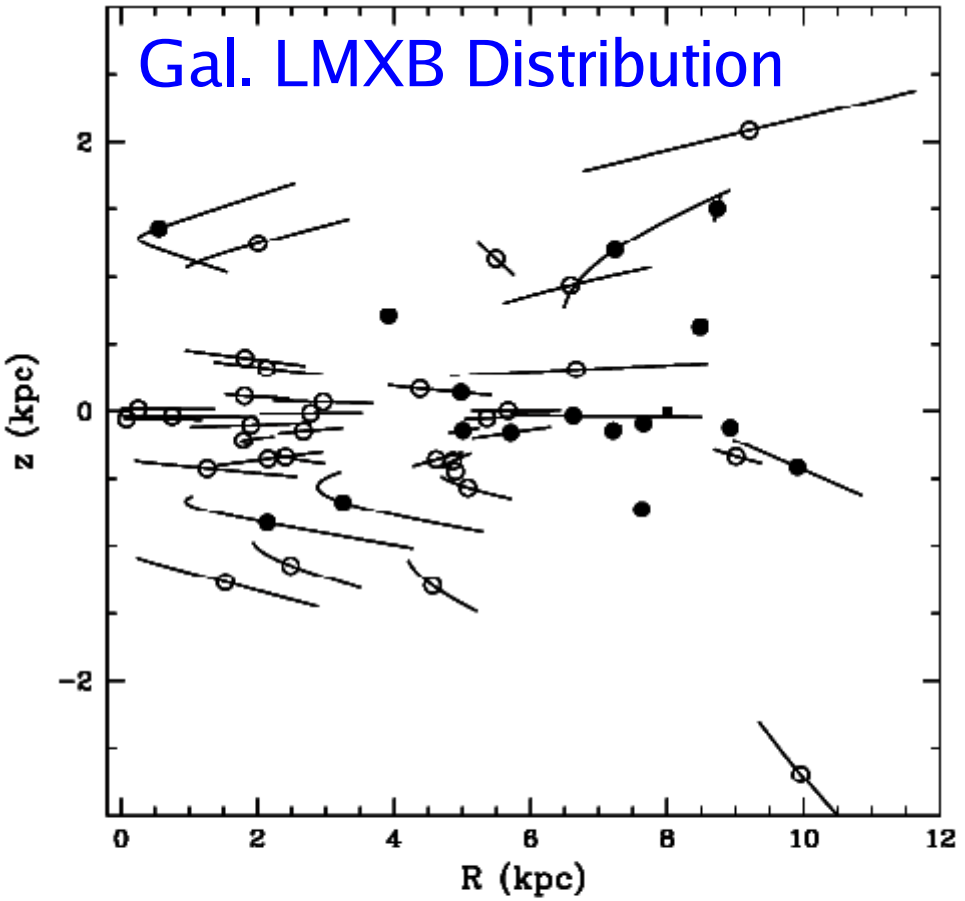

Figure 1. Galactic distribution of NS-LMXBs (open circles) and BH-LMXBs (filled circles). The radial distance from the Galactic Centre is $R = \sqrt{x^2 + y^2}$, where x and y are the Cartesian coordinates in the Galactic plane, whereas the distance from the plane of the Galaxy is $z = d \sin b$. Two NS binaries fall off the figure: XTE J2123−058 and Cyg X−2. The solid lines account for the uncertainty of the distance from the Sun for each binary. The Sun is indicated as a square.

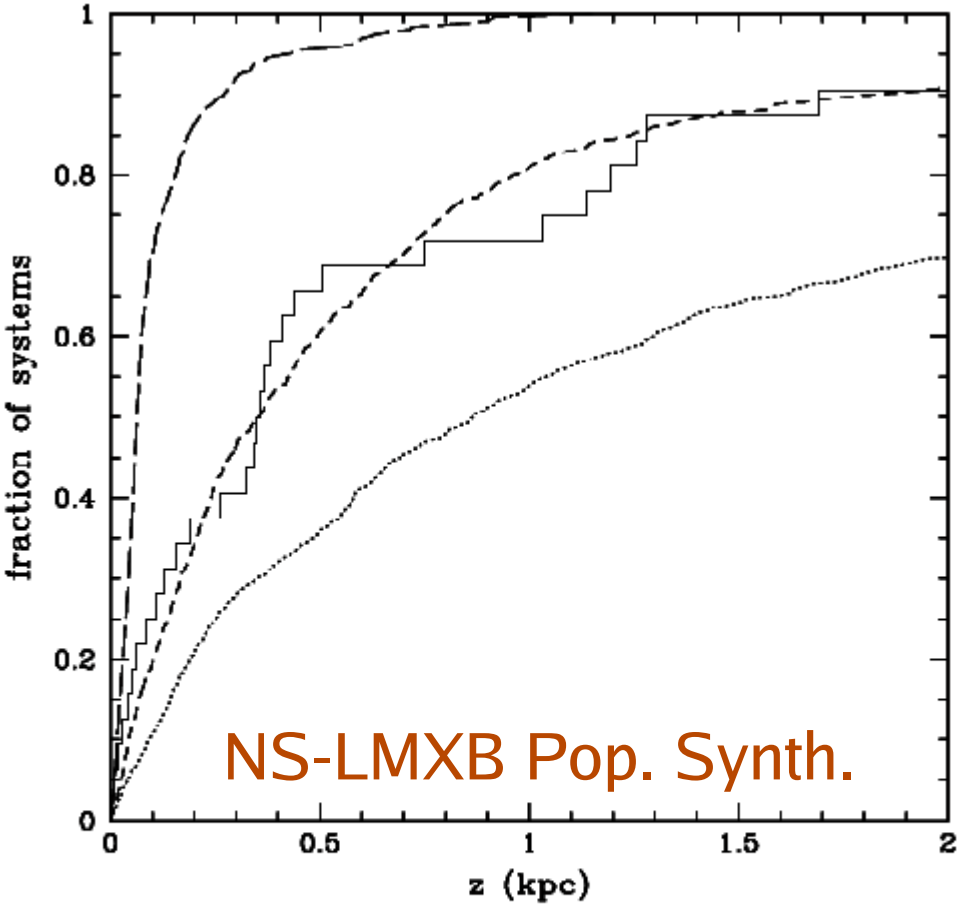

Figure 8. Cumulatives which show the fraction of NS-LMXBs versus the distance from the Galactic plane, for the four different NKs (dotted line is for a Hansen & Phinney NK, short-dashed line is for an Arzoumanian NK, whereas a zero NK scenario corresponds to the long-dashed line). Cumulatives are to be compared with the observed one (solid line).

Repetto, Davies, & Sigurdsson, MNRAS 425 (2012) 2799

Neutron Star Recoil and Nickel Production

Nickel production is enhanced in direction of stronger explosion, i.e. opposite to NS kick

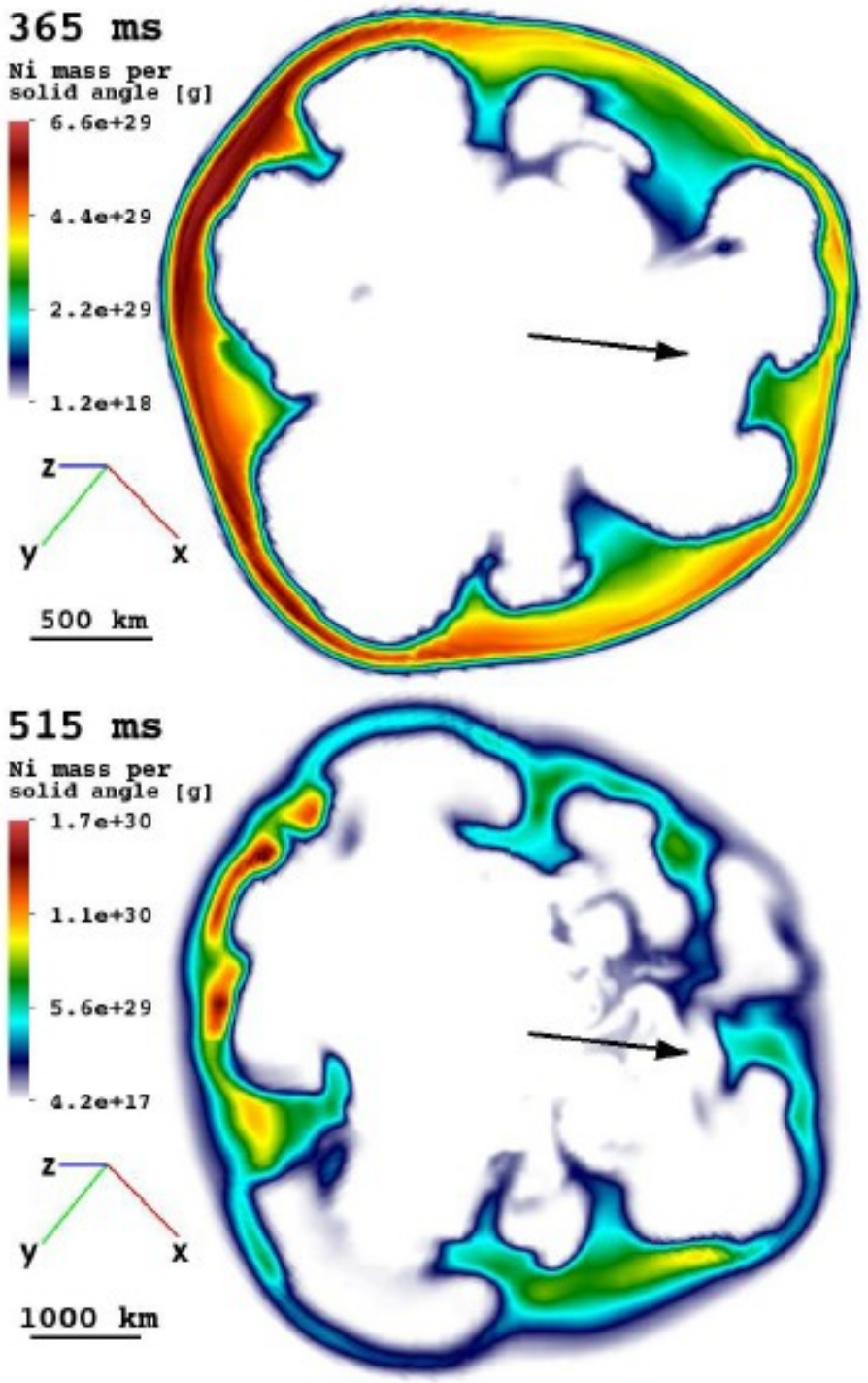

Wongwathanarat, Janka, Müller, A&A 552 (2013) A126

Neutron Star Recoil and Nickel Production

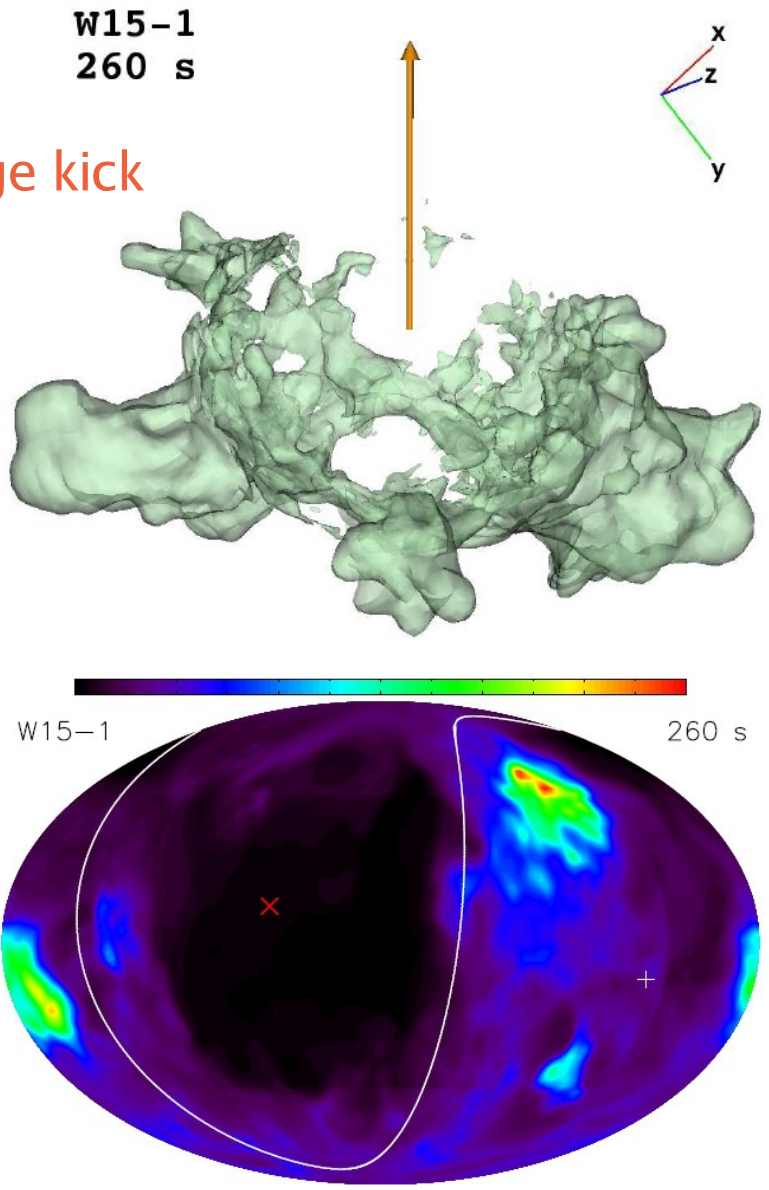

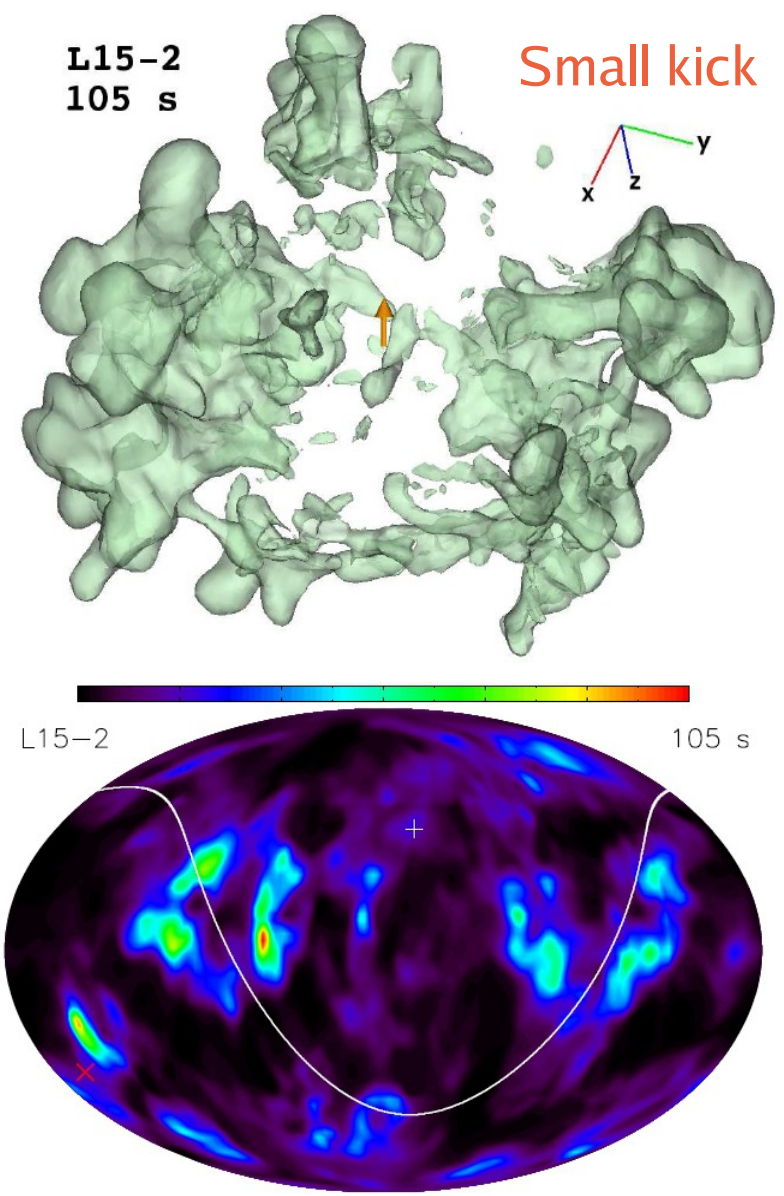

Wongwathanarat, Janka, Müller, A&A 552 (2013) A126

Enhanced concentration of iron in supernova remnants opposite to direction of large pulsar kick can be observable consequence of hydrodynamical kick mechanism.

Black Hole Kicks of Galactic BH-LMXBs

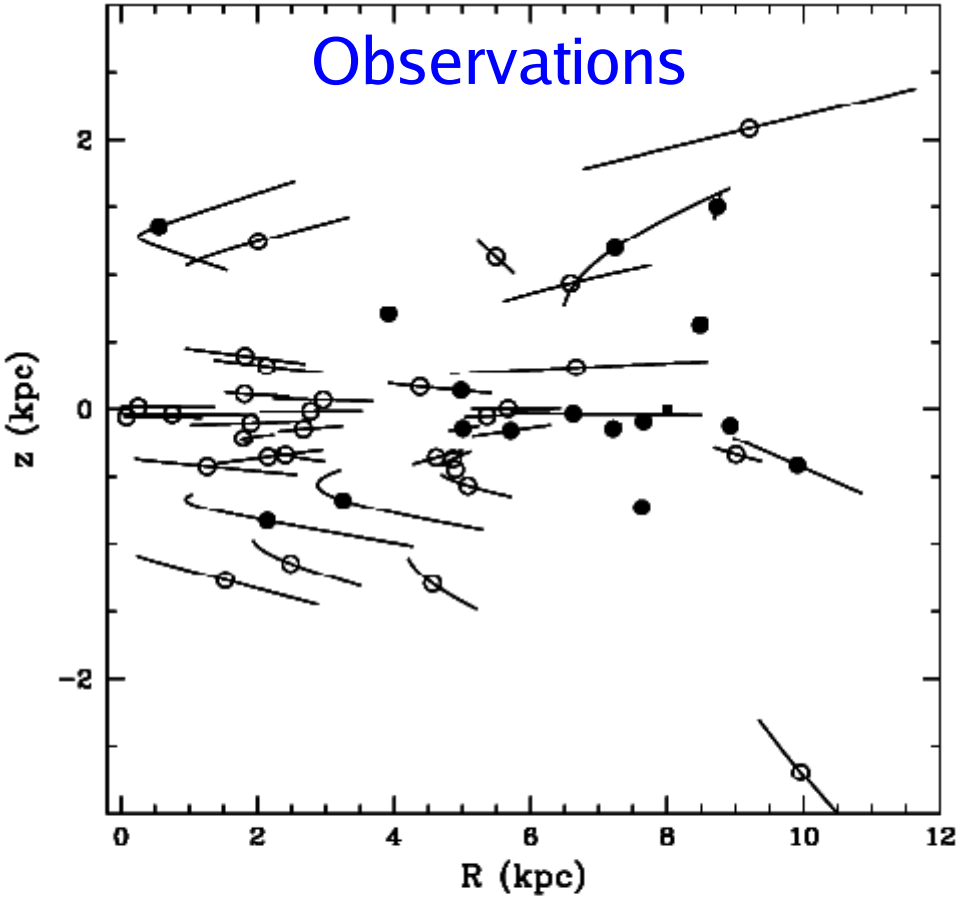

Figure 1. Galactic distribution of NS-LMXBs (open circles) and BH-LMXBs (filled circles). The radial distance from the Galactic Centre is $R = \sqrt{x^2 + y^2}$, where x and y are the Cartesian coordinates in the Galactic plane, whereas the distance from the plane of the Galaxy is $z = d \sin b$. Two NS binaries fall off the figure: XTE J2123−058 and Cyg X−2. The solid lines account for the uncertainty of the distance from the Sun for each binary. The Sun is indicated as a square.

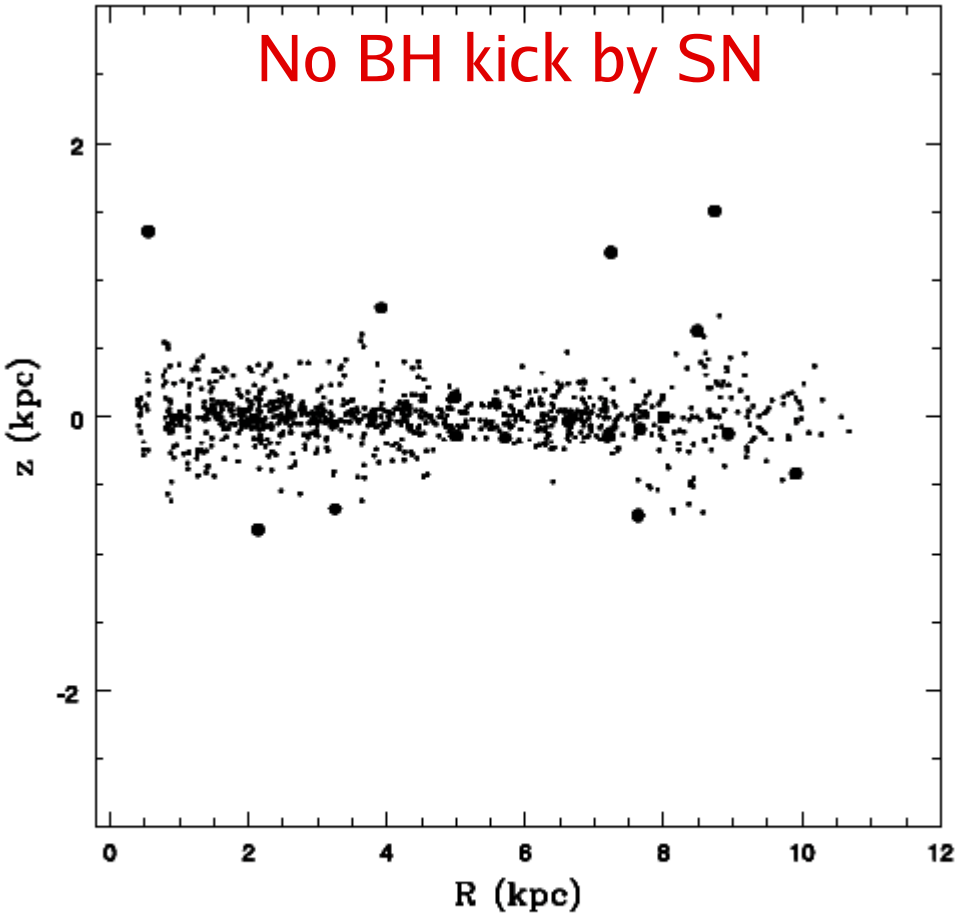

Figure 5. BPS for a sample of BH-LMXBs. No NK has been imparted to the BH. The smaller dots correspond to the synthetic population, the bigger ones to the observed binaries and the position of the Sun is denoted with a square.

Repetto, Davies, & Sigurdsson, MNRAS 425 (2012) 2799

Black Hole Kicks of Galactic BH-LMXBs

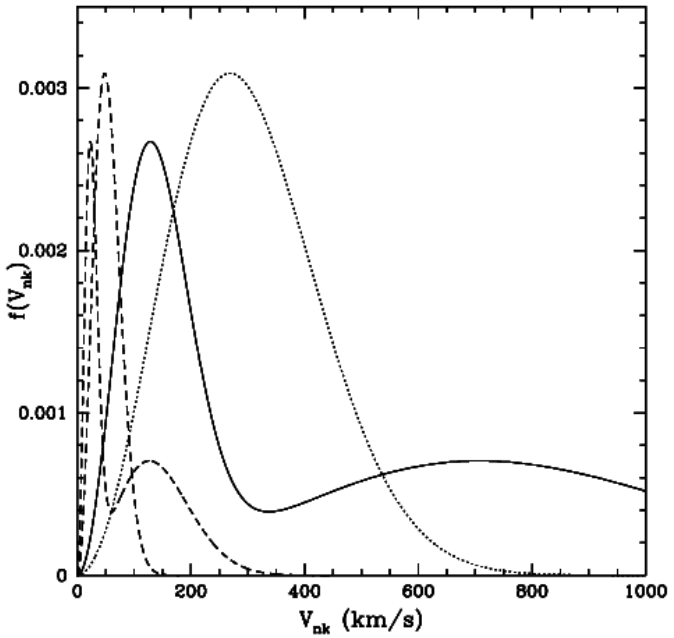

Figure 3. NK distributions used in our BPS calculations. The solid line corresponds to Arzoumanian distribution, the dotted line to Hansen & Phinney and the two dashed lines correspond to these two distributions but with kick speeds reduced, assuming that the momentum imparted to the BH is the same as the momentum imparted to the NS.

Repetto, Davies, & Sigurdsson,
MNRAS 425 (2012) 2799

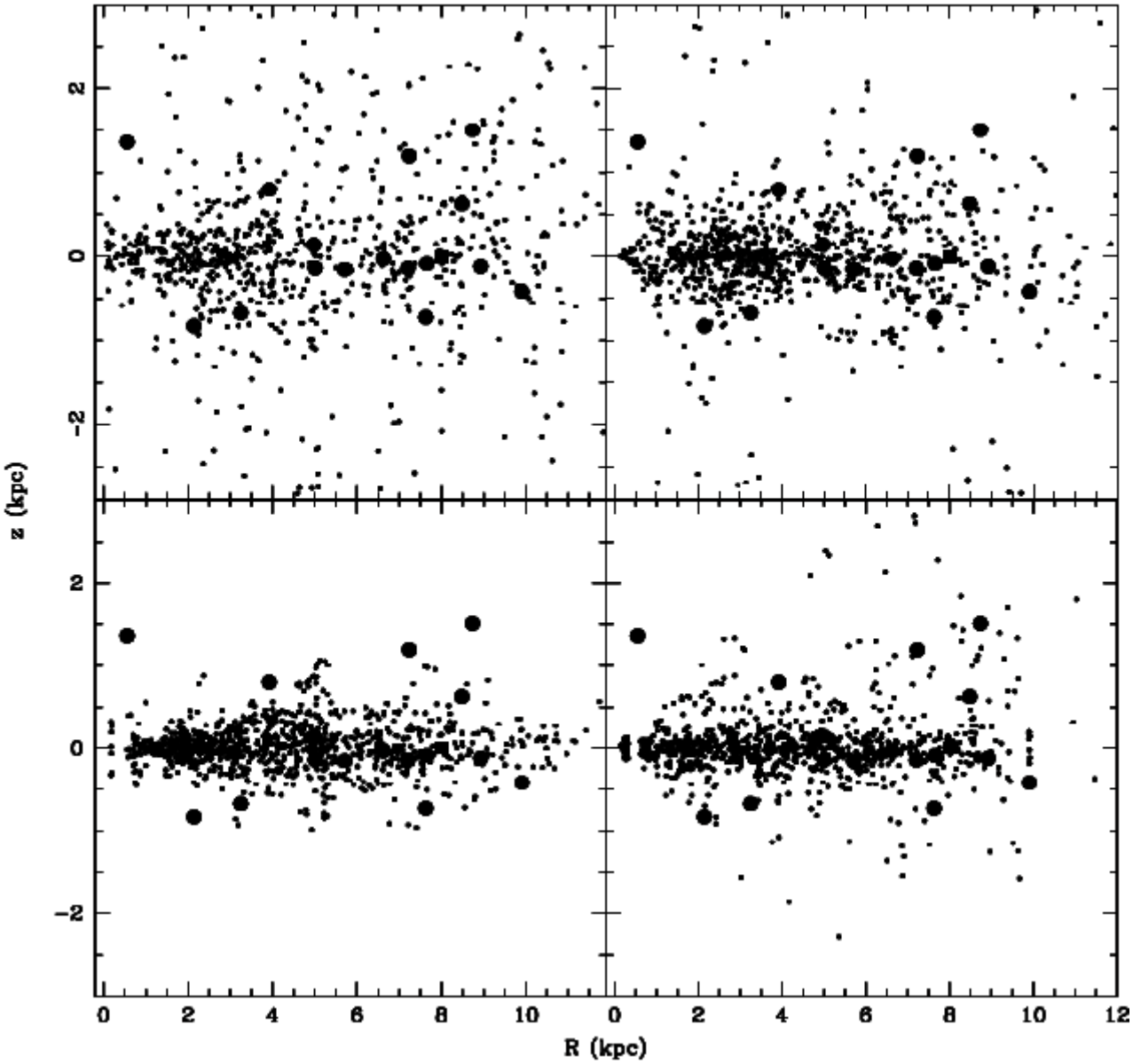

Figure 6. BPS for a sample of BH-LMXBs. NKs have been drawn from the Hansen & Phinney (top-left) distribution, a bimodal distribution (top-right), whereas the bottom figures correspond to the reduced NKs. The smaller dots correspond to the synthetic population, the bigger ones to the observed binaries and the position of the Sun is denoted with a square.

Black Hole Recoil by Hydrodynamical "Gravitational Tug-Boat" Mechanism

This mechanism can also explain the observed black hole kick velocities of Galactic BH-binaries by BH formation in fallback SNe.
BH kick velocities are NOT reduced by ratio of NS/BH mass!

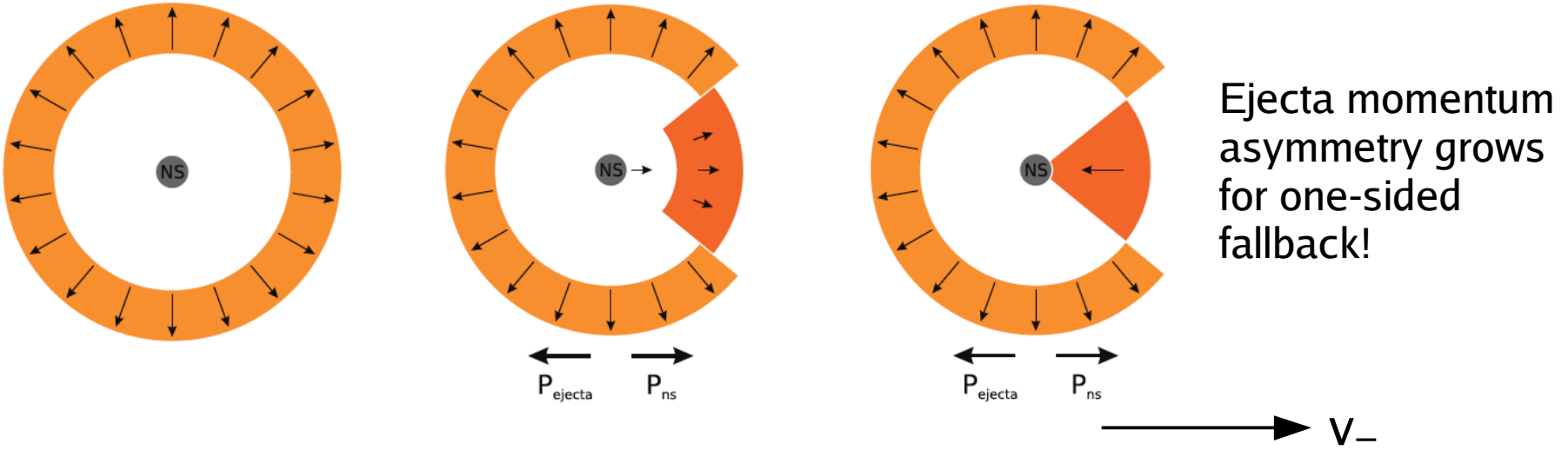

Ejecta momentum asymmetry grows for one-sided fallback!

$$M_{\rm BH} = M_{\rm NS} + M_{\rm fb}$$

THJ, MNRAS 434 (2013) 1355

$$p'_{\rm ej} = p_{\rm BH} = m_+ v_+ - (m_- - M_{\rm fb})\, v_- = p_{\rm NS} + M_{\rm fb}\, v_-$$

$$v_{\rm BH} = \frac{M_{\rm NS}}{M_{\rm BH}}\, v_{\rm NS} + \frac{M_{\rm fb}}{M_{\rm BH}}\, v_- \approx \frac{M_{\rm NS}}{M_{\rm BH}}\, v_{\rm NS} + v_-$$

3D Explosions and Supernova Asymmetries

Mixing Instabilities in 3D SN Models

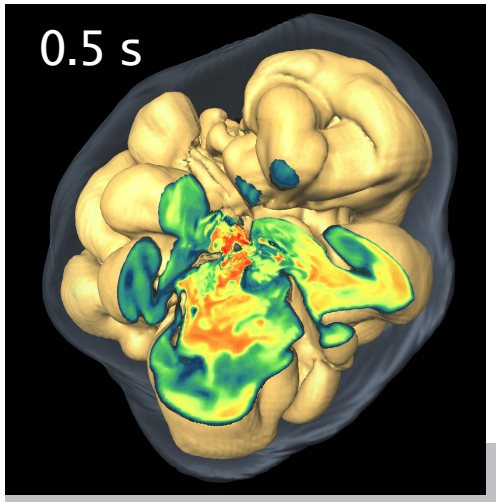

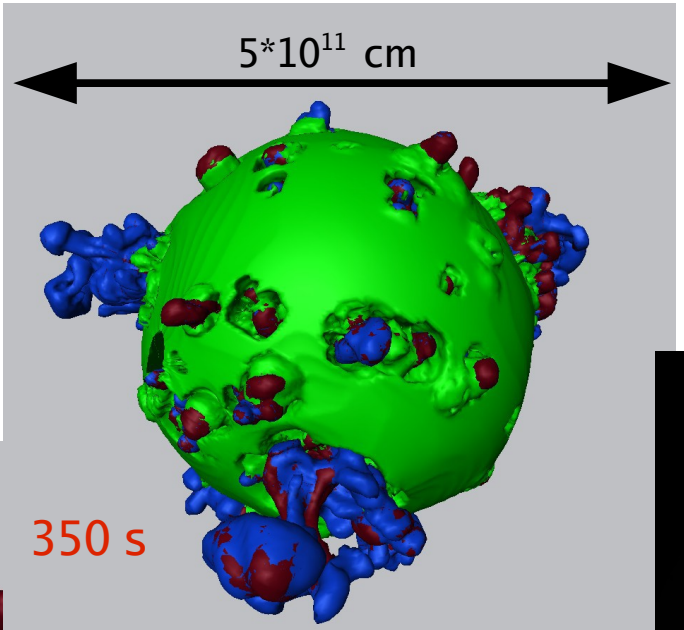

green: carbon
red: oxygen
blue: nickel

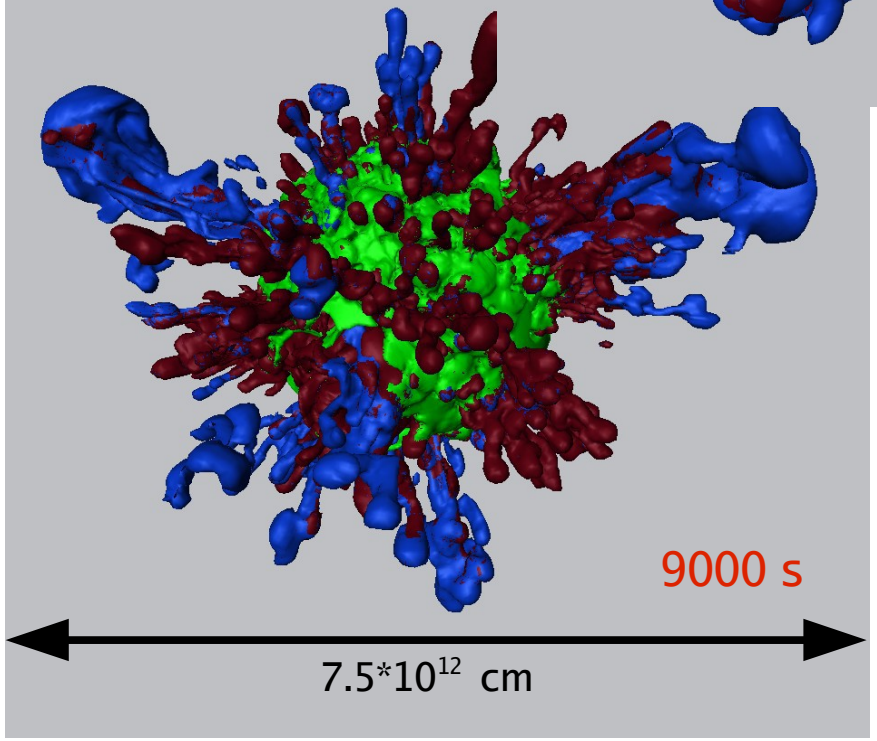

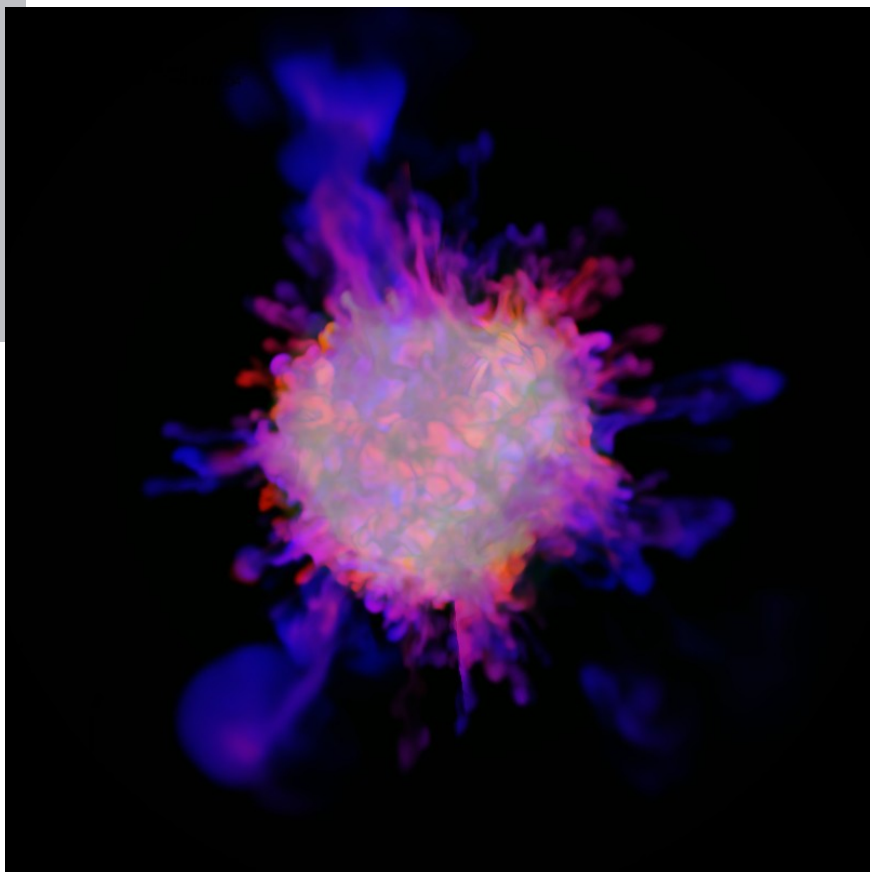

(Hammer, Janka, Müller, ApJ 2010)

Mixing Instabilities in 3D SN Models

Isosurfaces of constant mass fraction X(Ni) = 3%

B15: 15 M_{sun}

BSG

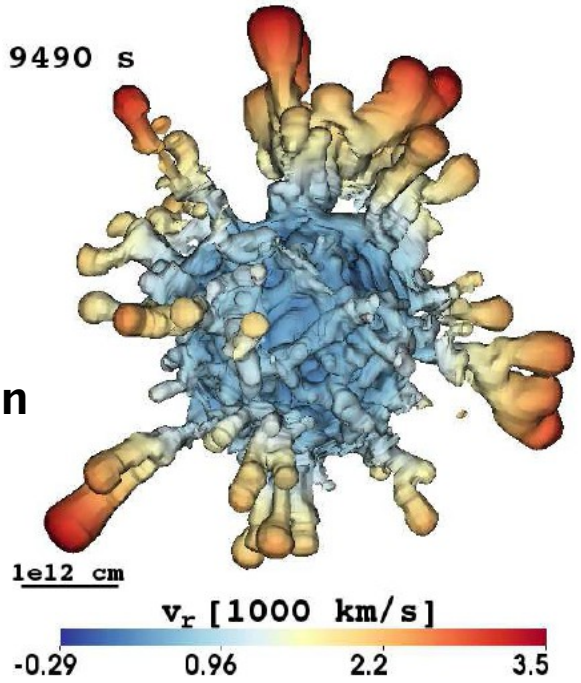

L15: 15 M_{sun}

RSG

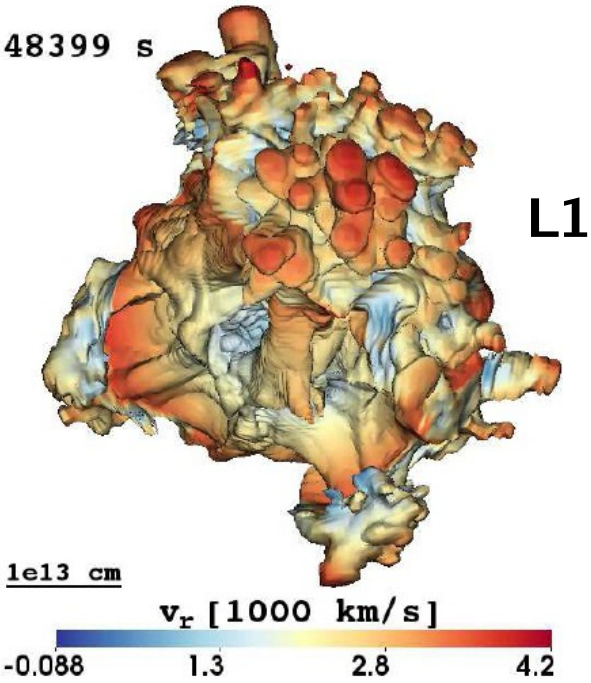

N20: 20 M_{sun}

BSG

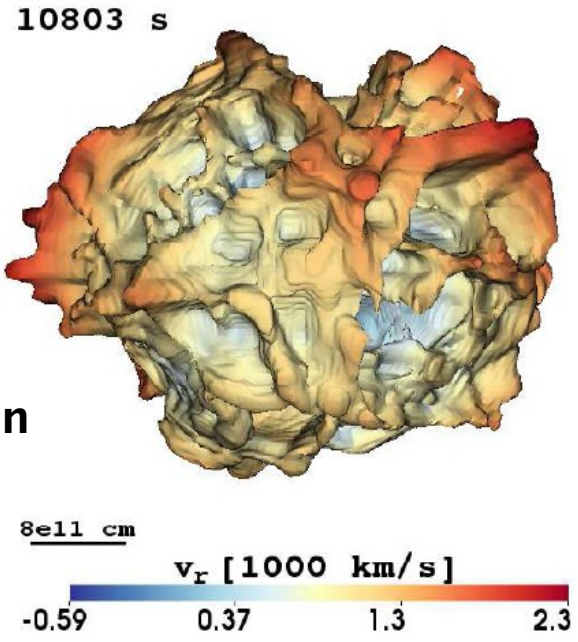

W15: 15 M_{sun}

RSG

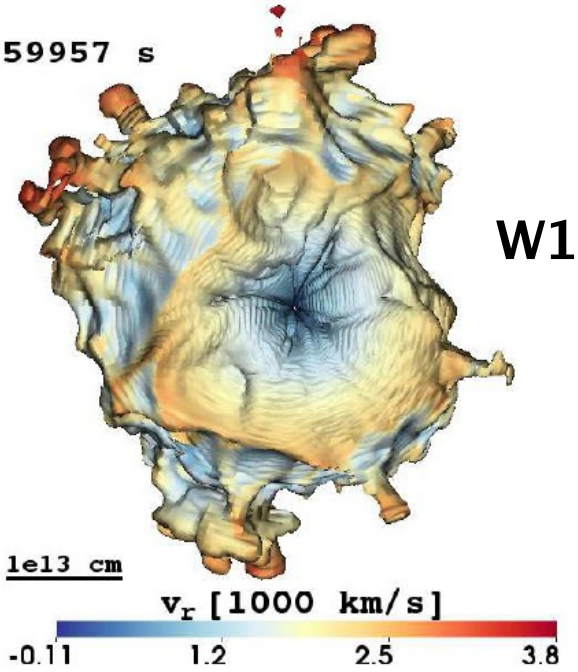

(Wongwathanarat, Müller, Janka, in preparation)

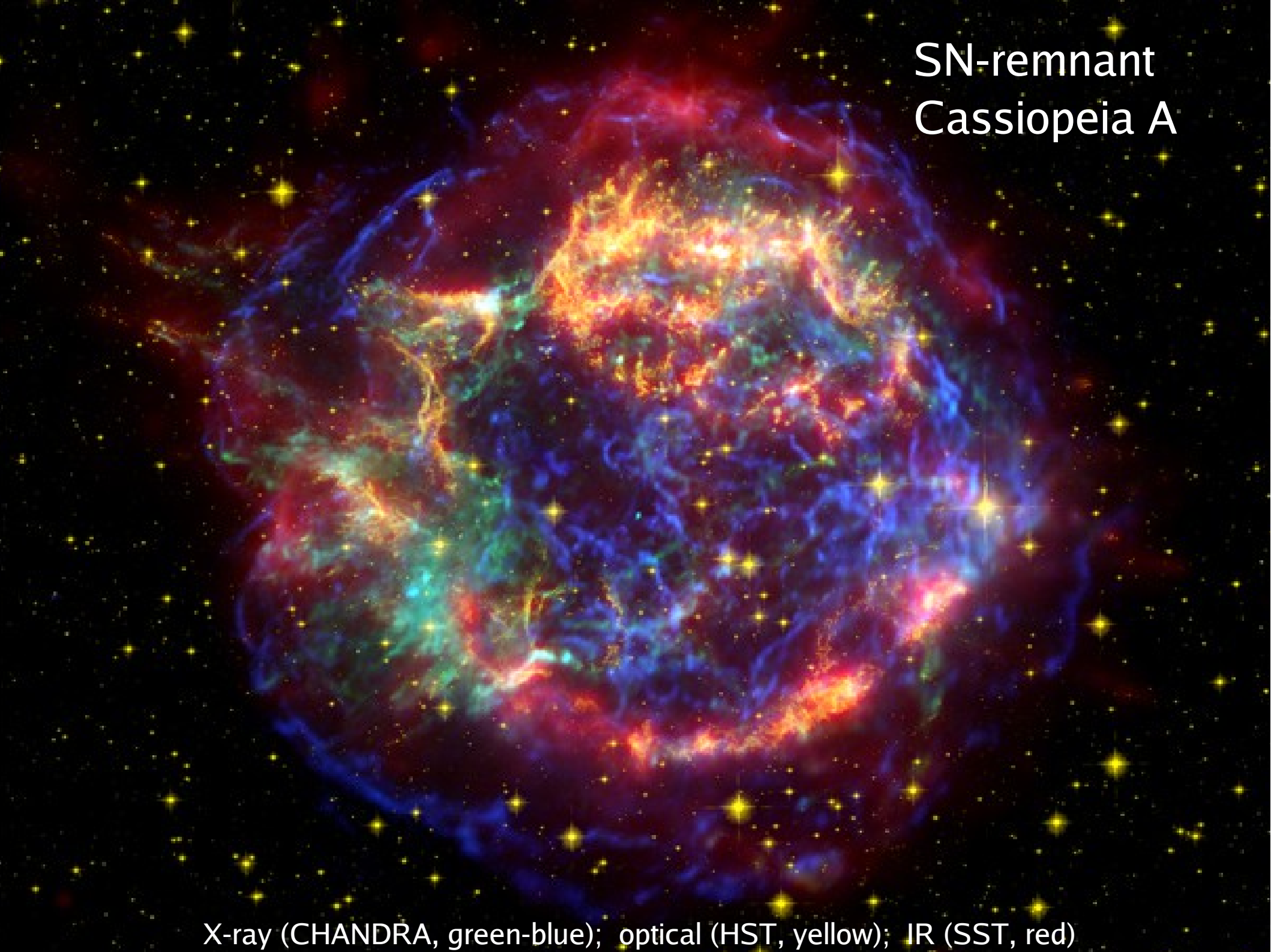
SN-remnant
Cassiopeia A
X-ray (CHANDRA, green-blue); optical (HST, yellow); IR (SST, red)

Mixing Instabilities in 3D SN Models

Progenitor: 15 solar masses RSG (Limongi et al. 2000)
$E_{exp} = 1.74 * 10^{51}$ erg

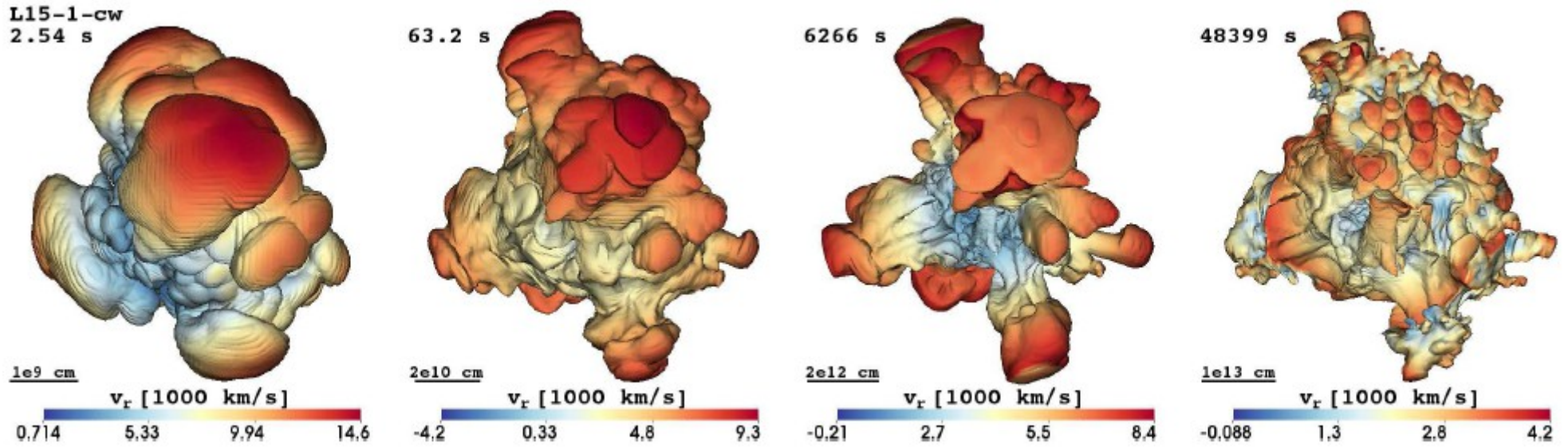

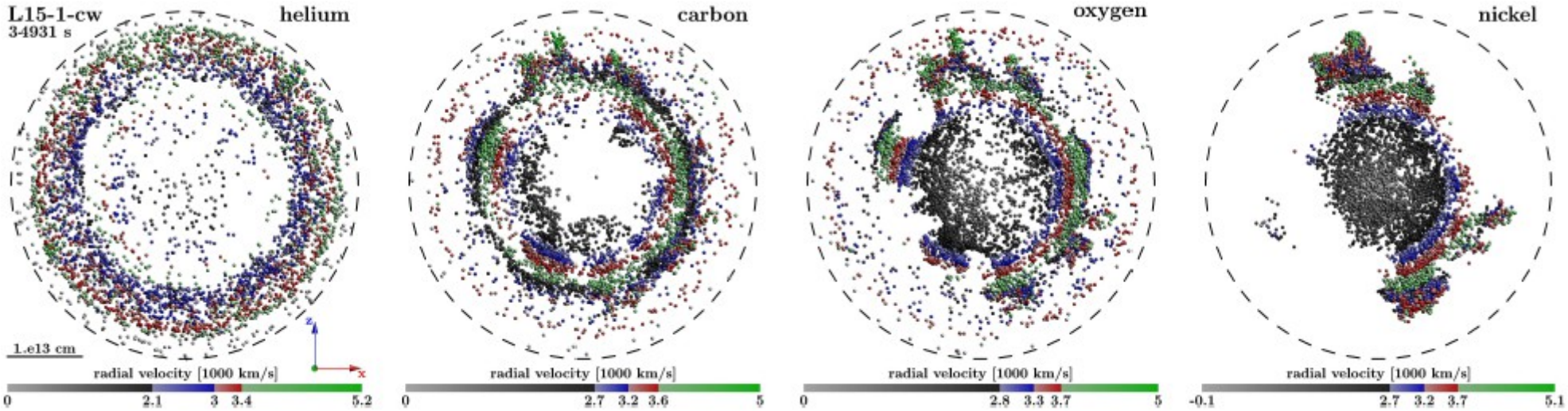

(Wongwathanarat, Müller, Janka, in preparation)

Supernova 1987A

Progenitor-Explosion and SN-Remnant Connections

Large Set of 1D SN Explosion Models

(Ugliano, THJ, Marek, & Arcones, ApJ 757, 69 (2012))

- Hydrodynamic simulations of neutrino-driven explosions in 1D:
  Neutron-star cooling after onset of explosion followed for 15–20 s,
  SN explosion followed continuously with fallback for days to weeks.

- Analytic neutron-star core-cooling model,
  including self-consistent treatment of accretion luminosity.

- Parameters of NS core-cooling calibrated for SN1987A:
  For ~20 M_{sun} progenitors yields explosion energy, nickel mass,
  and neutrino-energy loss and emission timescale as observed.

- Core-collapse simulations for 101 solar-metallicity progenitors
  (from Woosley, Heger, & Weaver, RMP 2002)

Cosmic CCSN and Star Formation Rates

Horiuchi et al., ApJ 738 (2011) 154

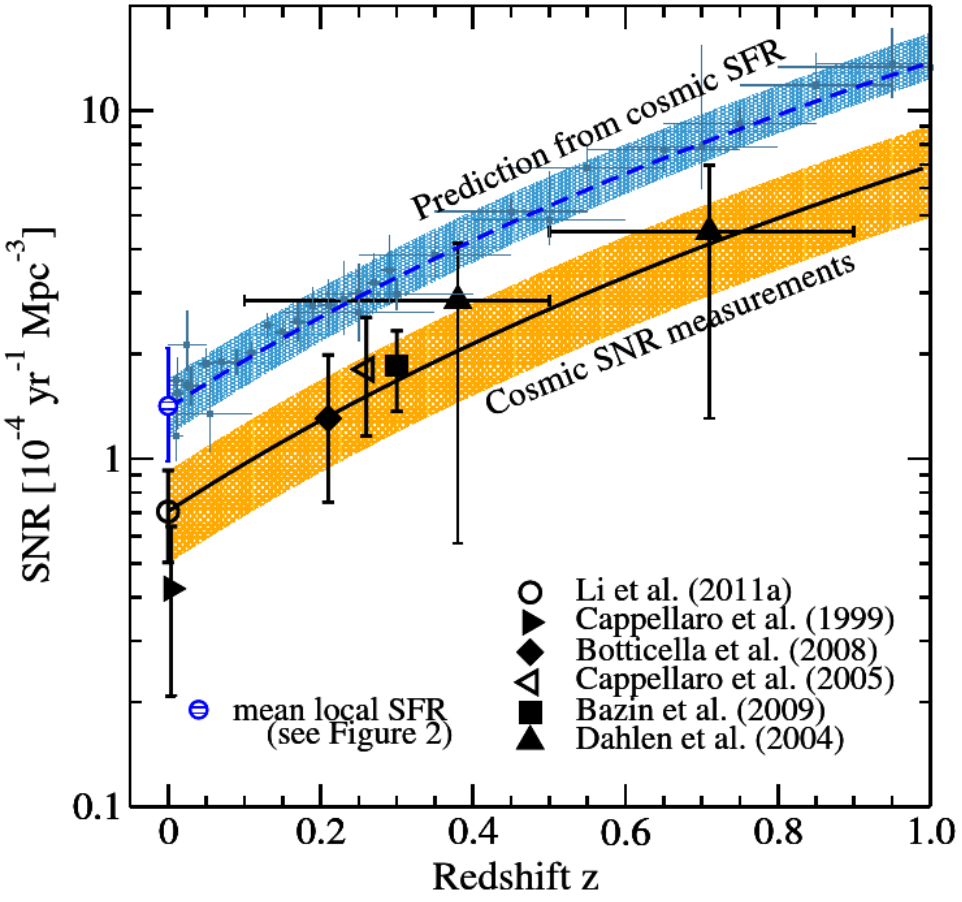

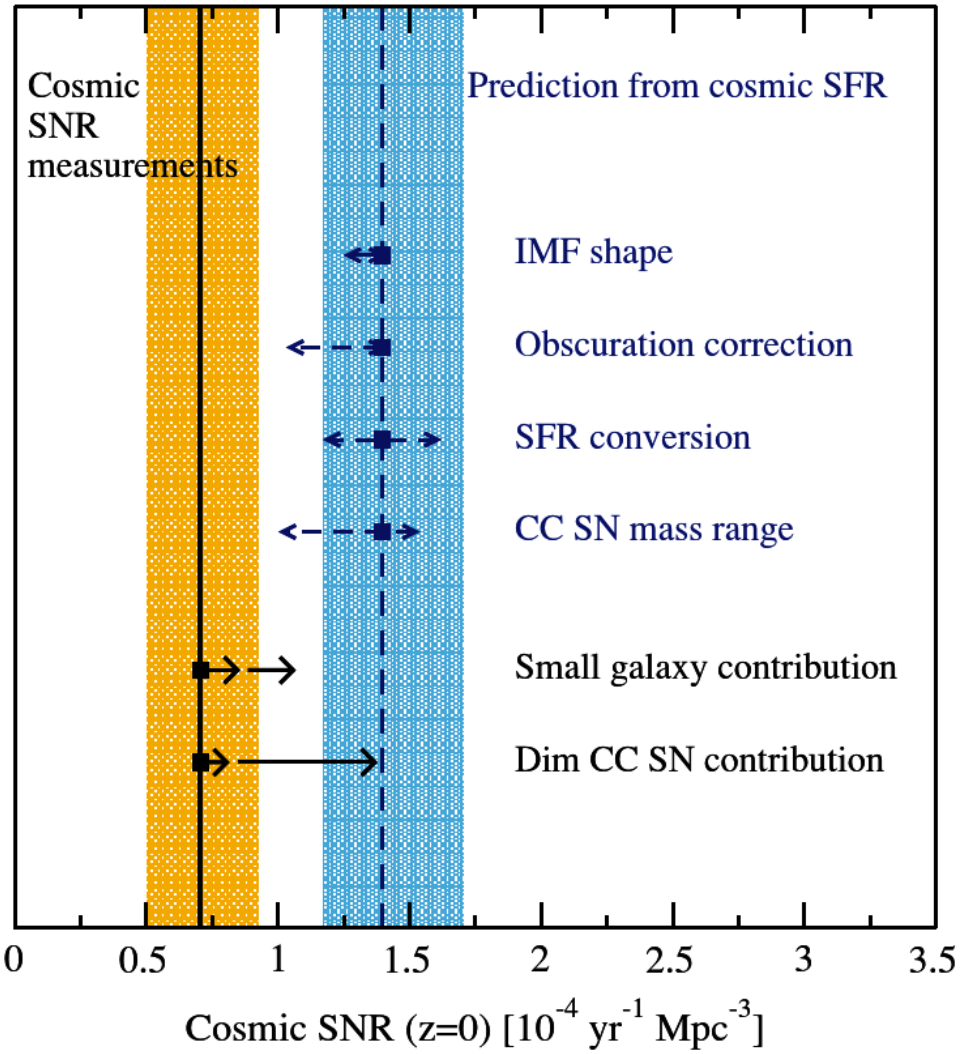

NS and BH Regimes

O'Connor & Ott, ApJ 730:70 (2011)

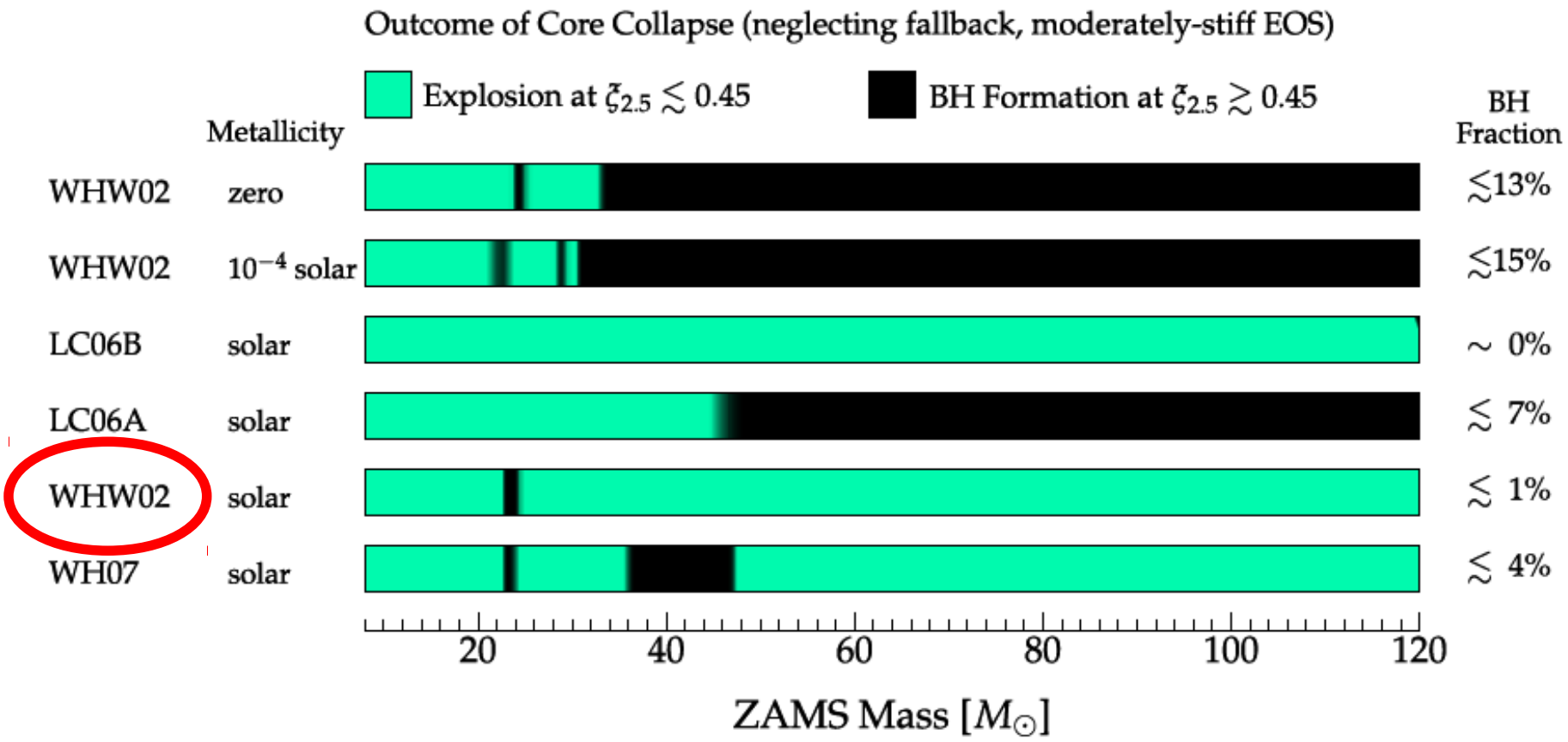

Employed assumption: Progenitors with compactness $\xi_{2.5} > 0.45$ collapse to BHs

Progenitor Variations

Progenitor models from Woosley, Heger, & Weaver (RMP 2002)

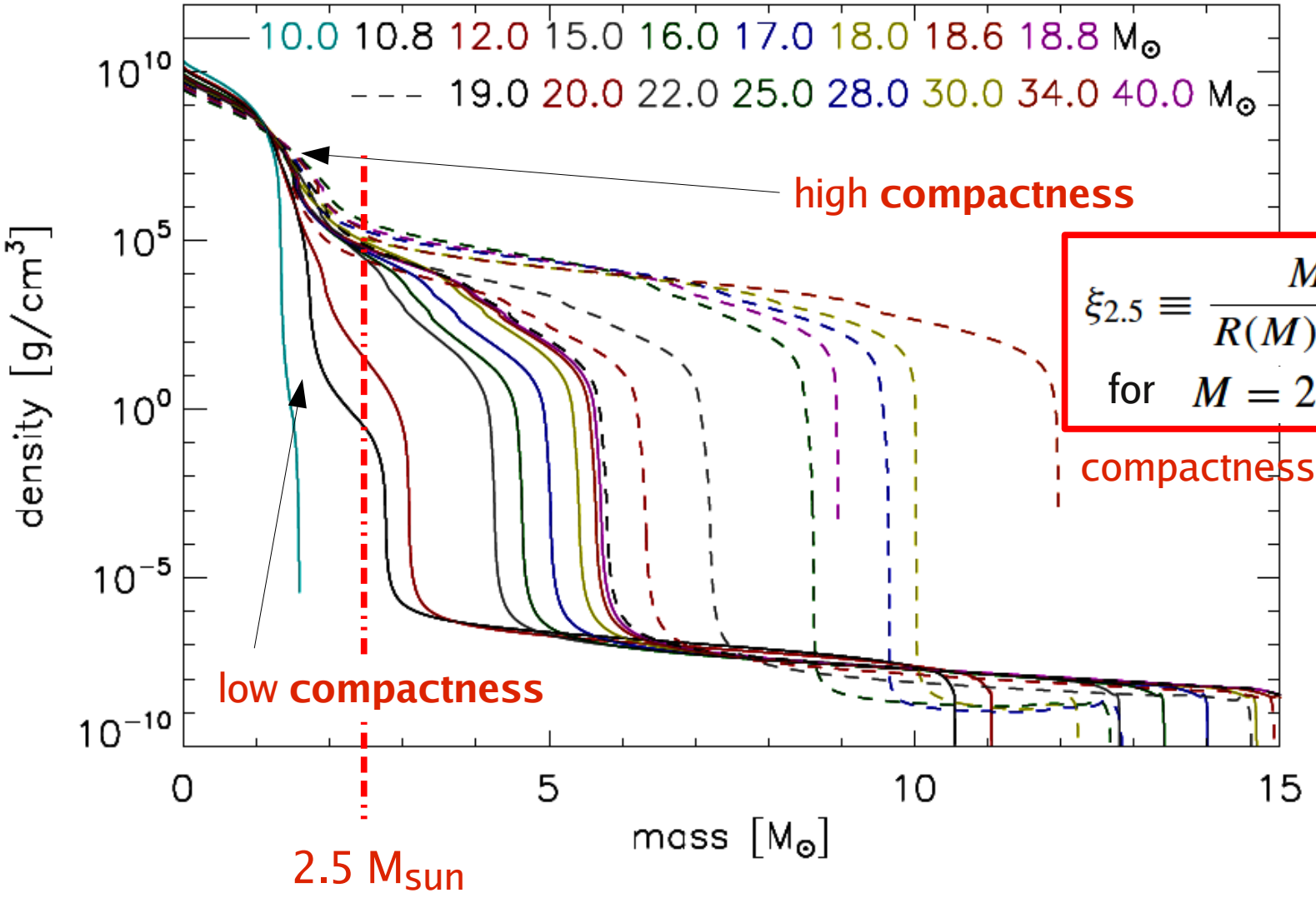

$$\xi_{2.5} \equiv \frac{M/M_\odot}{R(M)/1000\,\mathrm{km}} \quad \text{for} \quad M = 2.5\ M_\odot$$

compactness parameter

O'Connor & Ott, ApJ 730:70 (2011)

Progenitor Variations: Compactness

Core compactness can be nonmonotonic function of ZAMS mass

$$\xi_{2.5} \equiv \frac{M/M_\odot}{R(M)/1000\,\mathrm{km}}\,,$$

$$\text{mass } M = 2.5\ M_\odot$$

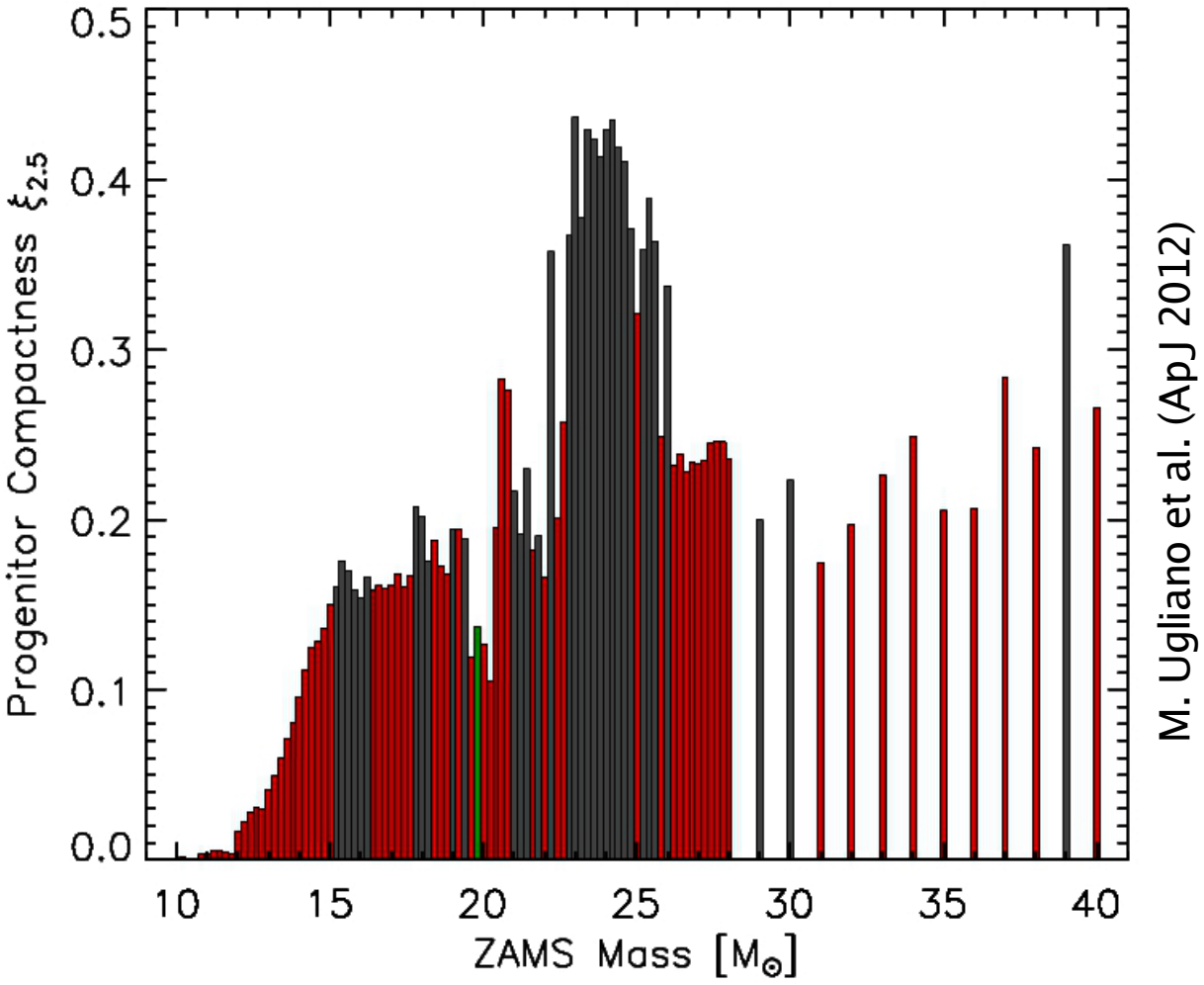

Progenitor models: Woosley et al. (RMP 2002)

Stellar Compactness and Explosion

Core compactness can be nonmonotonic function of ZAMS mass

Progenitor models: Woosley et al. (RMP 2002)

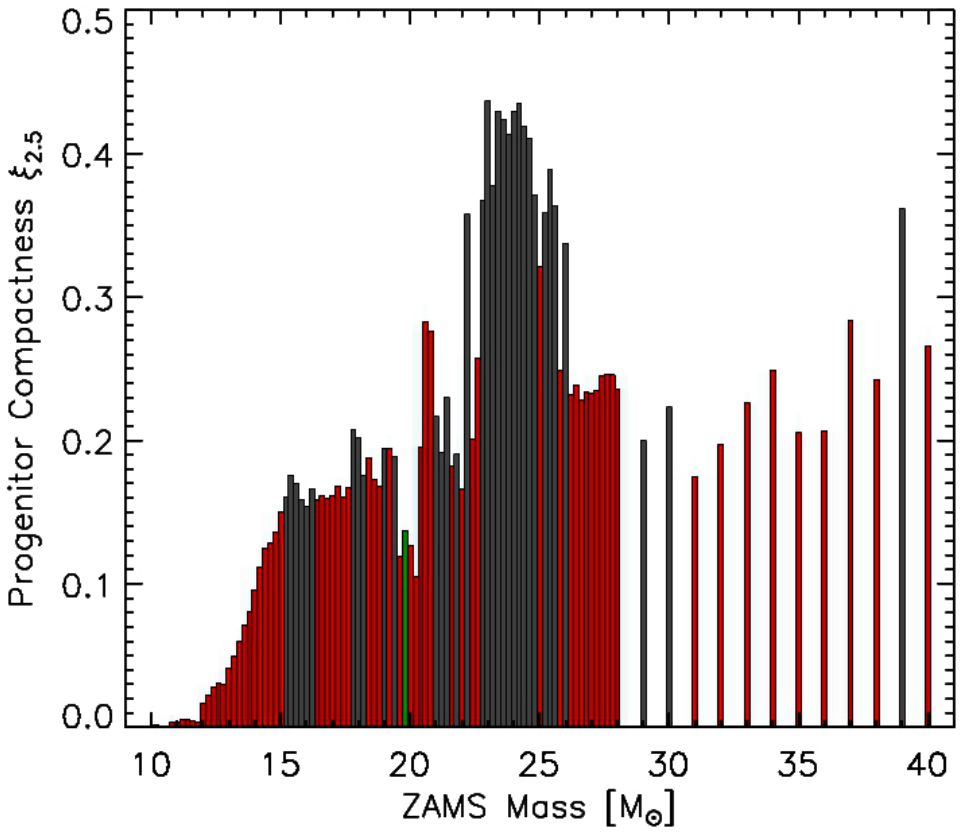

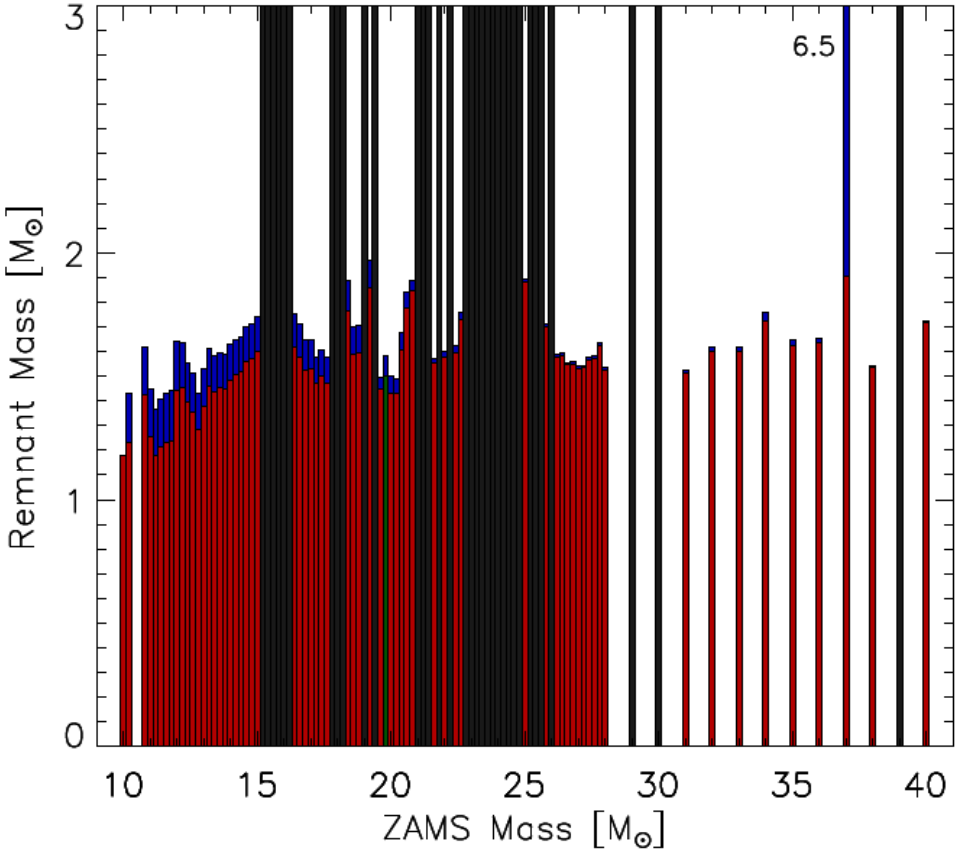

$$\xi_{2.5} \equiv \frac{M/M_\odot}{R(M)/1000\,\mathrm{km}}, \quad \text{mass } M = 2.5\ M_\odot$$

O'Connor & Ott, ApJ 730:70 (2011)

(Ugliano, THJ, Marek, Arcones, ApJ 757, 69 (2012))

Progenitor Properties

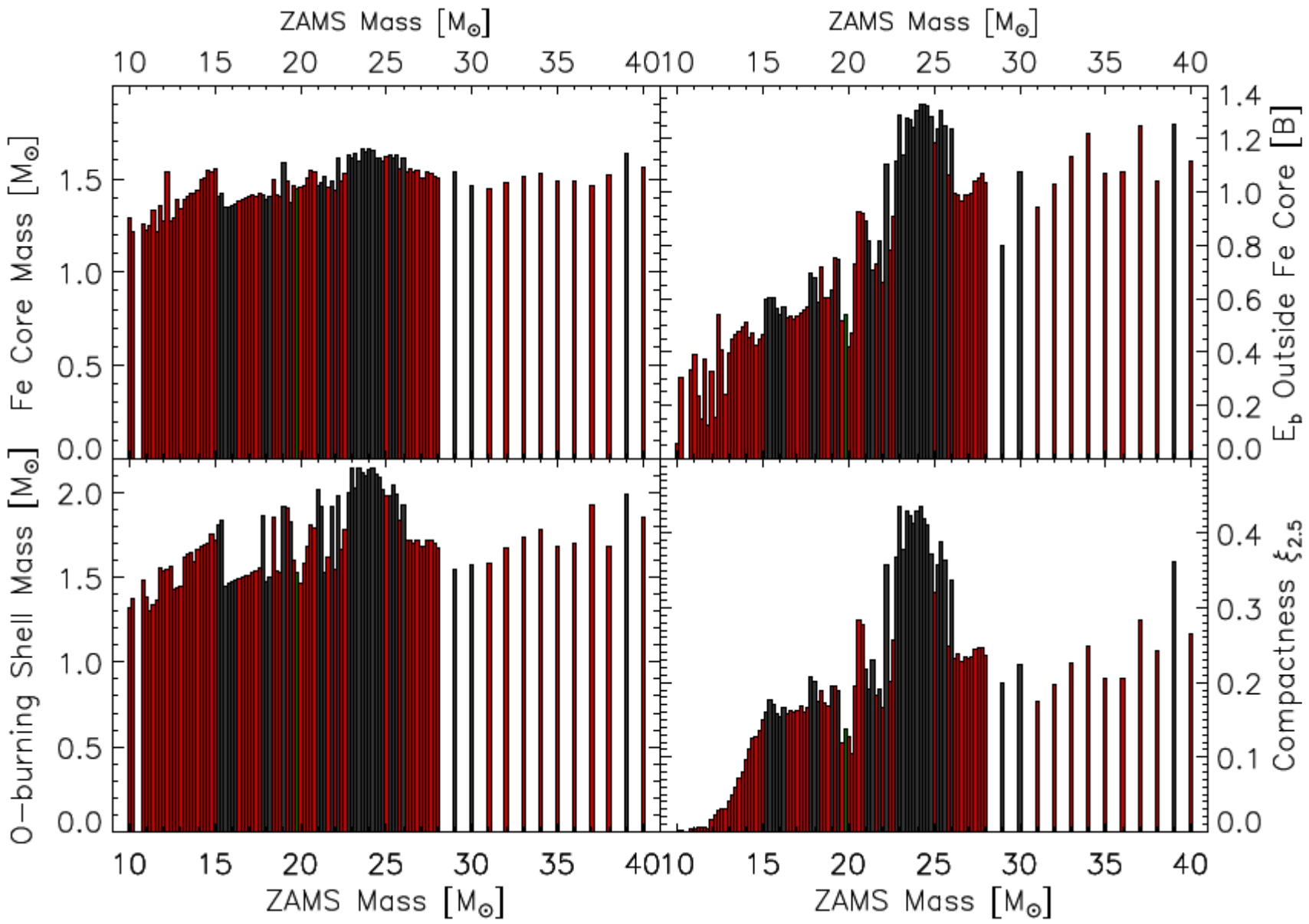

Grey = BH formation cases

(Ugliano, THJ, Marek, Arcones, ApJ 757, 69 (2012))

Explosion Energy and Ejected Ni Mass

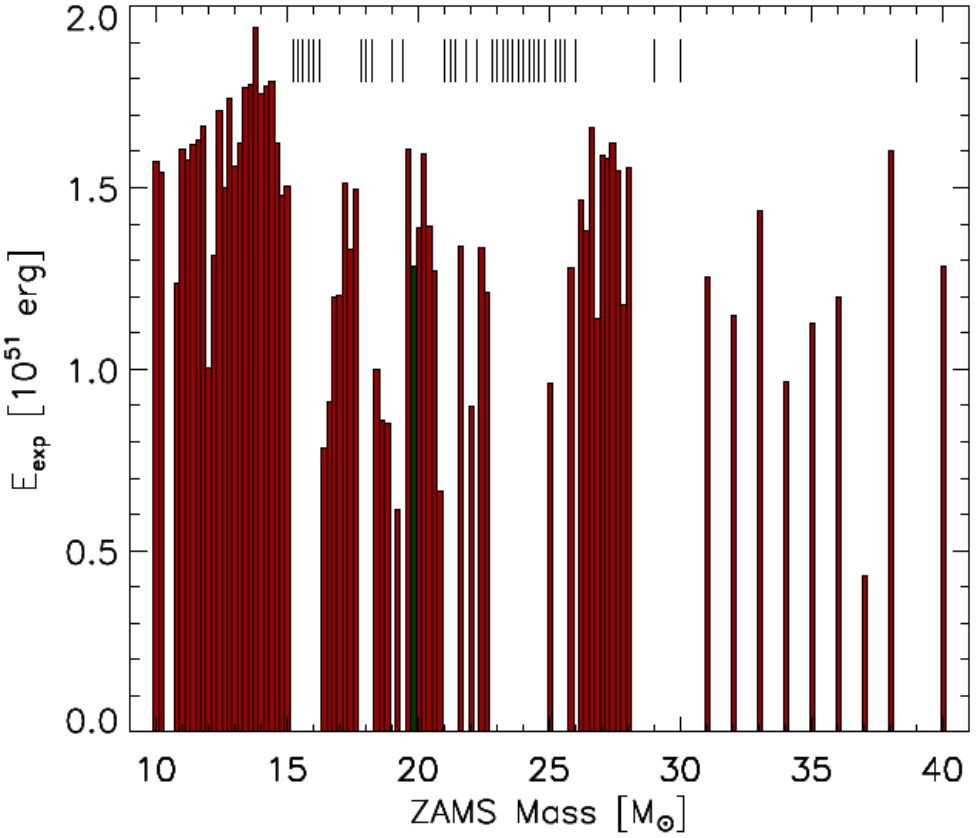

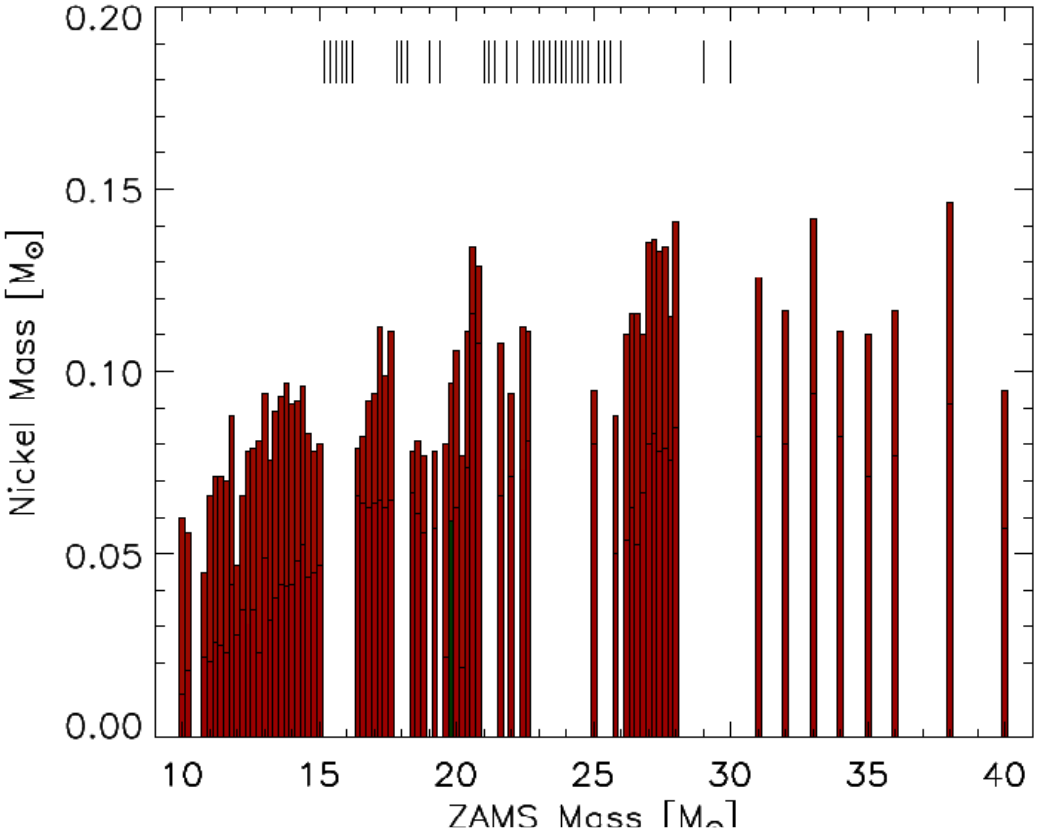

(Ugliano, THJ, Marek, Arcones, ApJ 757, 69 (2012))

Remnant Mass Distribution

Model results folded with Salpeter IMF:
23% of all stellar core collapses produce BHs

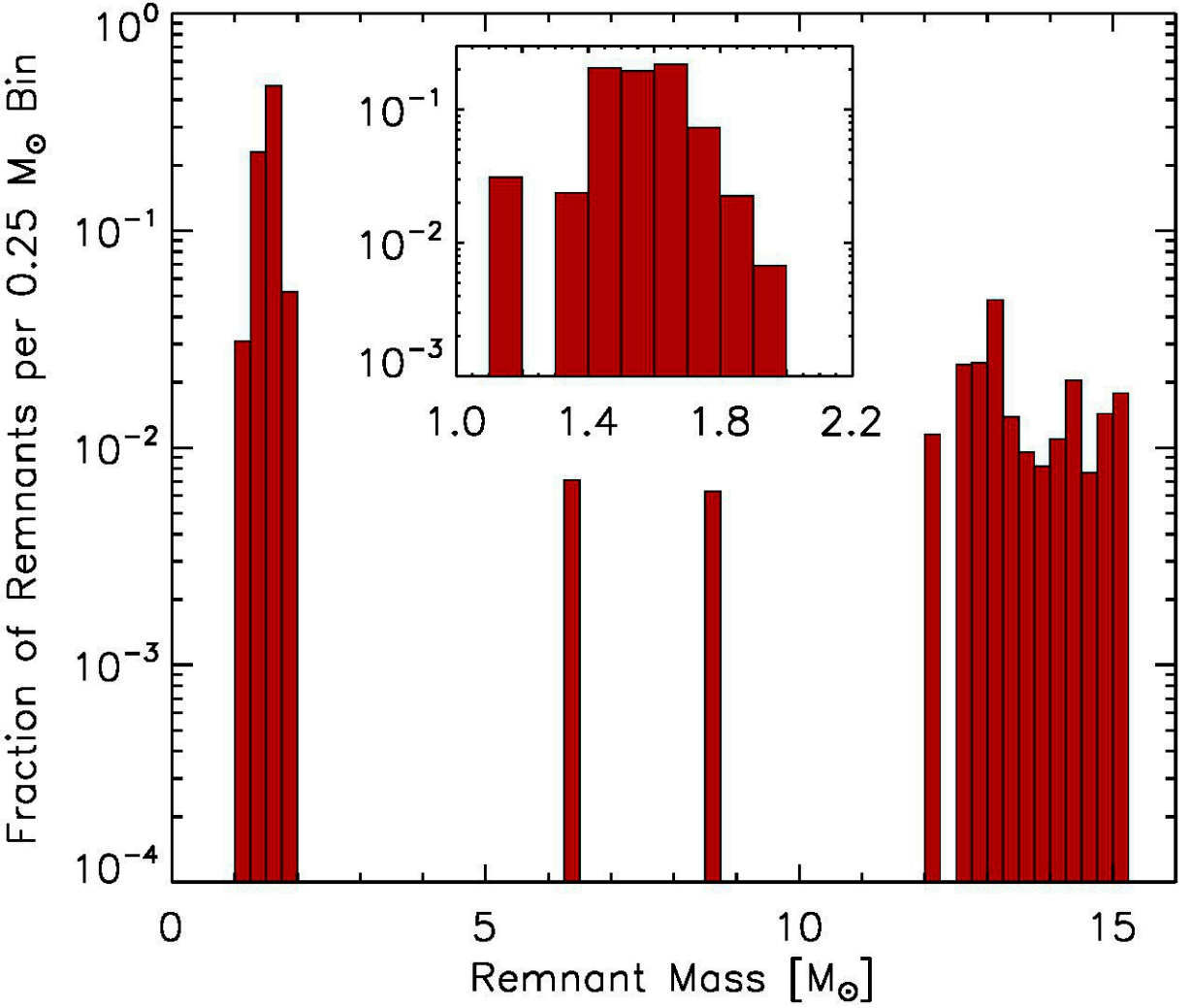

Note:
BH masses need to be corrected/reduced due to stripping of stellar H-envelope of several solar masses

(Nadezhin 1978, Lovegrove & Woosley 2012, Kochanek 2013)

(Ugliano, THJ, Marek, Arcones, ApJ 757, 69 (2012))

Bayesian analysis: Observed double NS systems vs. theoretical mass distribution

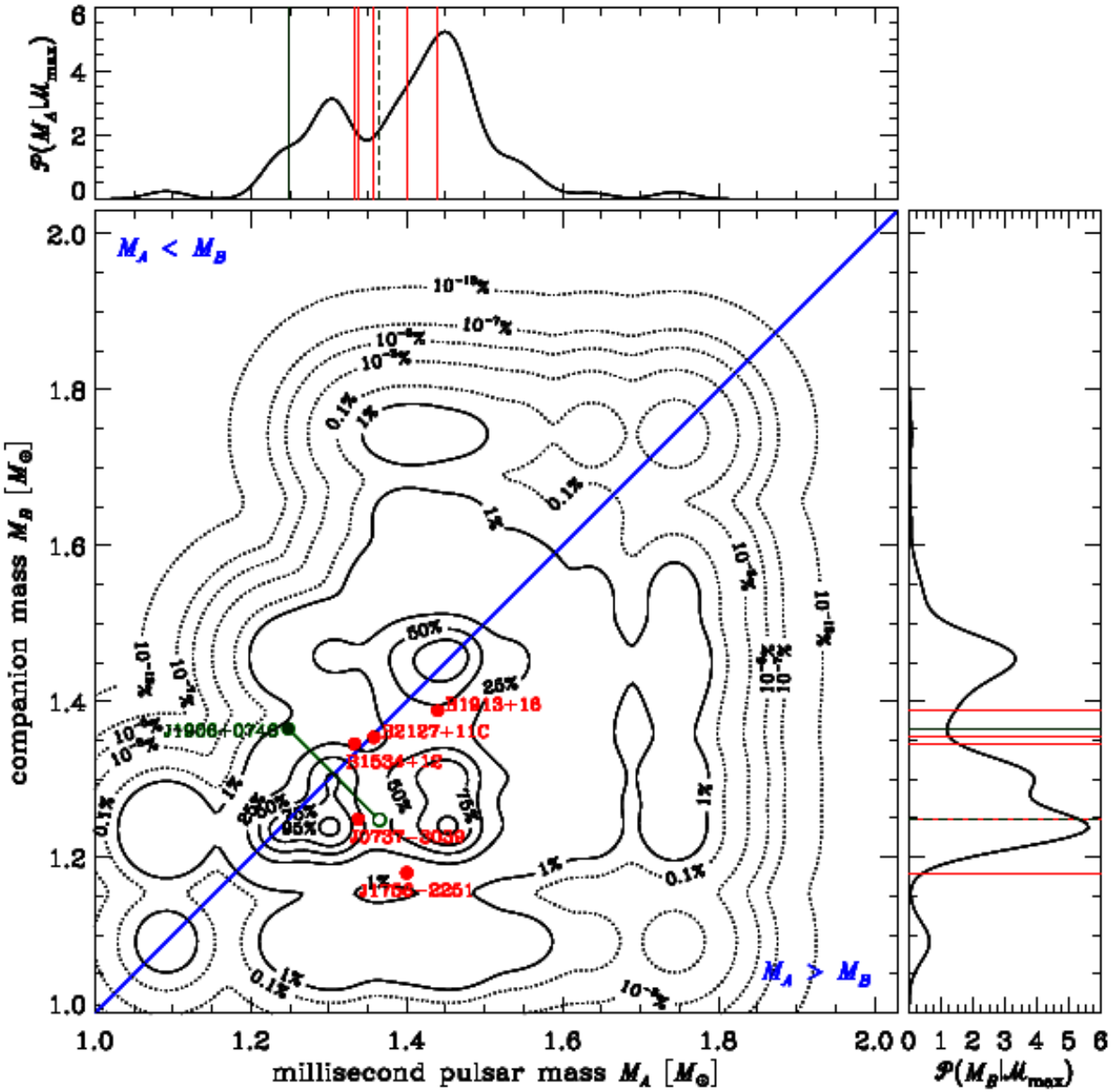

Pejcha, Thompson & Kochanek, MNRAS (2012)

Observed Remnant Mass Distribution

Observed distribution of NS and BH masses exhibits possible gap between neutron stars and black holes

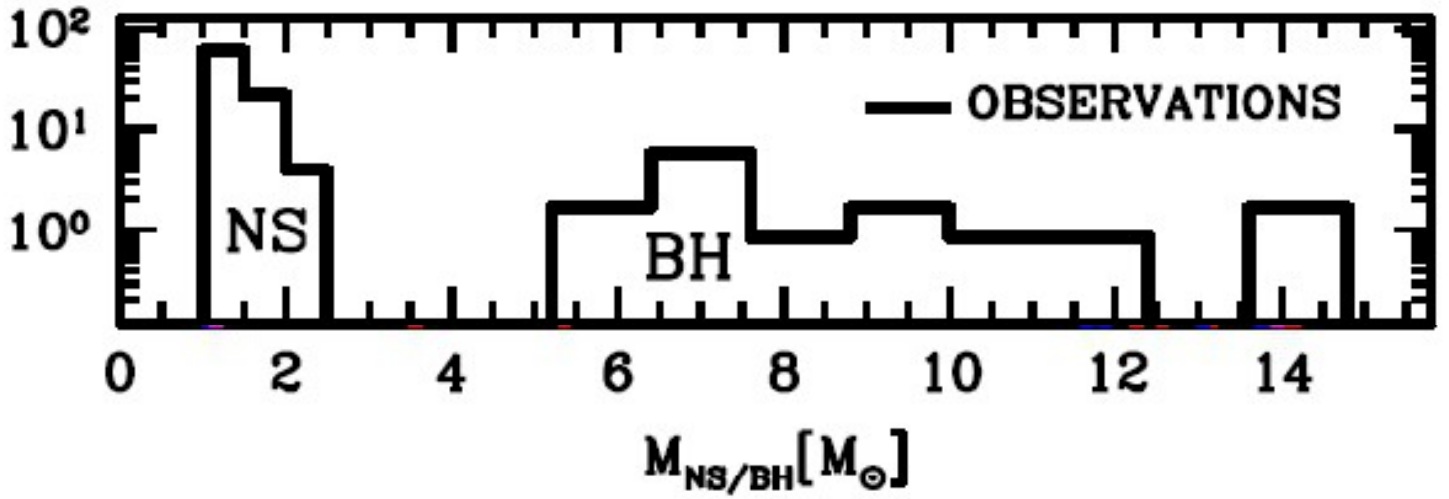

Belczynski et al., ApJ (2012)

Theoretical Remnant Mass Distribution

Our model results reproduce possible gap
in the observed distribution of NS and BH masses if
H-shell stripping for BH formation without SN is included.

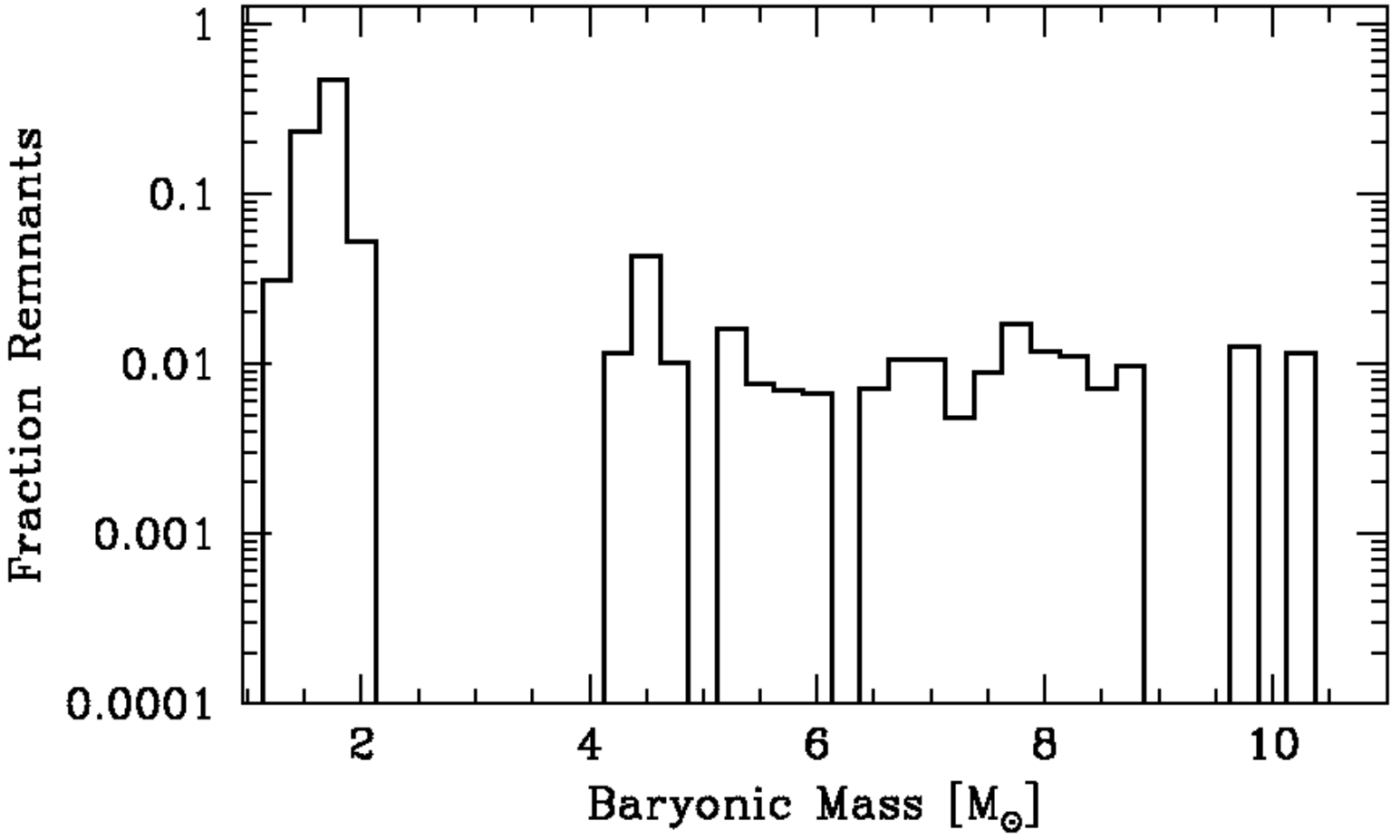

Summary

- BH formation possible for progenitors with $M_{ZAMS} > 15\ M_{sun}$.
- Large fraction of BH formation cases (~25% at solar metallicity).
- Neutrino mechanism yields $E_{exp} < 2*10^{51}$ erg and $M_{Ni} < 0.2\ M_{sun}$.
- Hypernovae with higher energies and more Ni ejection require different mechanism.
- Gap between NS and BH masses naturally occurs because of rarity of fallback SNe.

The Origin of the Heaviest Chemical Elements

Nucleosynthesis in Supernovae Ejecta

Crucial parameters for nucleosynthesis in neutrino-driven outflows:

* Electron-to-baryon ratio Y_e (<---> neutron excess)
* Entropy (<----> ratio of (temperature)^3 to density)
* Expansion timescale

Determined by the interaction of stellar gas with neutrinos from nascent neutron star:

$$\nu_e + n \rightarrow e^- + p$$
$$\bar{\nu}_e + p \rightarrow e^+ + n$$

$$Y_e \sim \left[1 + \frac{L_{\bar{\nu}_e}(\epsilon_{\bar{\nu}_e} - 2\Delta)}{L_{\nu_e}(\epsilon_{\nu_e} + 2\Delta)}\right]^{-1}$$

$$\text{with} \quad \epsilon_\nu = \frac{\langle \epsilon_\nu^2 \rangle}{\langle \epsilon_\nu \rangle} \quad \text{and} \quad \Delta = (m_n - m_p)c^2 \approx 1.29\,\text{MeV}.$$

If $L_{\bar{\nu}_e} \approx L_{\nu_e}$, one needs for $Y_e < 0.5$ (i.e. neutron excess):

$$\epsilon_{\bar{\nu}_e} - \epsilon_{\nu_e} > 4\Delta.$$

R-Process Nucleosynthesis in SN Ejecta?

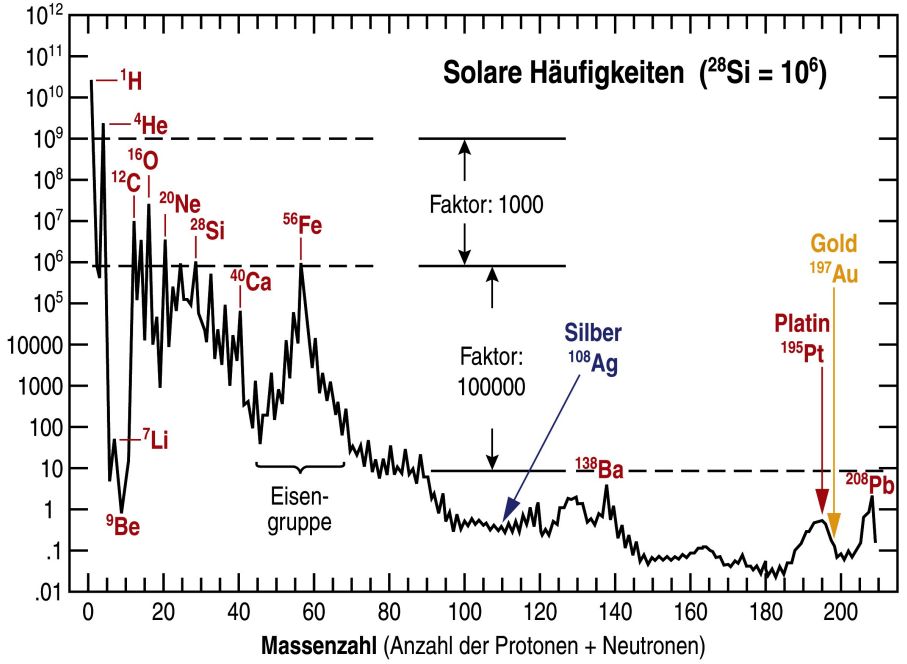

Rapid neutron-capture process (r-process) is responsible for production of ~50% of n-rich nuclei heavier than iron.

Astrophysical site of r-process is still unknown;

One of greatest mysteries of nuclear astrophysics.

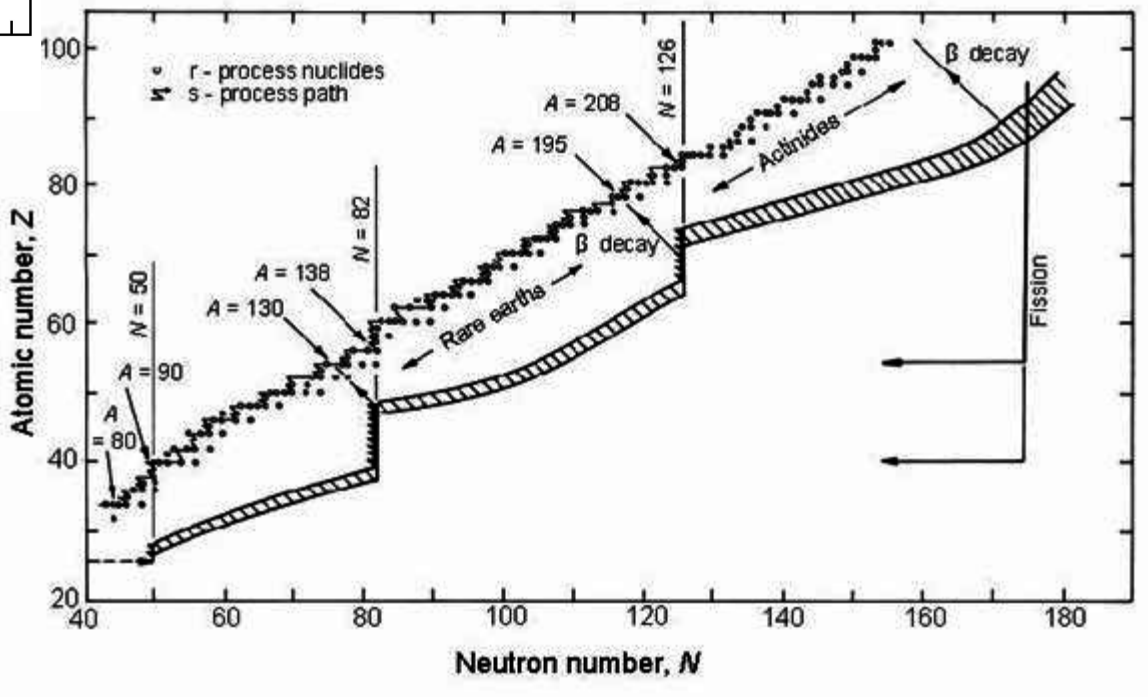

Neutrino-Driven Wind From Proto-Neutron Stars

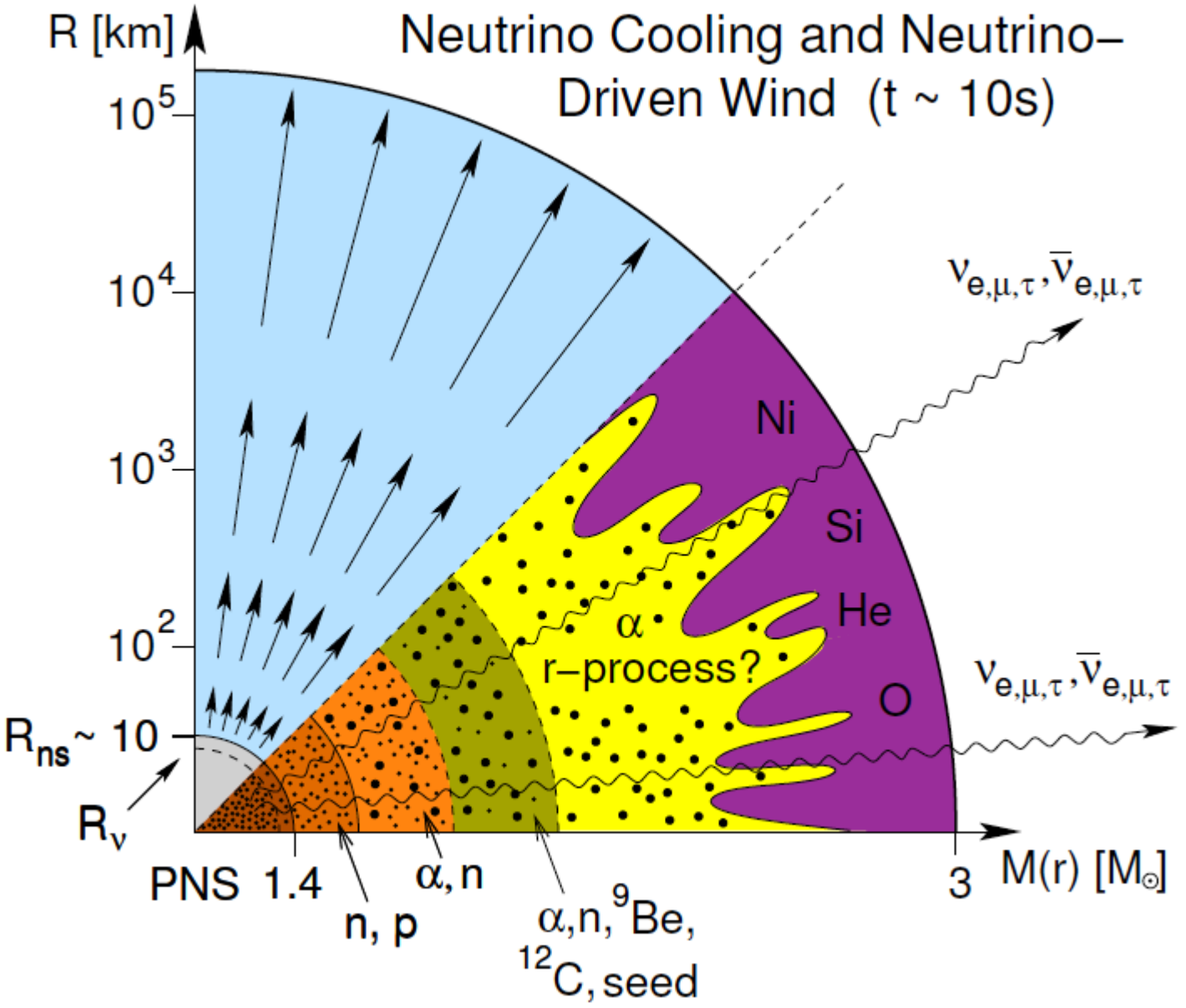

PNS Cooling in O-Ne-Mg-Core SNe

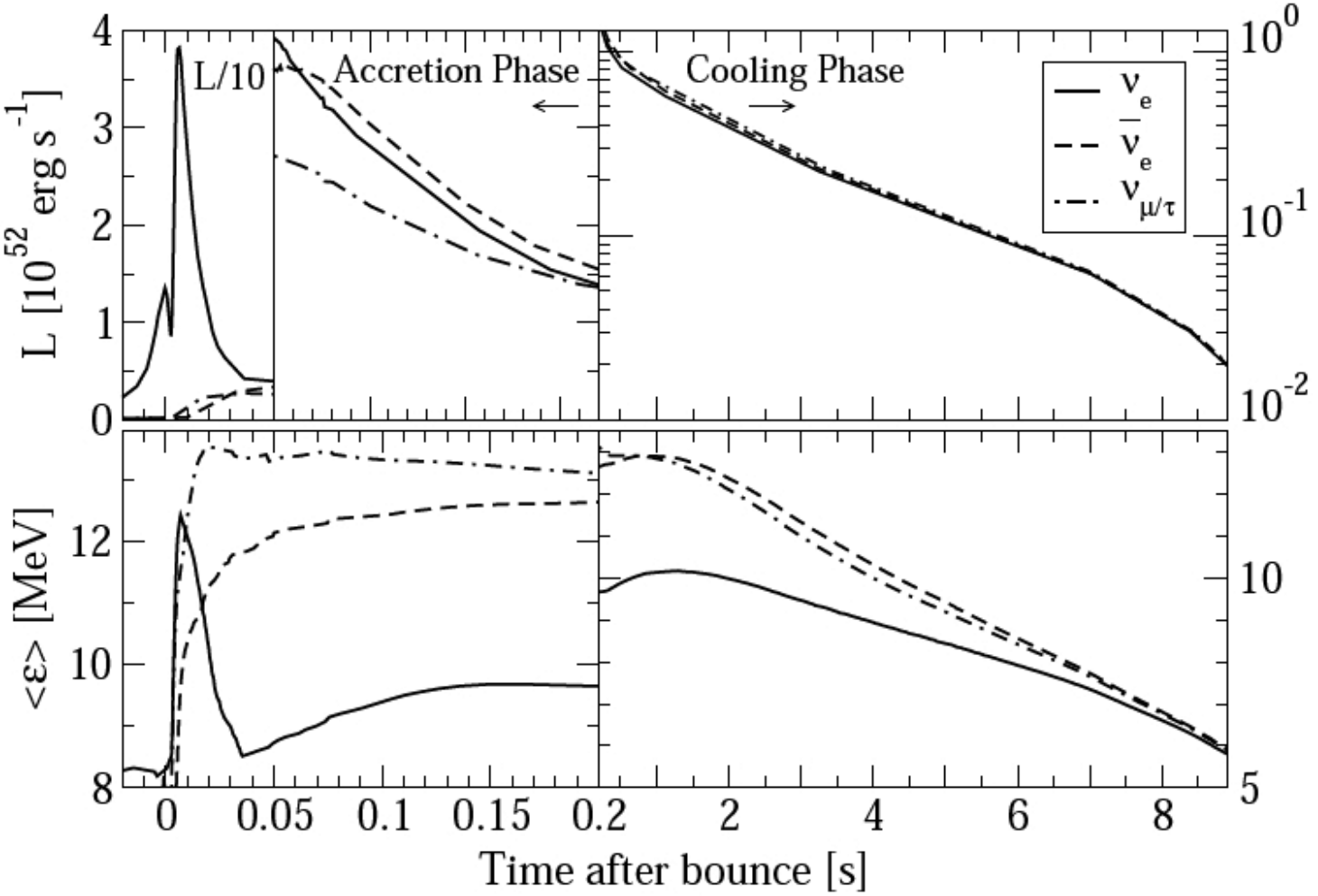

Hüdepohl et al. (PRL 104 (2010)); arXiv:0912:0260

Luminosities and mean energies very similar for all neutrinos during the proto-neutron star (PNS) cooling evolution.

Nucleosynthesis in O-Ne-Mg Core SNe

- Neutrino-driven wind remains p-rich for >10 seconds!
- No r-process in the late neutrino-driven wind!
- Holds also for more massive progenitos (Fischer et al. 2009)

Hüdepohl (Diploma Thesis 2009);
Hüdepohl et al. (PRL 104 (2010);
arXiv:0912:0260)

No favorable conditions for a strong r-process in ONeMg-core explosions and neutrino-driven winds of PNSs!

? What is the astrophysical site for the creation of the heaviest r-process elements (A > 130)? ?

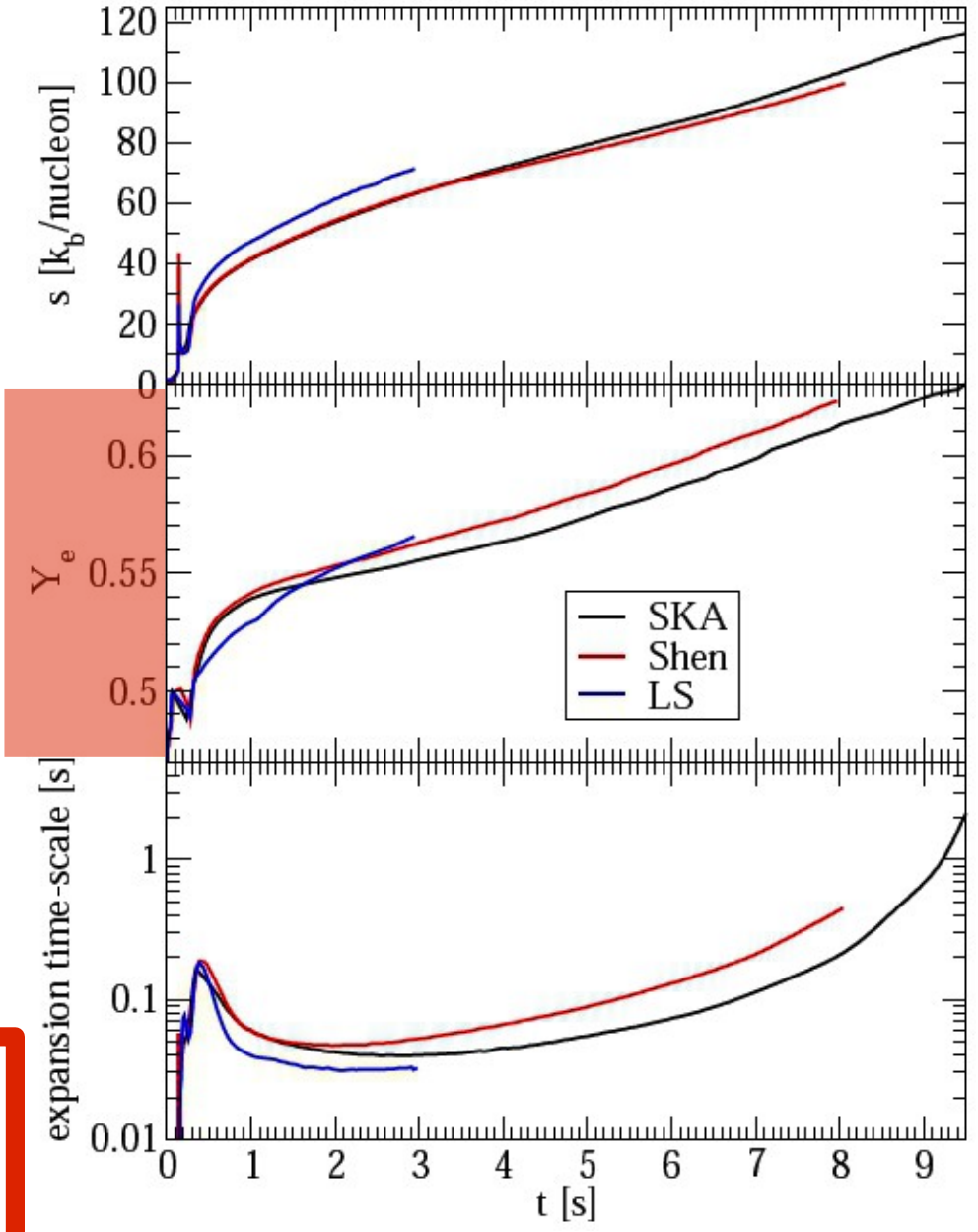

Gamma-Ray Bursts

GRB Phenomenology I

- Isotropic on sky
- Bimodal duration distribution
- High diversity
- Rapid time variations

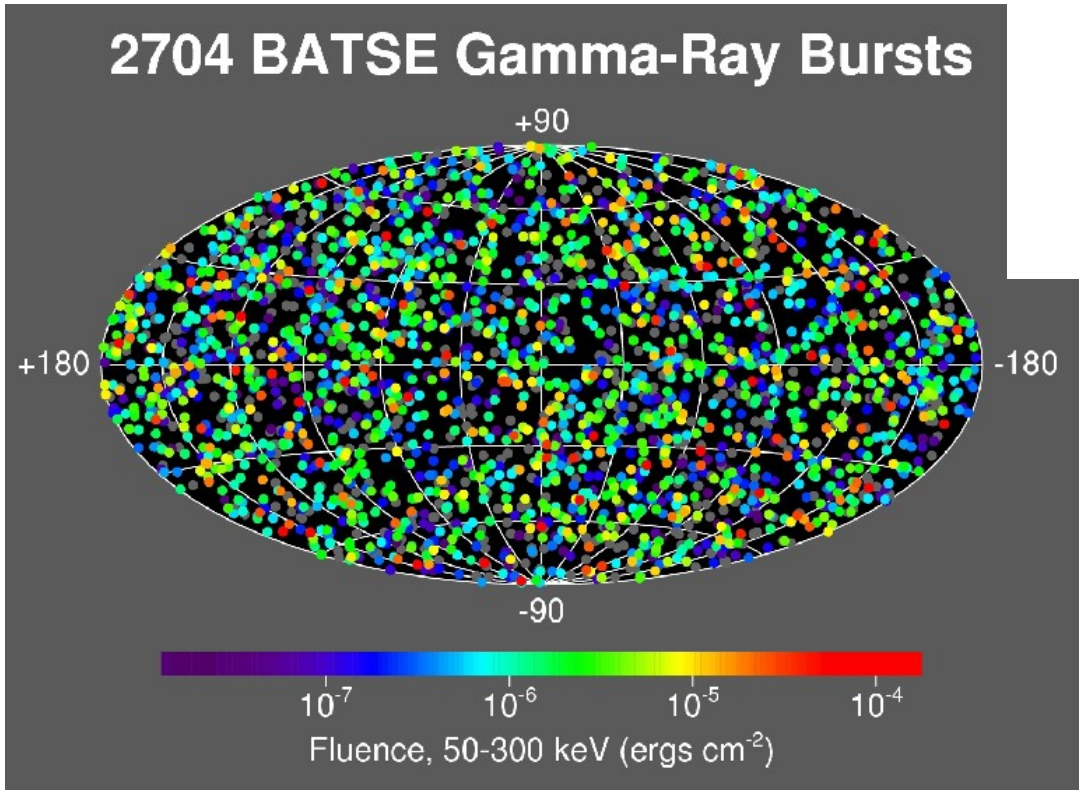

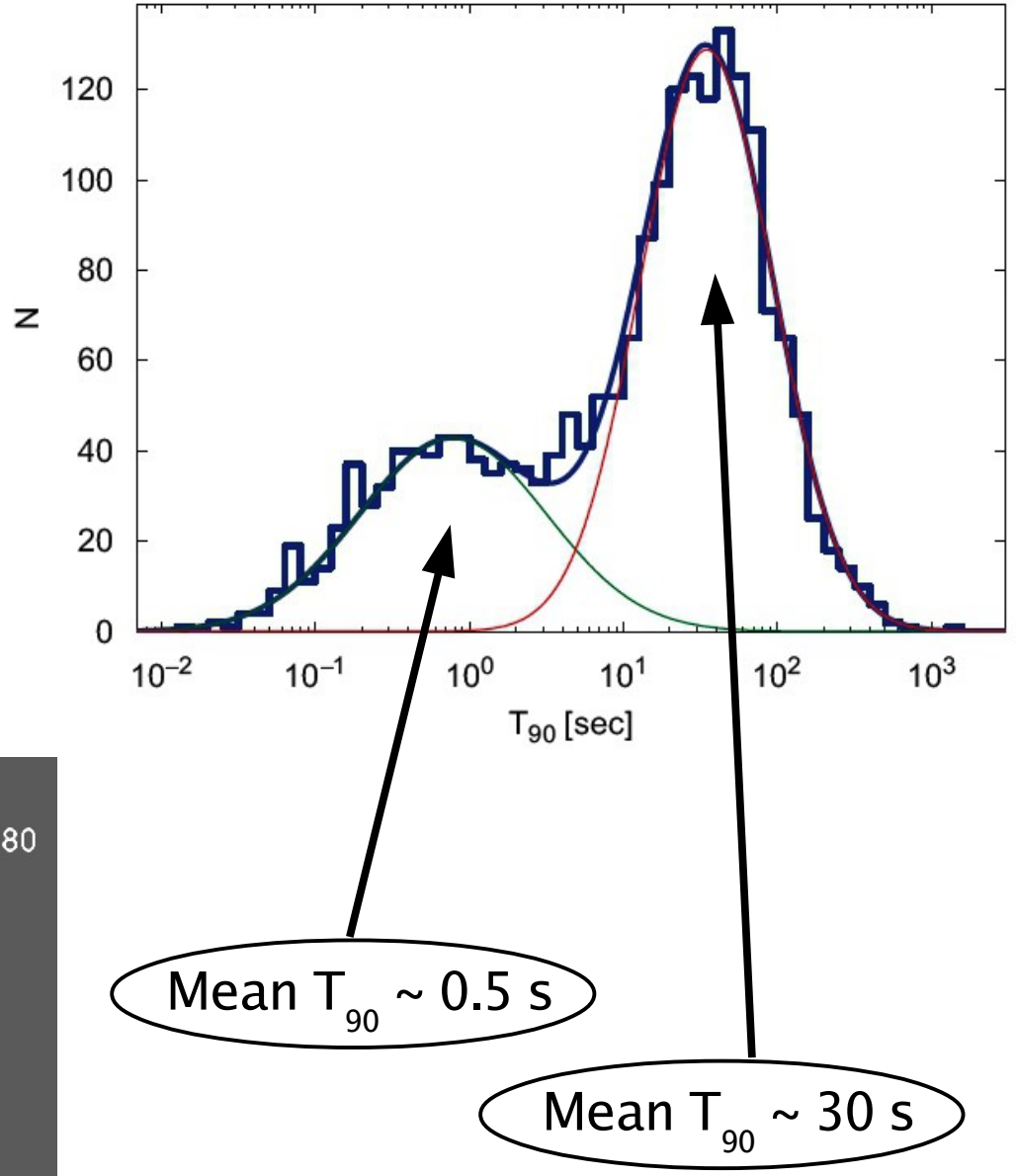

GRB Phenomenology II

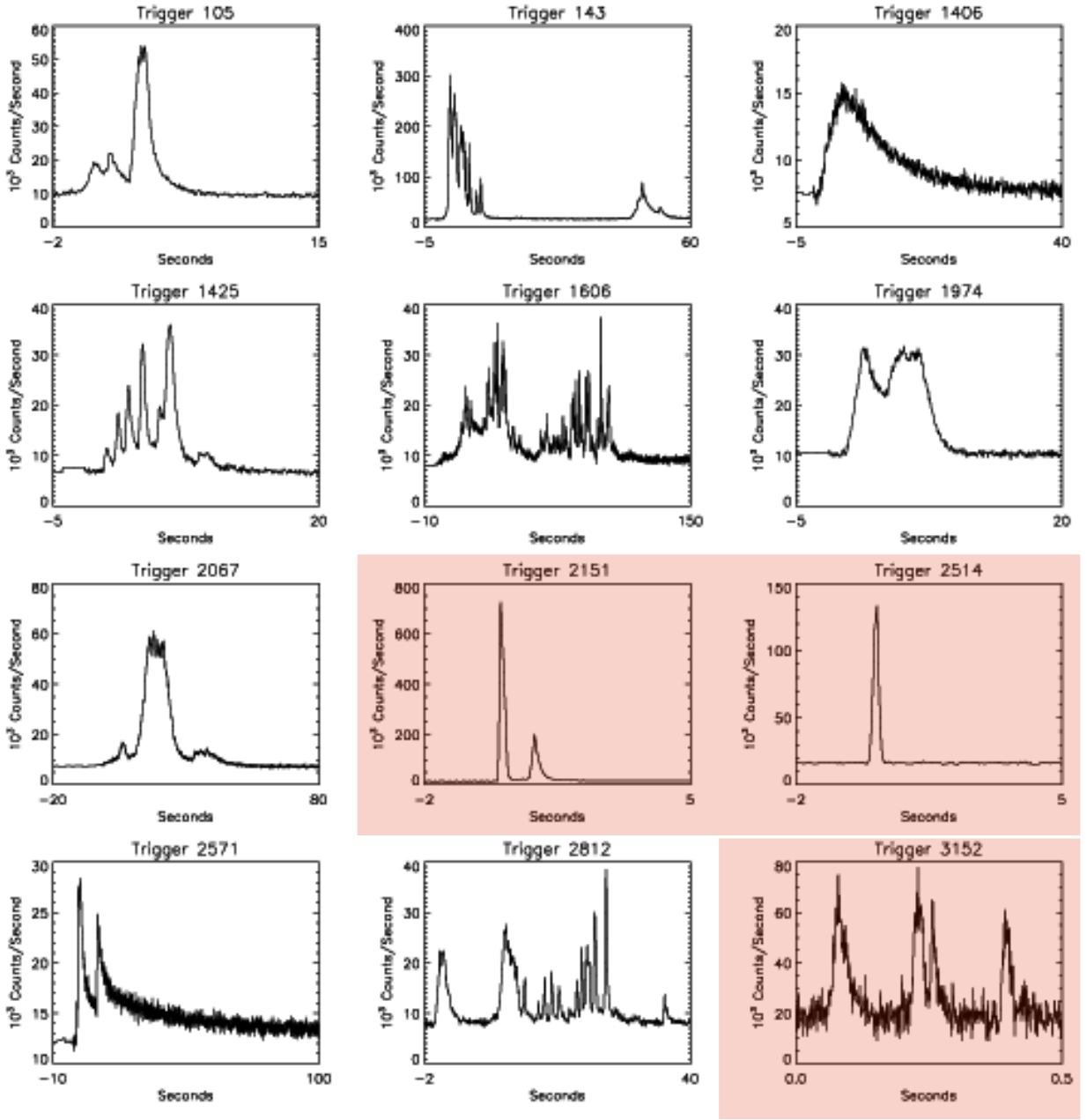

- Isotropic on sky
- Bimodal duration distribution
- Very high diversity
- Rapid time variations

- Swift, HETE-2, Integral: good localization -----> afterglows (x-ray, optical, radio could be observed) at cosmological distances

short GRBs

Short GRBs

- Harder spectra
- ~100 times less energetic than long GRBs
- ~21 with arcsec and sub-arcsec localizations HETE-2, Integral)
- From host identification:
  ~12 with determined redshifts;
  ~ half a dozen more with redshift limits
- ~ 6 with extended-duration, soft emission after first short-hard event

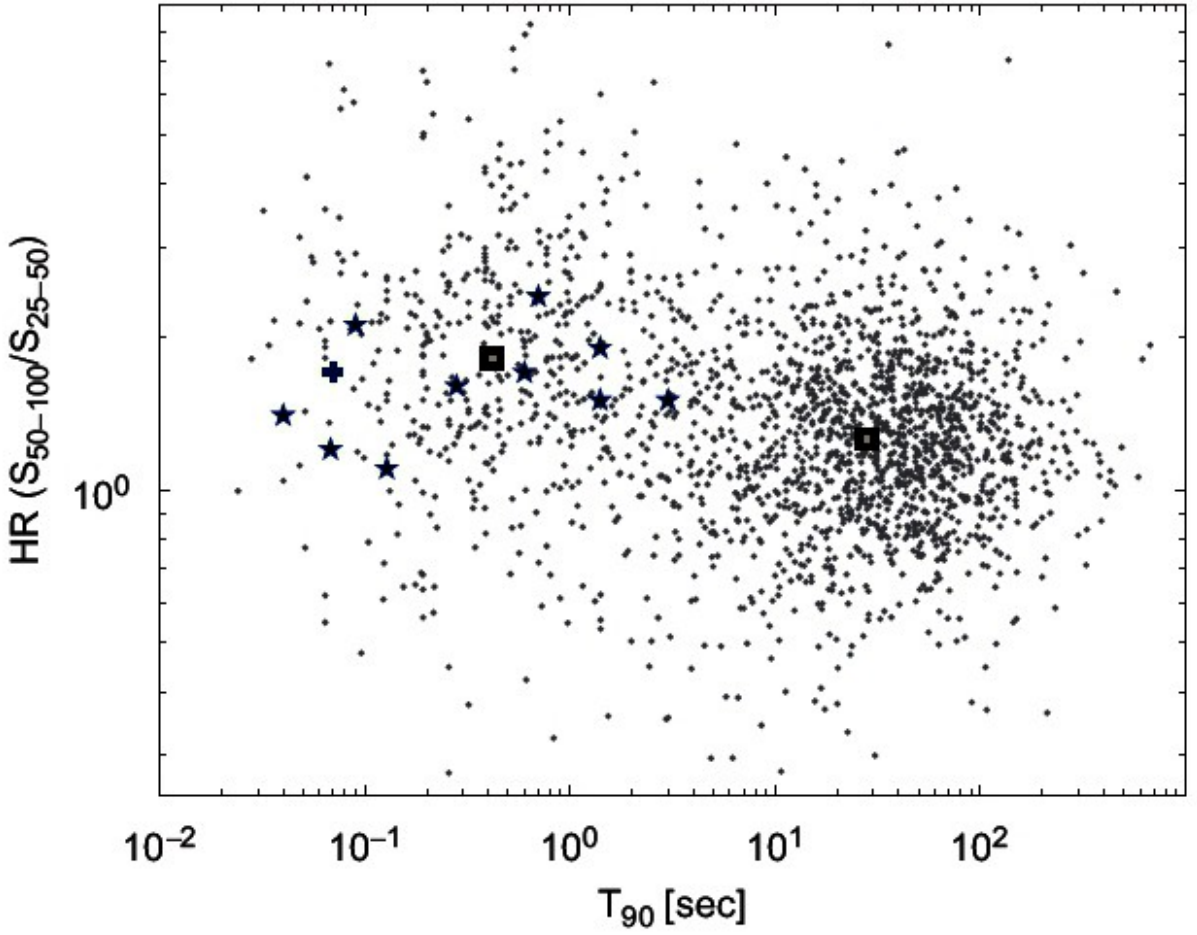

Nakar (2007)

Comparison: LGRBs vs. SGRBs

short GRBs

- T_{90} < 3 sec
- Hard γ spectrum
- $E_{\gamma,iso} \sim 10^{49\text{-}51}$ ergs
- <z> ~ 0.5
- Early & late type galaxies
- SFR < 1 M_{sun}/yr
- Small & large offsets
- Old & young stellar populations
- No SN associated
- Progenitor: probably DCO ??

long GRBs

- T_{90} > 3 sec
- Soft γ spectrum
- $E_{\gamma,iso} \sim 10^{52\text{-}54}$ ergs
- <z> ~ 2-3
- In star forming galaxies
- SFR ~ 10 M_{sun}/yr
- Small offsets
- Dense environments with lots of gas and dust
- SN associated
- Progenitor: massive star

Hyperaccreting Black Holes

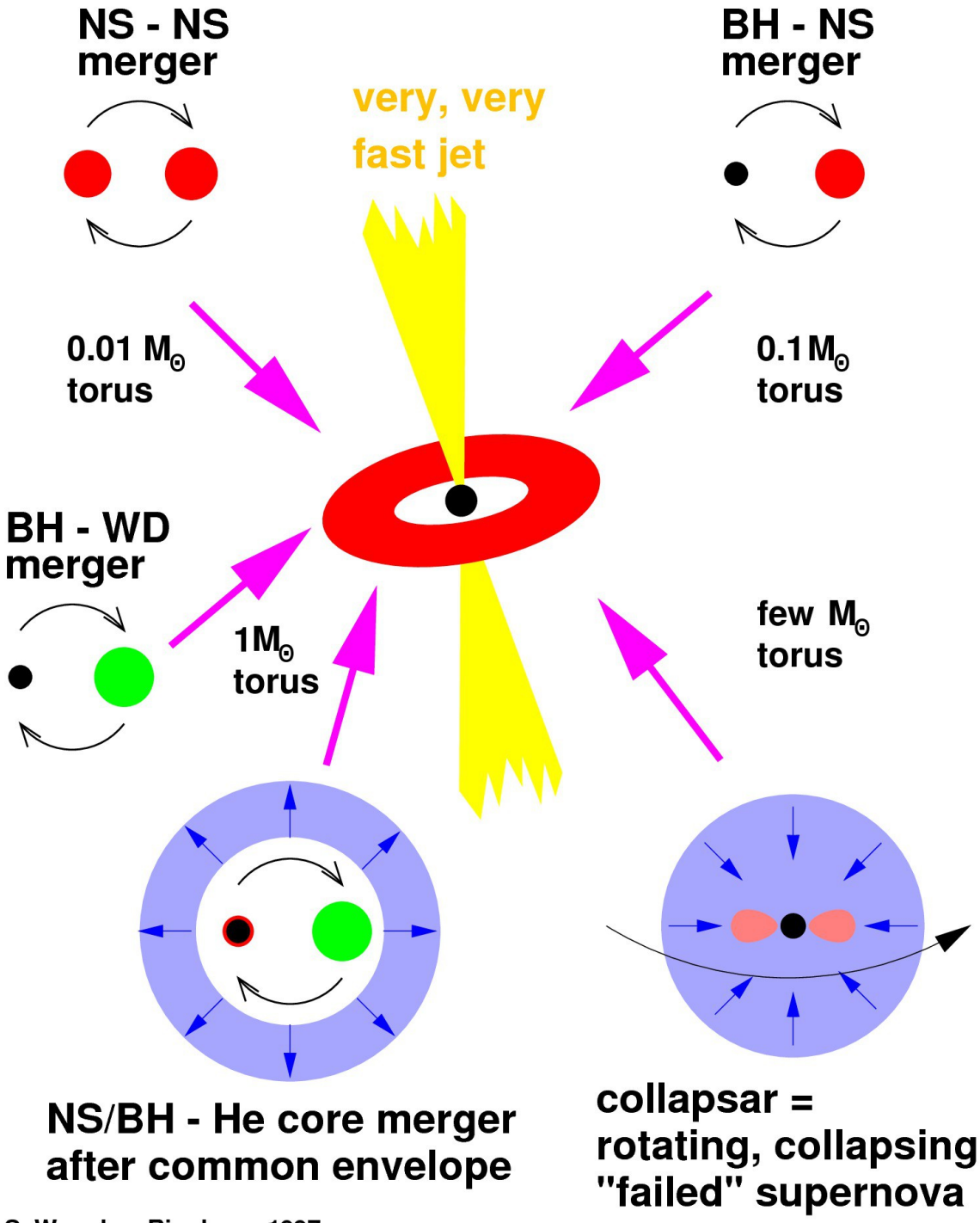

S. Woosley, Ringberg, 1997

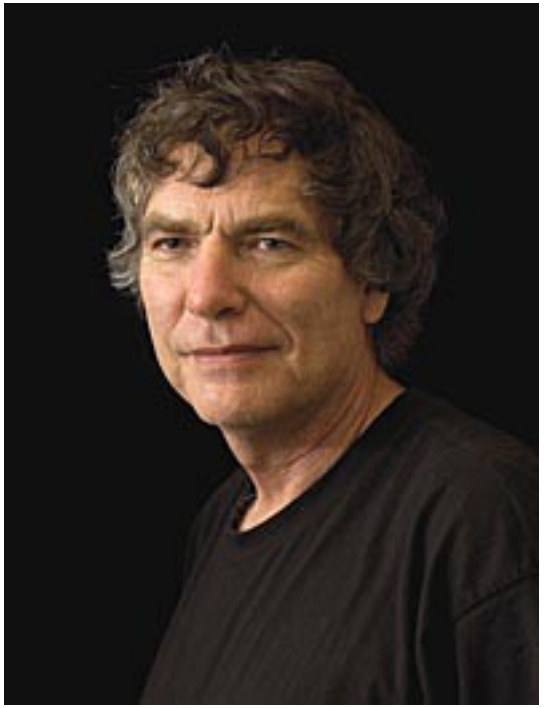

Stan Woosley

Long Gamma-Ray Bursts

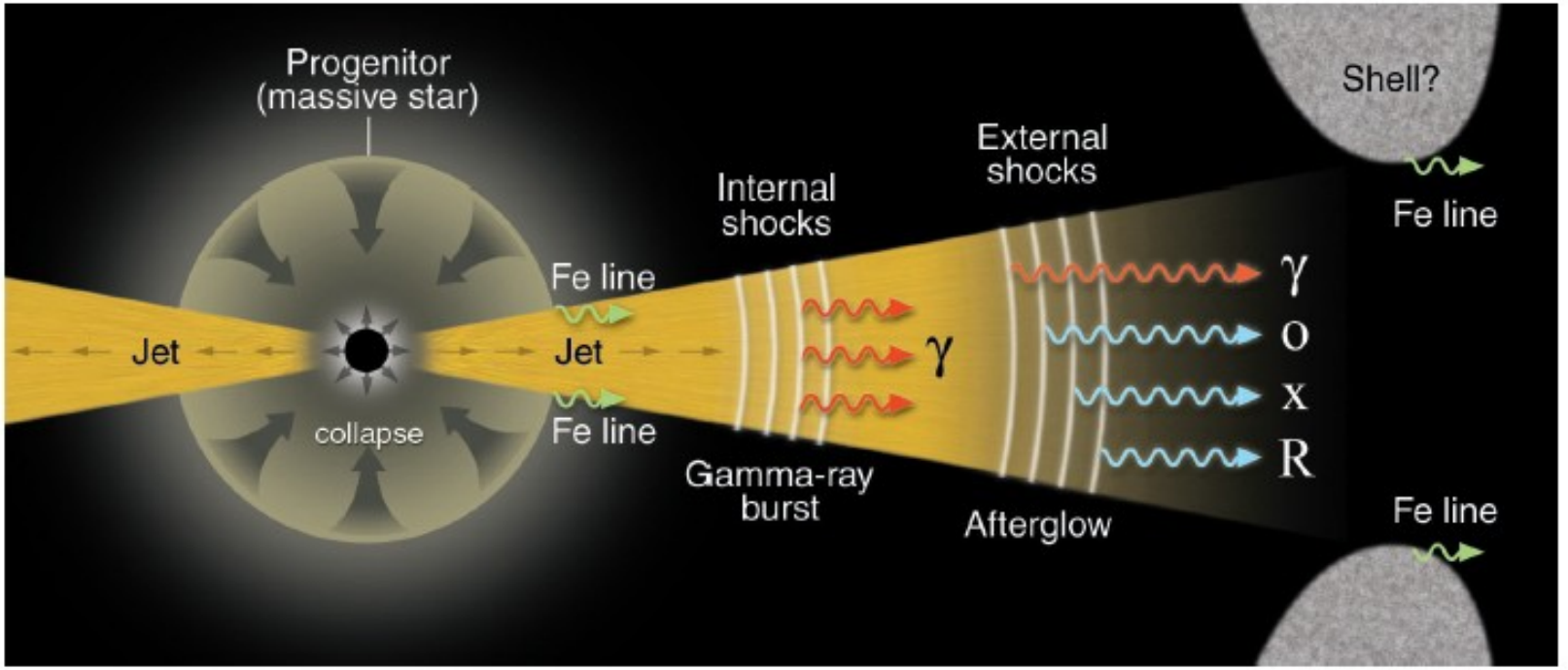

(Meszaros (2002)

- Associated with massive star explosions ("GRB-SNe"):
  SN bumps, direct SN/GRB associations
- Jets (opening angles: 1°–5°; collimation factor: 100–1000)
- Energies: 10^{50}–10^{51} erg in gamma rays, similar in AG

Gamma-Ray Bursts and Hypernovae

- Occur in rare cases of very rapidly rotating, very massive stars with sufficient mass loss until collapse
- Black hole formation
- BH accretion and ejection of very narrow, ultrarelativistic GRB jet, can be accompanied by hypernova explosion
- Jet is driven by magnetohydrodynamic (MHD) effects and/or neutrino-antineutrino annihilation
- Extremely energetic stellar explosion by MHD mechanism or viscous energy release in accretion disk

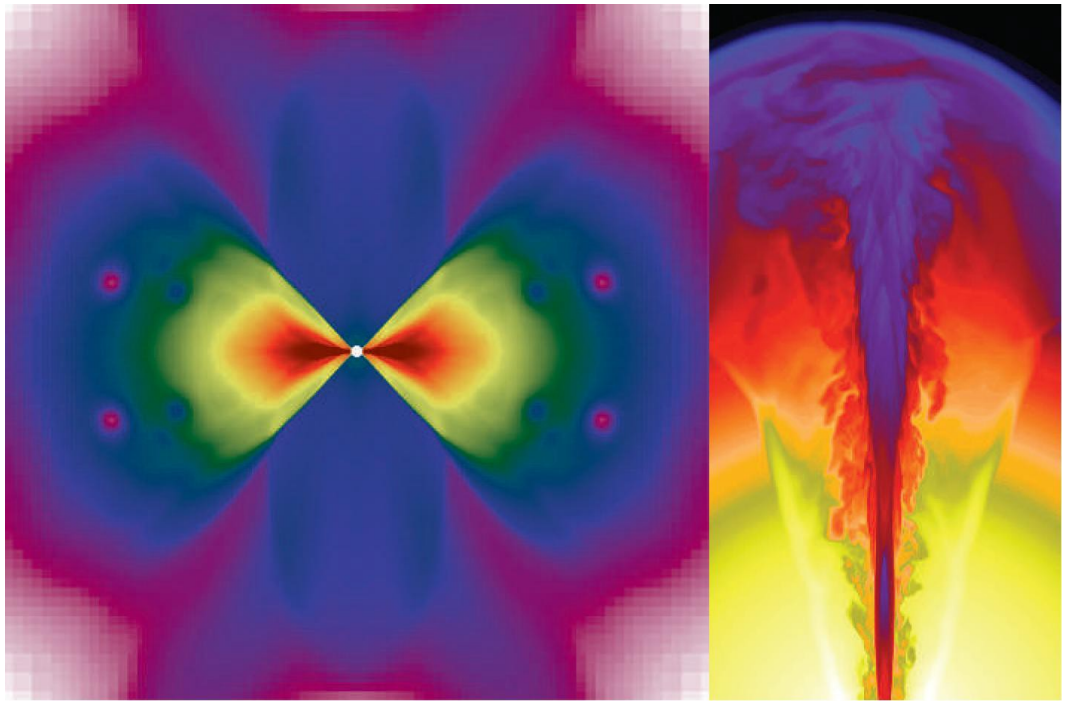

Zhang & Woosley (2005)

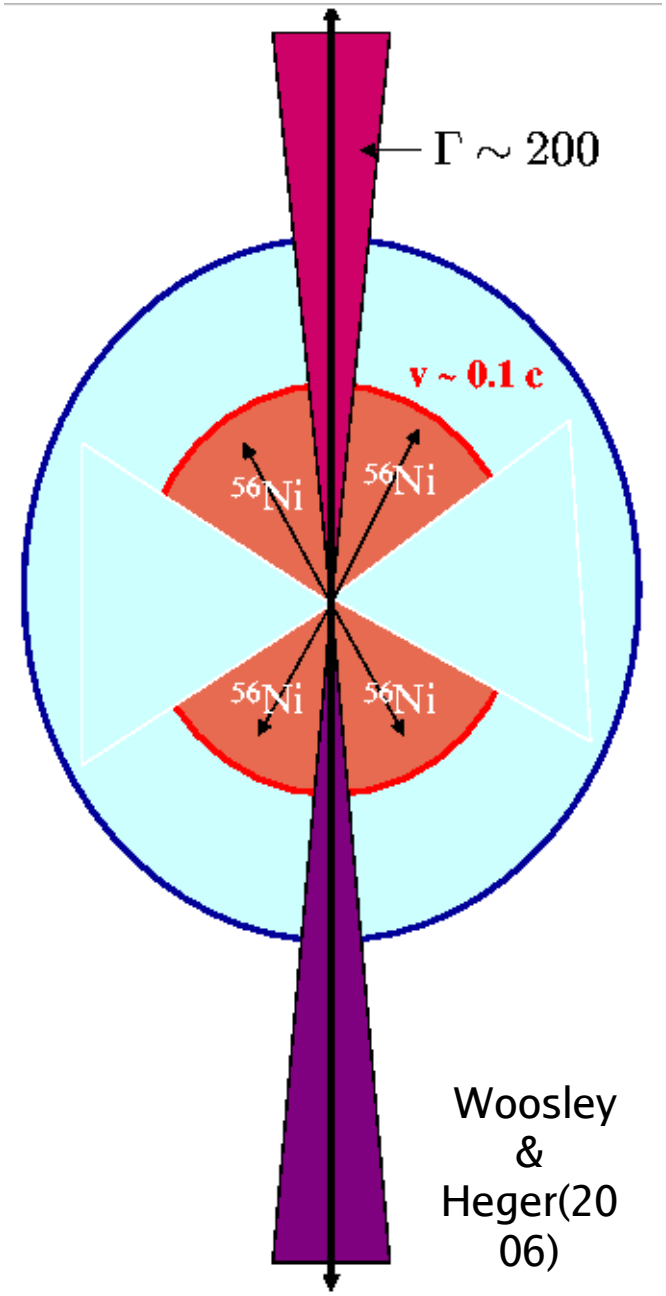

Woosley & Heger(2006)

NS+NS/BH Mergers

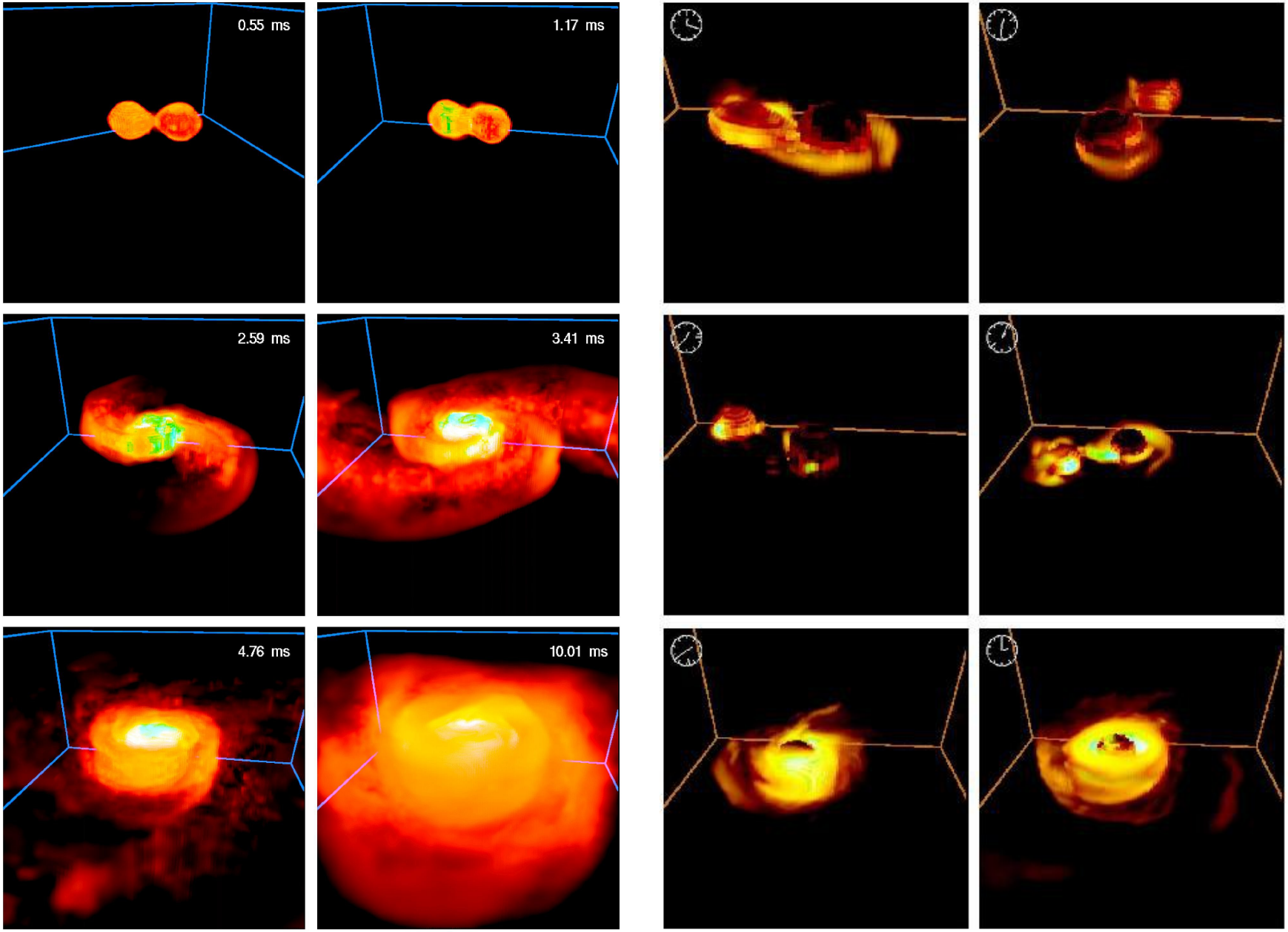

Ruffert et al.
Rosswog et al.
Oechslin et al.
Shibata et al.
Rezzolla et al.
Rasio et al.
Lehner et al.
etc.

Ejecta from NS+NS/BH Mergers

mass loss phases during NS–NS and NS–BH merging

1st phase: dynamical interaction with mass ejection

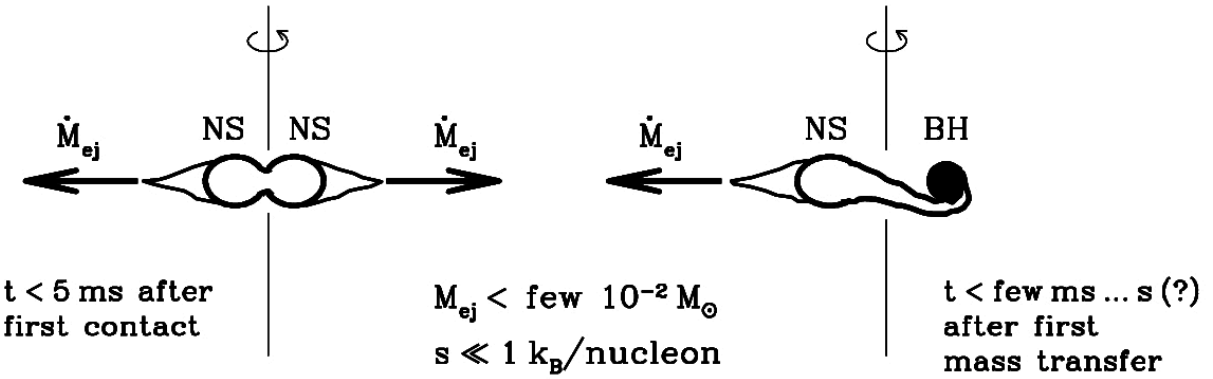

2nd phase: massive, ν emitting accretion torus around BH

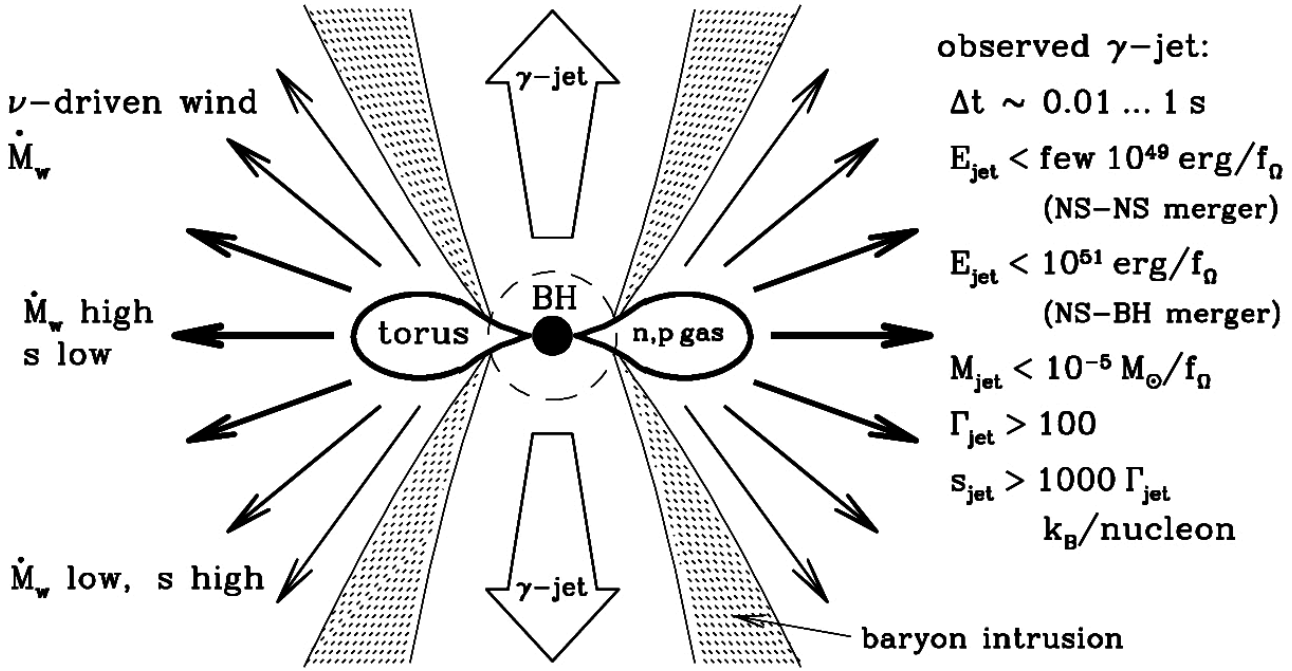

Ruffert & Janka (1999, 2001)

Properties of Dynamical Merger Ejecta

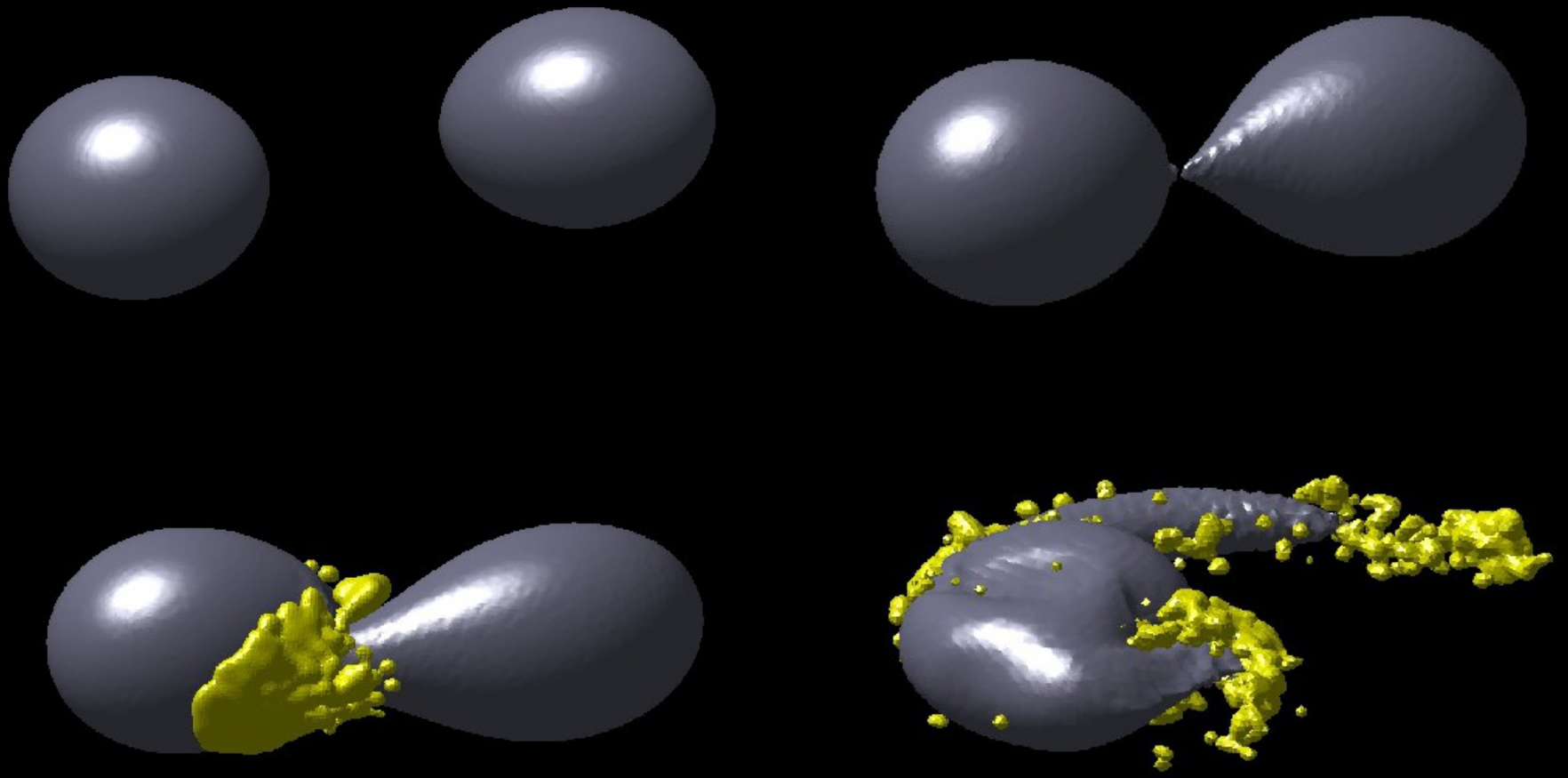

(Goriely, Bauswein, THJ, ApJL 738 (2011) L32)

Asymmetric NS-NS merger

Nucleosynthesis in Dynamical Merger Ejecta

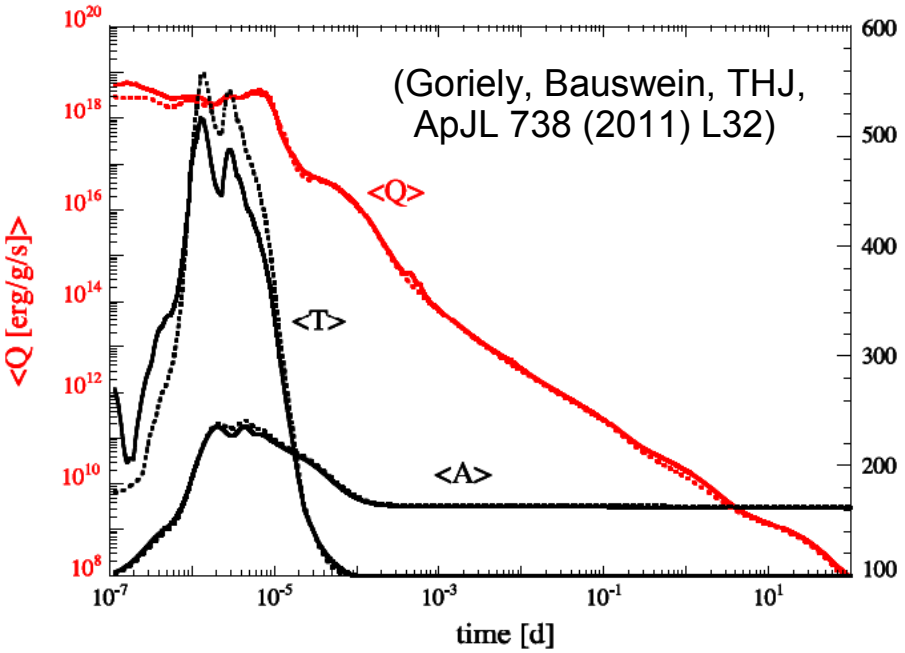

During r-processing fission recycling takes place and produces roughly solar abundances for A > 130.

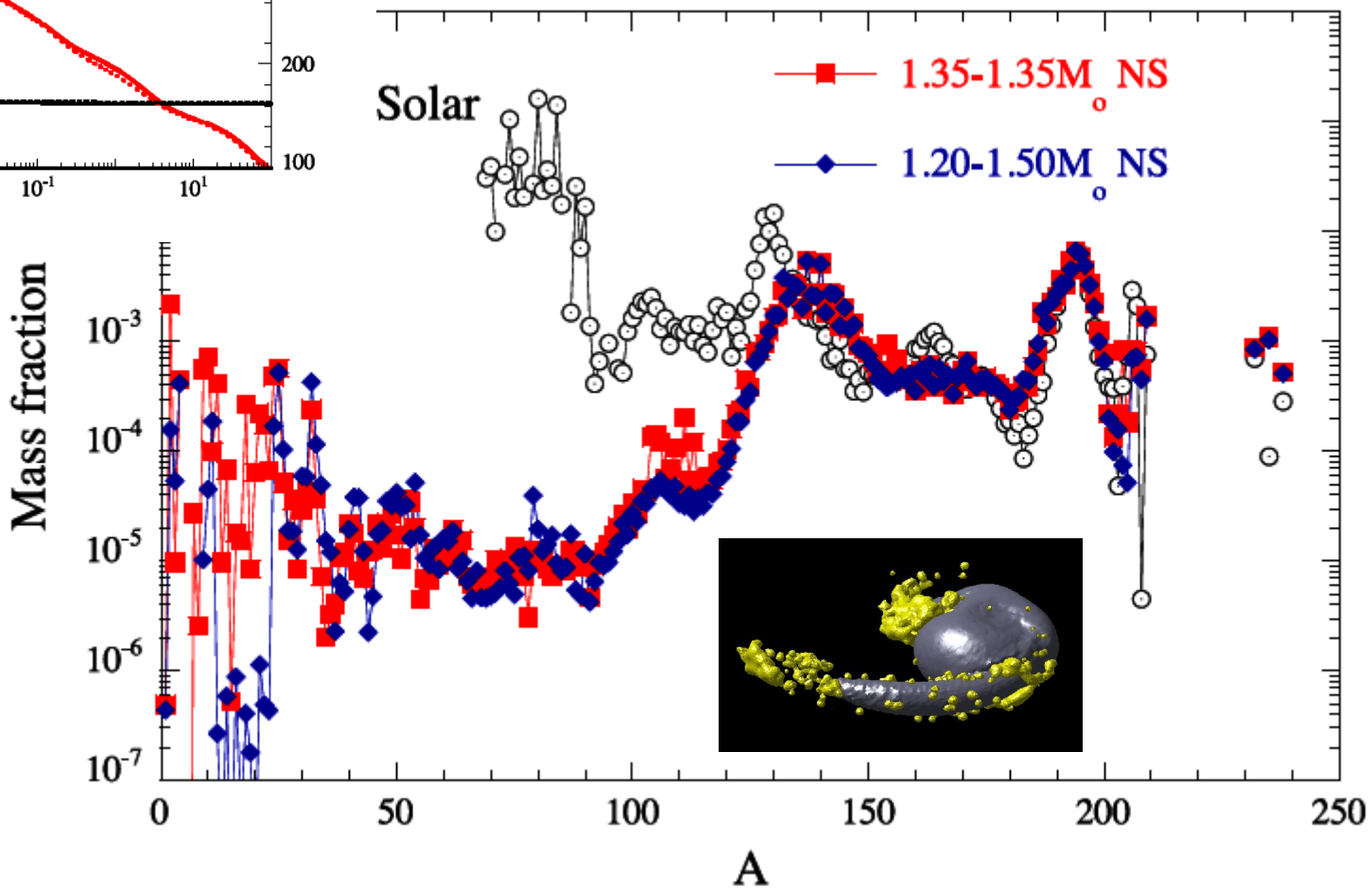

Per merger event 10^{-3}–10^{-2} M_{sun} are ejected.

With rate of 10^{-5} events per year and galaxy, NS mergers could be the main source of heavy r-process material.

Optical Transients associated with r-Process Heating

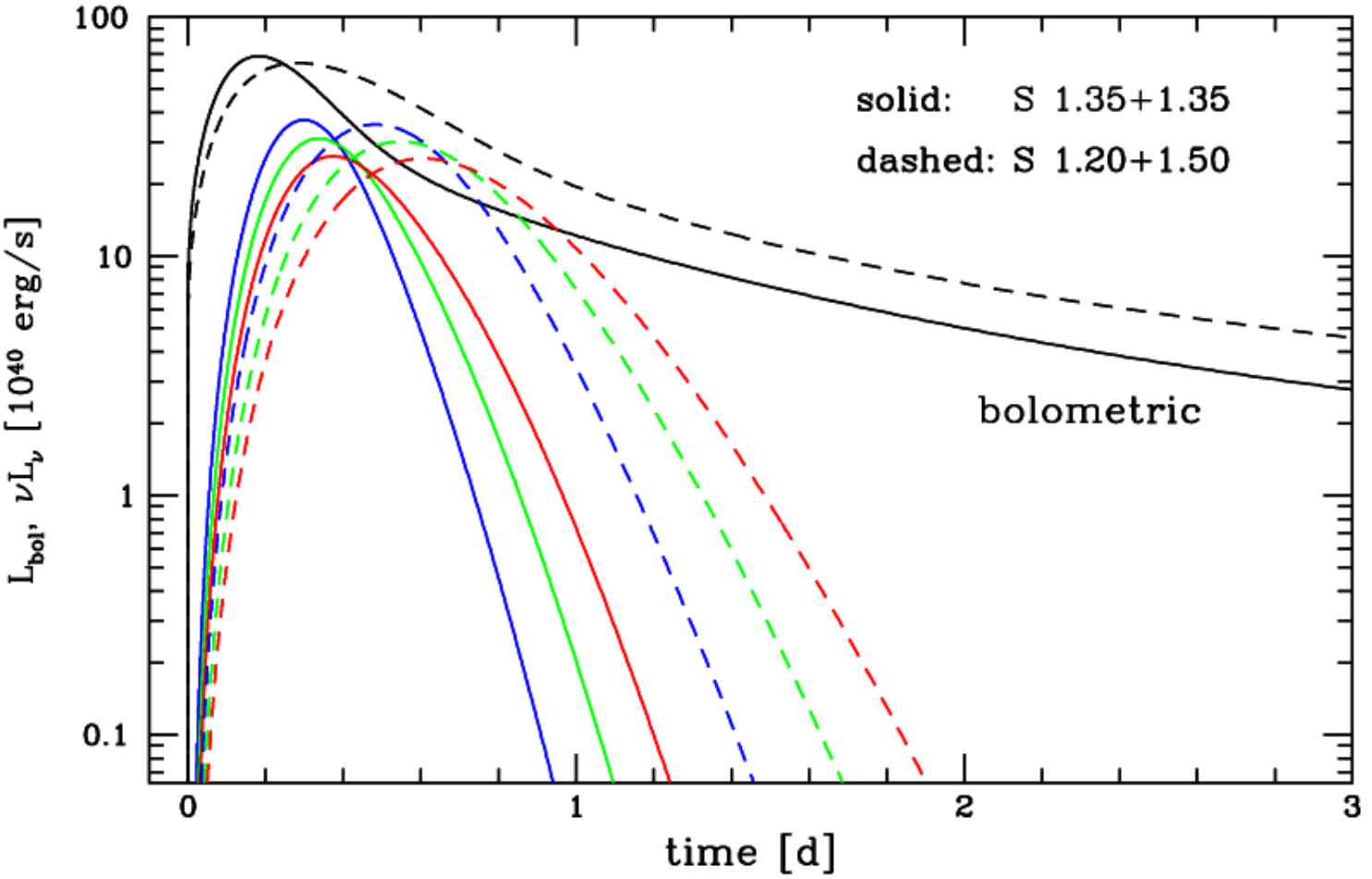

Goriely, Bauswein, HTJ, ApJ (2011)

Astronomers are searching for optical transients and orphan afterglows. **One potential discovery of infrared transient!**